Chapter 4

Results & Discussion

Section 1

Photophysical Properties of Fluorescent PMMA Films

A series of fluorescent PMMA thick films embedded with different concentrations (10, 20.....100 ppm) of a coumarin dyestuff (MACROLEX Fluorescent Red G); were investigated. Spectroscopic tools were applied to study the polymer-dye interactions and the photophysical processes in order to determine the optimum dye concentration corresponding to the maximum efficiency of the absorbed solar photons accompanied with both high conversion, guiding and optical efficiencies.

4.1.1 FT-IR Spectral Characterization

FT-IR transmission spectra were studied in order to know some information about the interactions between the vibrational energy states of the molecules of both polymer and dye molecules. Fig.(4.1.1) shows the FT-IR transmission spectra for the two films of extreme dye concentrations (pure PMMA and 100 ppm MACROLEX Fluorescent Red G) in the wavenumber range (4000-400 cm^{-1}); the main vibrational characteristic groups are depicted on the spectra. An inspection of the spectra showed the disappearance C=C stretching mode (1650-1610 cm^{-1}) characterizing MMA, pointing to the complete polymerization of the monomer [18]. The comparison shows that the most interesting feature is the shape and position of carbonyl group of PMMA (C=O stretching mode) expanded in the band (1800-1500 cm^{-1}), Fig.(4.1.2). It is observed that the vibrational peaks of C=O stretching mode are identical since they appear at the same wavenumber (1728 cm^{-1}) as well as the same band width (FWHM=50 cm^{-1}); this clarifies that there is no chemical bonds raised between PMMA and dye molecules [20].

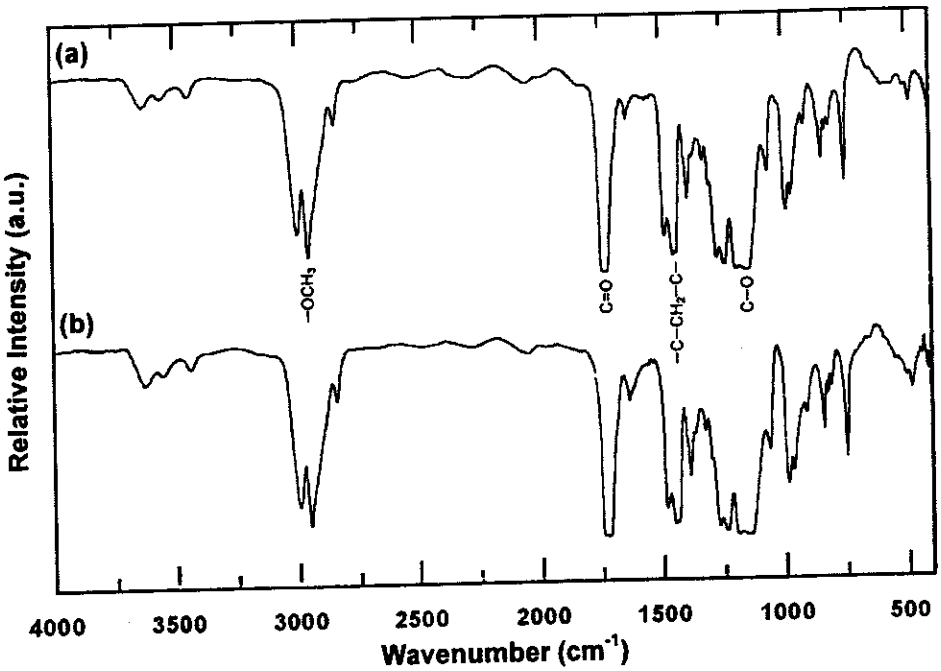

Fig.(4.1.1): FT-IR transmission spectra of (a) PMMA and (b) PMMA/100 ppm MACROLEX Fluorescent Red G films; the main characteristic groups are depicted on the spectra.

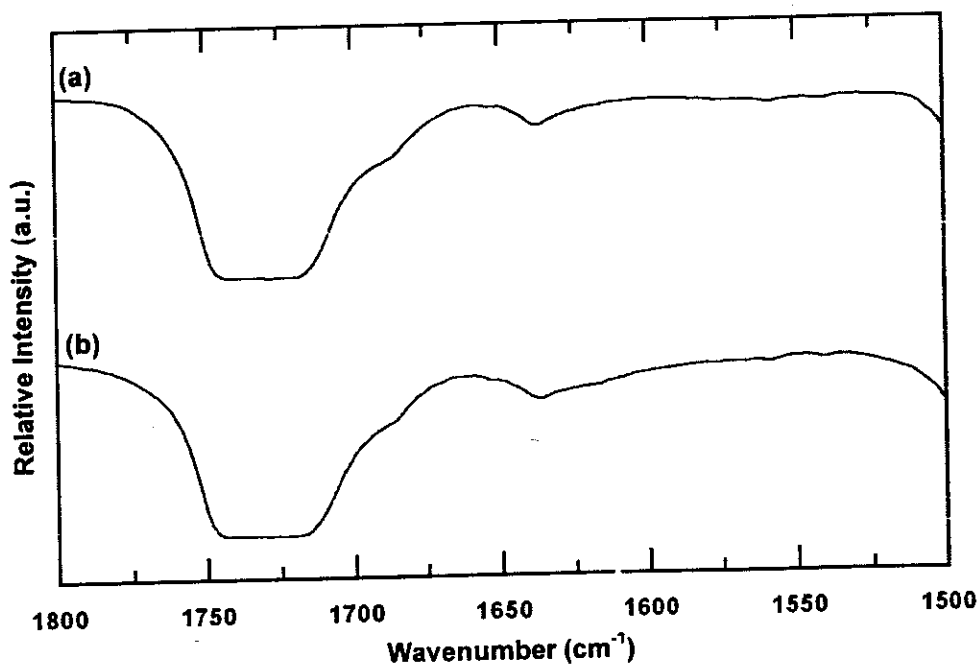

Fig.(4.1.2): Expanded FT-IR transmission spectra in the range (1800-1500 cm^{-1}) (a) PMMA and (b) PMMA/100 ppm MACROLEX Fluorescent Red G films.

4.1.2 Optical Absorption Spectroscopy

The absorption spectra for all the prepared fluorescent PMMA films were recorded in the wavelength range (190-1100 nm) and plotted in Fig. (4.1.3). Two major bands are observed, the first one lies in the UV region around ≈214 nm characterizing π-π^* transition in the carbonyl group of PMMA. The second one appears around ≈520 nm corresponding to the electronic transition to the first excited singlet state ($S_0 \rightarrow S_1$) of the dye [18,113]. The increase in the absorbance value by increasing the dye concentration is attributed to the increase of the number of the absorbing species (chromophores) according to Beer's law [90,91] (Eq. (2.3)),

$$A = \varepsilon(\nu)\, c\, d$$

where $\varepsilon(\nu)$ is the molar absorptivity (molar absorption coefficient), c is the sample concentration and d is the film thickness.

The absorption efficiency, η_{abs} was calculated from Eq. (2.32) as [55],

$$\eta_{abs} = 1 - 10^{-\alpha d}$$

where α is the absorption coefficient at the maximum absorption wavelength and d is the film thickness. Fig.(4.1.4) shows the dependence of η_{abs} on the dye concentration. It is noticed that the absorption efficiency increases by increasing the dye concentration and reaches a maximum value of 55.23 % at the dye concentration 100 ppm. The matrix efficiency η_{mat} for all the fluorescent PMMA films can be calculated by using Equation (2.41) [55],

$$\eta_{mat} = 10^{-\alpha(\lambda_F)\bar{d}}$$

where $\alpha(\lambda_F)$ is the absorption coefficient of the host PMMA matrix at the

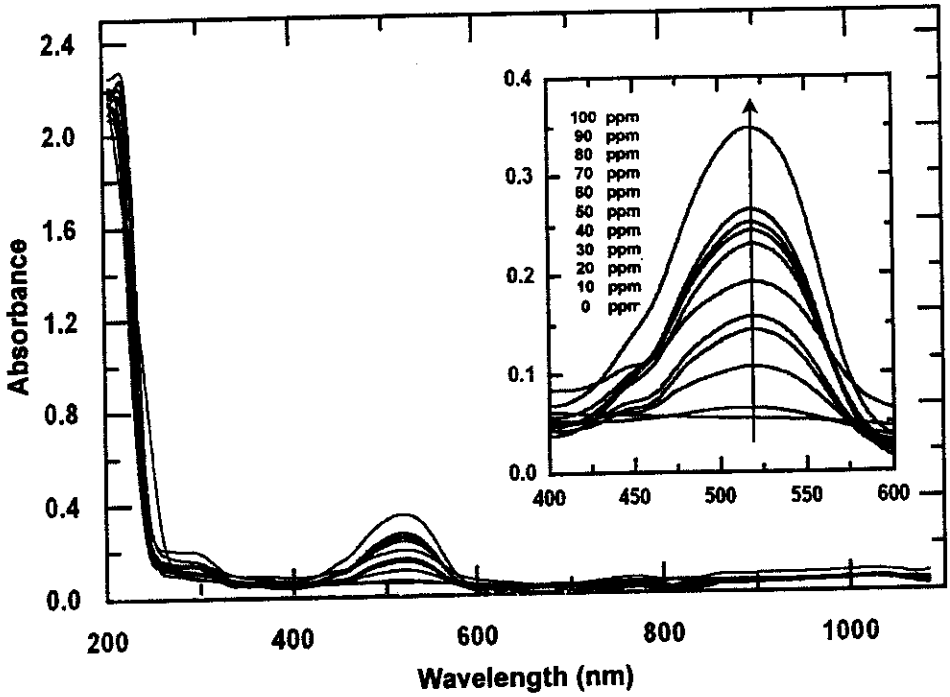

Fig.(4.1.3): The effect of MACROLEX Fluorescent Red G concentration on the absorption spectra of PMMA films; the bands concerning the dye only are magnified (inset).

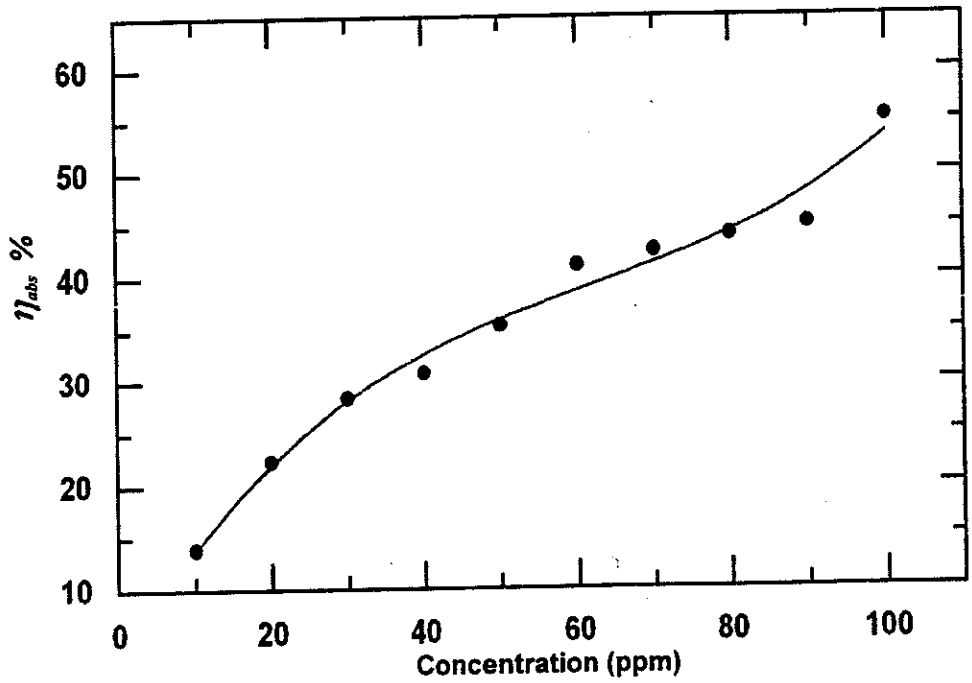

Fig.(4.1.4): Concentration dependence of the absorption efficiency, η_{abs} , for (PMMA/ MACROLEX Fluorescent Red G) films.

fluorescence maximum, and $\overline{d}$ is the mean optical pathlength calculated as mentioned in Eqs.(2.39 - 40)[54,55].

Fig.(4.1.5) shows that the values of η_{mat} are slightly increased by increasing the dye concentration, until reaching a highest value (89.61%) for the film of 100 ppm. This value indicates low losses of the fluorescent light due to the matrix absorption [38, 40].

4.1.3 Fluorescence Spectroscopy

The effect of the dye concentration on the fluorescence spectra of the investigated films are illustrated in Fig.(4.1.6); the intensity and position of the fluorescent peaks are plotted against the dye concentration in Fig.(4.1.7). It is observed that the fluorescence intensity is enhanced by increasing the dye concentration up to 50 ppm, this enhancement is followed by a dramatic reduction accompanied with the appearance of a new fluorescence band red shifted to 623 nm for the film of 100 ppm dye concentration. The formation of this new band may be originated from the existence of other electronic states which are completely different from those of a single dye molecule [103,104]. Fig.(4.1.8) illustrates that the vibrational states of the electronic transitions for such band are similar to some extent, since the excitation and fluorescence spectra for this film look like mirror image of each other [90].

The distribution of the new molecular entity formed in PMMA film of 100 ppm dye concentration can be explicated by the three-dimensional synchronous excitation and fluorescence spectra plotted in Fig.(4.1.9) and the corresponding contour plot as depicted in Fig.(4.1.10). One distinct maximum can be observed at the coordinates (exc., fluo.) = (518.8, 623.4 nm), the broadening of the contour lines indicates a wide distribution of the aggregated dye molecules due to the high concentration [114].

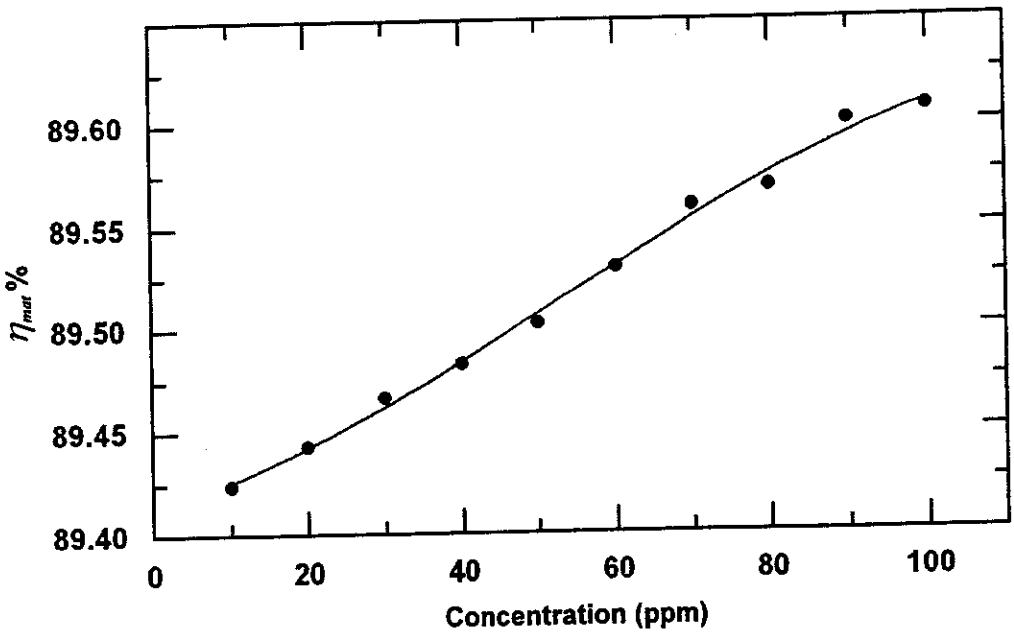

Fig. (4.1.5): Concentration dependence of the matrix efficiency, η_{mat}, for (PMMA/ MACROLEX Fluorescent Red G) films.

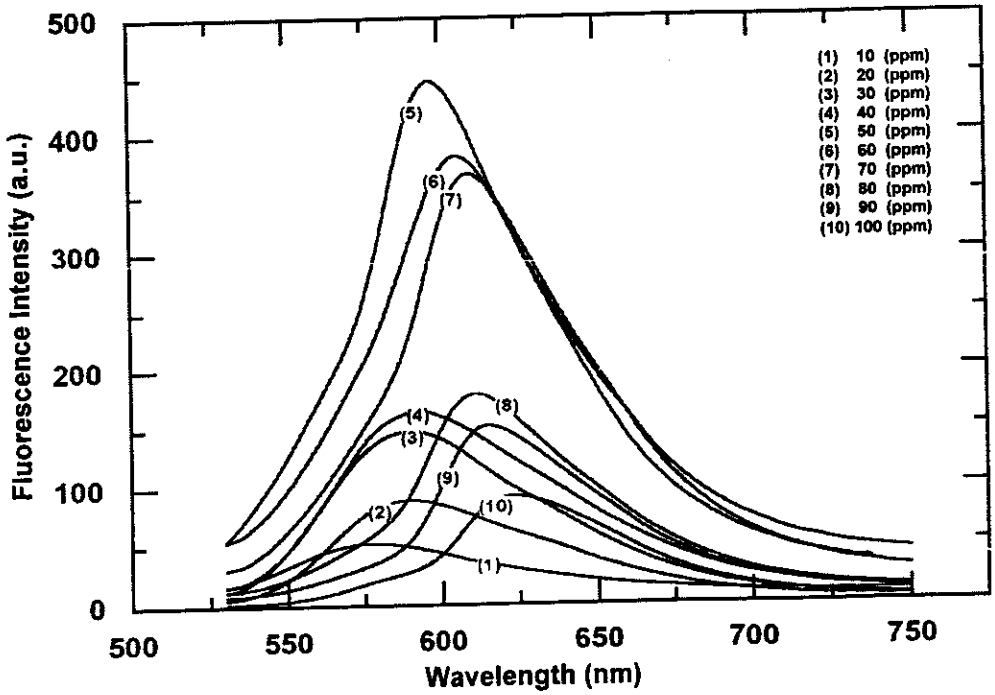

Fig.(4.1.6): Fluorescence spectra of (PMMA/MACROLEX Fluorescent Red G) films.

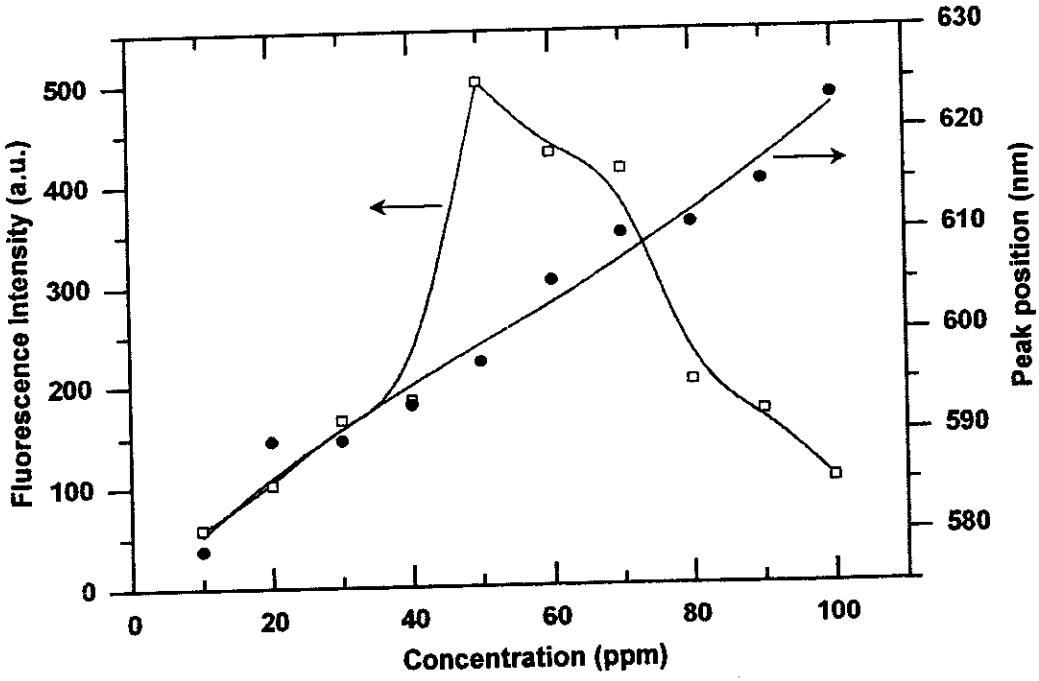

Fig.(4.1.7): The change of the fluorescence intensity and peak position for all the prepared (PMMA/MACROLEX Fluorescent Red G) films.

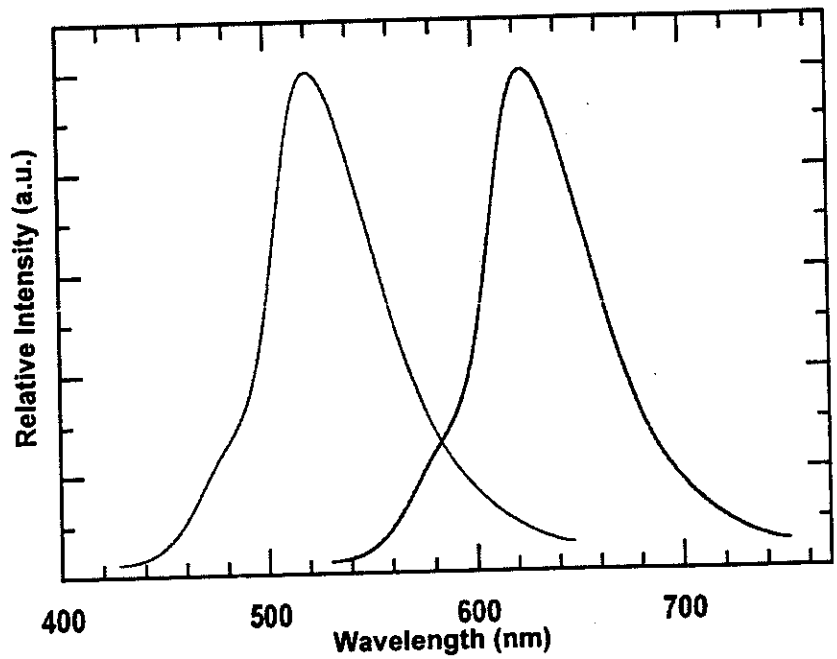

Fig.(4.1.8): Mirror image relationship of excitation (left) and fluorescence (right) spectra for (PMMA/100 ppm MACROLEX Fluorescent Red G) film.

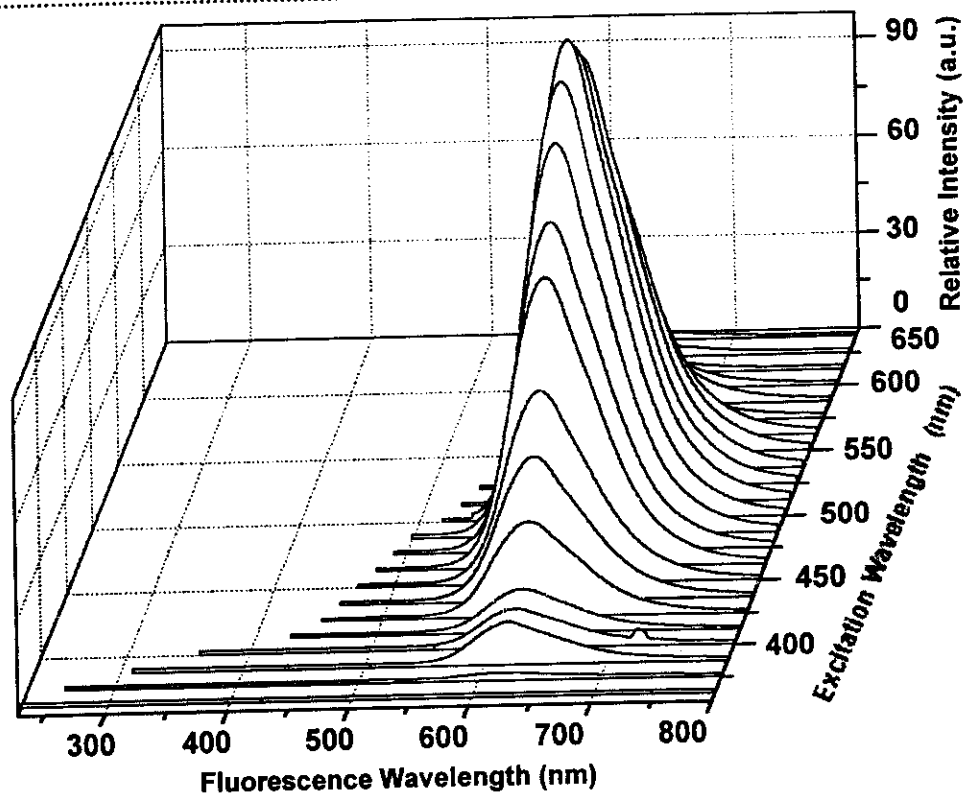

Fig.(4.1.9): Three dimensional representation of a synchronous excitation and fluorescence spectra of PMMA/100 ppm MACROLEX Fluorescent Red G film.

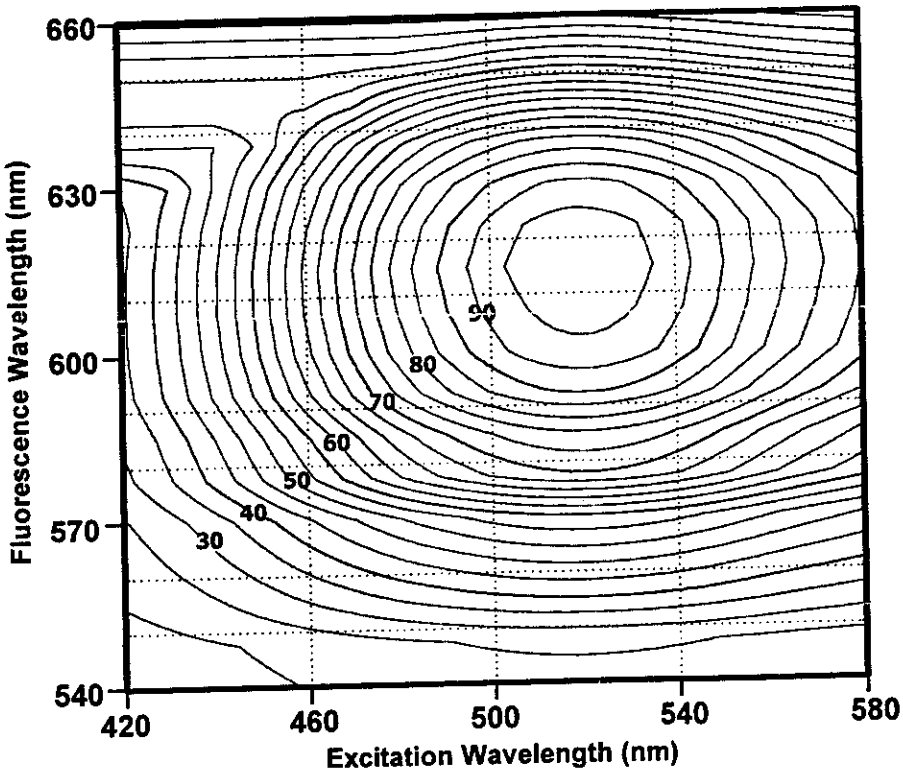

Fig.(4.1.10): Surface map representation of a synchronous excitation and fluorescence spectra of PMMA/100 ppm MACROLEX Fluorescent Red G film.

The absolute fluorescence quantum yield η_F, of fluorescent PMMA films was calculated, relative to Rhodamine 101 doped in PMMA film as a reference sample using Eq. (2.21) [103-107],

$$\eta_F = \eta_{ref} (a/a_{ref}) (n/n_{ref}) (S_{ref}/S)$$

where η_{ref} is the fluorescence quantum yield of the standard sample (reference), "a" is the absorbance, n is the refractive index of the matrix and S is the area under the fluorescence curve.

The Stokes shift $\Delta\lambda_s$, which is a measure of self-absorption of the fluorescent light, was calculated from Eq.(2.22) [19],

$$\Delta\lambda_s = \lambda_{F(max)} - \lambda_{a(max)}$$

where $\lambda_{F(max)}$ and $\lambda_{a(max)}$ are the wavelengths at the fluorescence and absorbance maxima respectively. The values of $\lambda_{a(max)}$, $\lambda_{F(max)}$, $\Delta\lambda_s$ and η_F are listed in Table (4.1.1). The observed decrease in η_F accompanied with larger values of $\Delta\lambda_s$ at concentrations higher than 50 ppm can be mainly attributed to the formation of excited state dimers (excimers) and higher aggregates which have small values of η_F. The strength of aggregation depends mainly on the dye nature, the host media and the other factors related to the preparation conditions. The decrease in the quantum yield at higher concentrations is caused by Förster-type energy transfer to the excited state dimers (excimers) [103]. In other words, the dimer (two bonded dye molecules) fluorescence is more predominant than that of the monomer (isolated dye molecule) if they are equally present in the matrix [115].

4.1.4 Interband Transitions

The UV absorption edge was analyzed in the range (190-350 nm)

Table (4.1.1): The effect of concentration on the absorption and fluorescence wavelengths $\lambda_{a(max)}$ and $\lambda_{F(max)}$, stokes shift $\Delta\lambda_S$ and fluorescence quantum yield η_F for the investigated (PMMA/ MACROLEX Fluorescent Red G) films.

Concentration (ppm)	$\lambda_{a(max)}$ (nm)	$\lambda_{F(max)}$ (nm)	$\Delta\lambda_S$ (nm)	η_F %
10	517.00	578.80	61.80	15.60
20	523.00	589.60	66.60	22.80
30	521.90	589.60	67.70	33.80
40	524.00	593.00	69.00	42.90
50	521.30	597.20	75.90	90.60
60	522.10	605.20	83.10	78.40
70	520.20	609.80	89.60	75.70
80	520.60	610.80	90.20	39.70
90	519.50	615.00	95.50	34.60
100	518.80	623.40	104.60	23.20

and the calculated values of the absorption coefficient α are found to lie in the range $1 \leq \alpha \leq 10^4$ cm^{-1}. The absorption coefficient for a simple parabolic band can be expressed by Eq.(2.9) [93],

$$\alpha E = M (E - E_{opt})^m$$

where E_{opt} is the optical band gap of the specimen and m is an index which has a value of 1/2, 3/2, 2 and 3 depending on the nature of electronic transition responsible for the absorption. Fig.(4.1.11) shows the dependence of $(\alpha E)^2$ on photon energy E for all the investigated fluorescent PMMA films. These figures show a linear behavior that can be considered as an evidence of the direct transition [116]. The approximate value of E_{opt} is determined from the extrapolation of the straight line part to zero photon energy, and listed in Table (4.1.2). The dependence of E_{opt} on the dye concentration shows a maximum value for the film of 50 ppm. This behaviour is well correlated to that observed in the calculated values of the fluorescence quantum yield (Table (4.1.1)). This means that adding the dye to PMMA introduces energy levels in the polymer band gap that produced light induced electron-hole pairs (exciton-like states) followed by the annhilation processes through a set of eqidistant energy levels that accordingly produced a set of very specific wavelengths by increasing the dye concentration [18,80].

On the otherhand, the absorption spectra show an extending tail for lower photon energies below the band edge, which can be described by Urbach's formula from Eq. (2.8) [101],

$$\alpha(\nu) = \alpha_o \exp (E/E_U)$$

where E_U is the Urbach's energy corresponding to the width of the band tails of the localized states in the optical band gap.

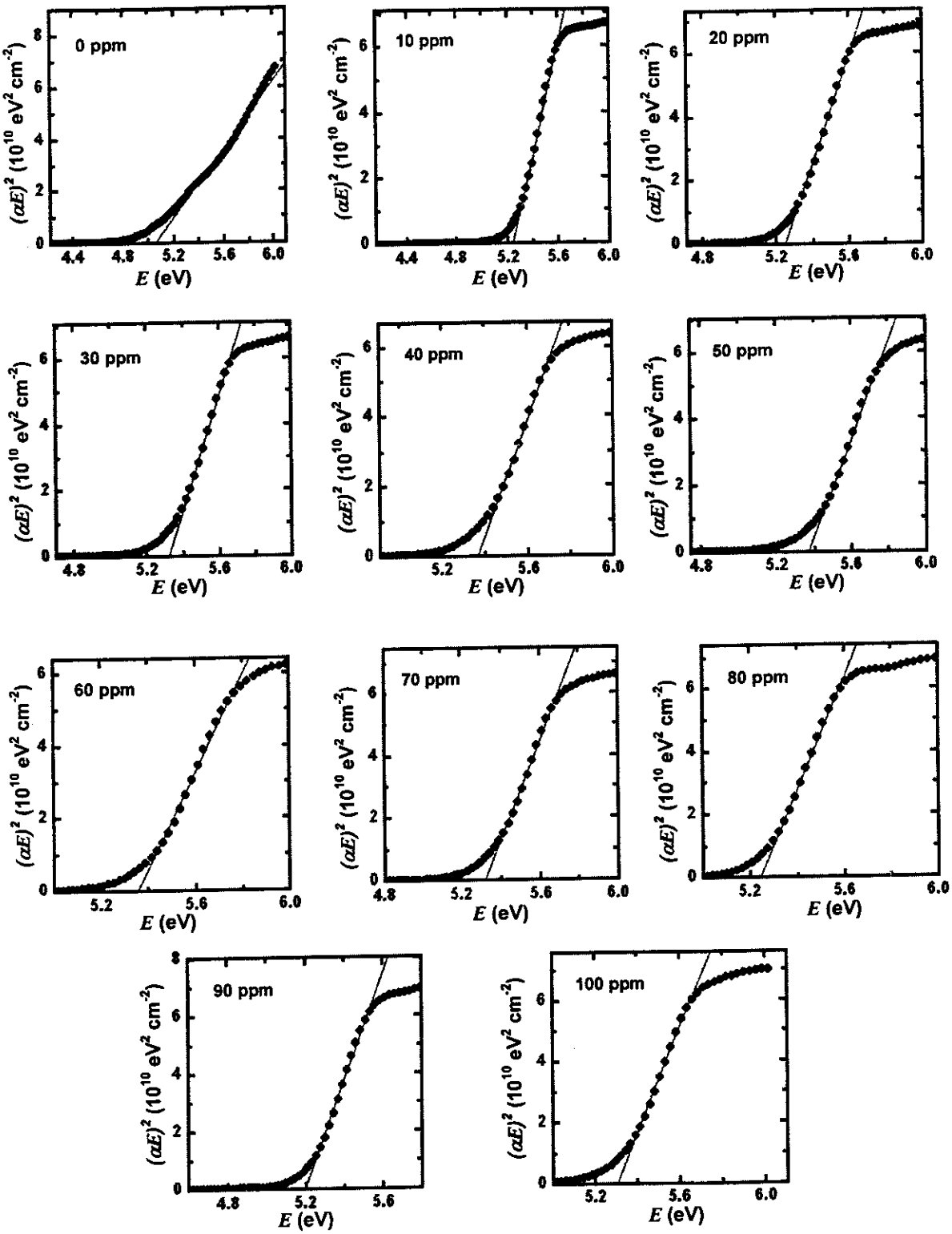

Fig.(4.1.11): The dependence of $(\alpha E)^2$ on photon energy (E) for the prepared (PMMA/MACROLEX Fluorescent Red G) films.

Table (4.1.2): The effect of concentration on the optical band gap E_{opt}, and the tail width E_U for the (PMMA/ MACROLEX Fluorescent Red G) films.

Concentration (ppm)	E_{opt} (eV)	E_U (eV)
0	5.005	0.199
10	5.242	0.197
20	5.253	0.208
30	5.320	0.229
40	5.369	0.235
50	5.374	0.259
60	5.359	0.243
70	5.320	0.232
80	5.244	0.207
90	5.197	0.198
100	5.307	0.248

The values of E_U were calculated as the reciprocal gradient of the obtained straight line, from the relation between $\ln\alpha$ versus the photon energy (Fig.4.1.12), and listed in Table (4.1.2). It is noticed that the dependence of E_U on the dye concentration does not match with E_{opt} values because the sample having a narrower band gap is expected to have a wider band tail. This can be attributed to the fact that the change in localized states is probably affected by internal potential fluctuations associated with the polymer structure. Unlike E_U behaviour, E_{opt} is not affected by the internal potential fluctuations because the initial (valance band) and final (conduction band) states are practically at the same potential [18,77].

4.1.5 Transmission Spectroscopy

The transmission spectra for all the prepared fluorescent PMMA films were recorded in the wavelength range (190-1100 nm) and plotted in Fig. (4.1.13). The effect of dye concentration on the film transmittance at the fluorescence maxima T_F is illustrated in Fig.(4.1.14), it is noticed that all the films under investigation exhibit high transmission with a maximum value (97.65%) at the film of 50 ppm dye concentration due to its excellent fluorescence properties.

4.1.6 Refractive Index and Guiding properties

The spectral dependence of the specular reflection spectra for all films in the wavelength range (300-1100 nm) is shown in Fig.(4.1.15). All the curves show a minimum peak in the wavelength range of the absorption band followed by a maximum one in the wavelength range of the fluorescence band. The determined wavelength of the maximum reflectance increases by increasing the dye concentration; in good agreement with the behavior observed in the fluorescence spectra.

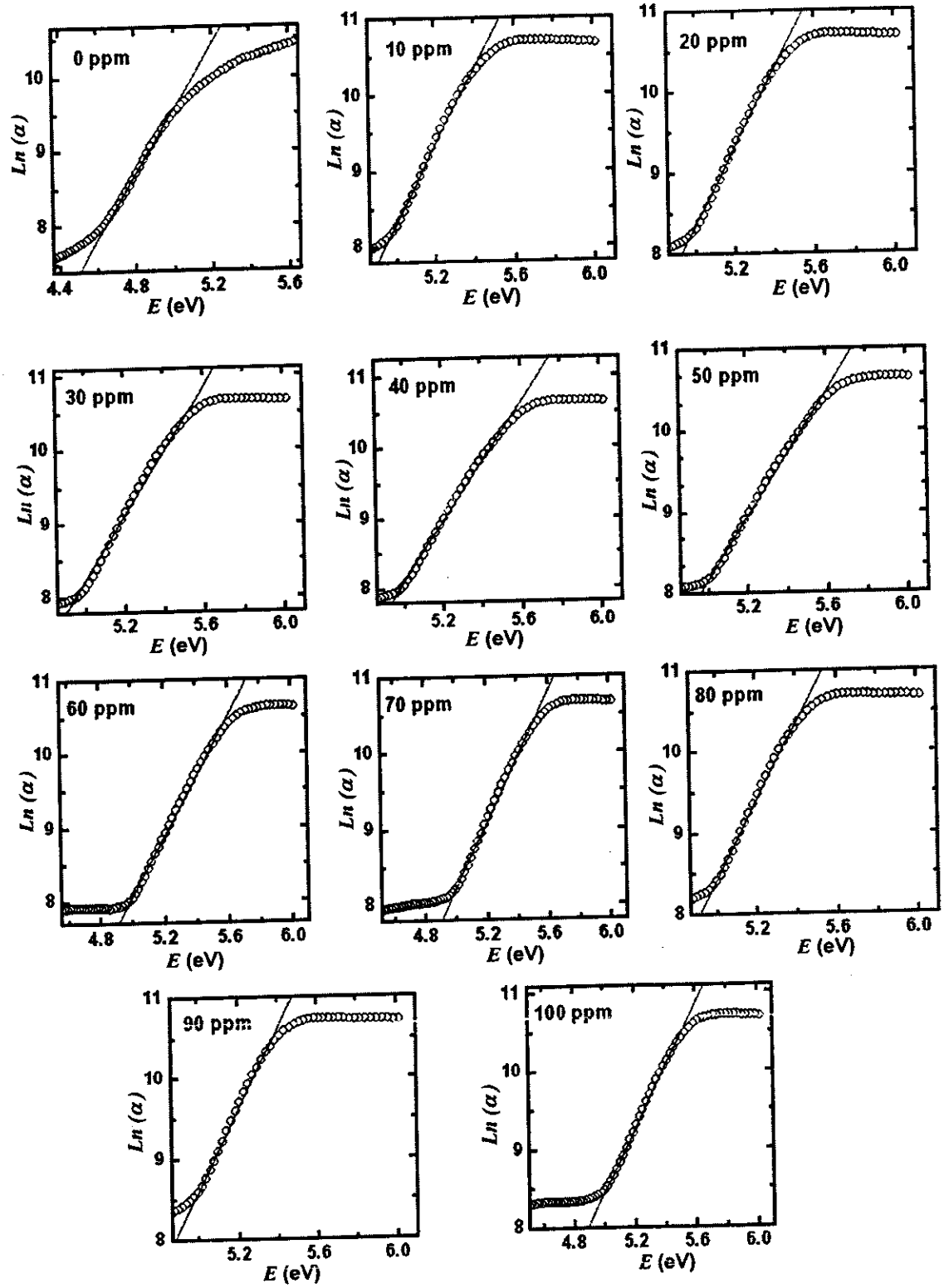

Fig.(4.1.12): The dependence of $ln(\alpha)$ on the photon energy (E) for the investigated (PMMA/ MACROLEX Fluorescent Red G) films.

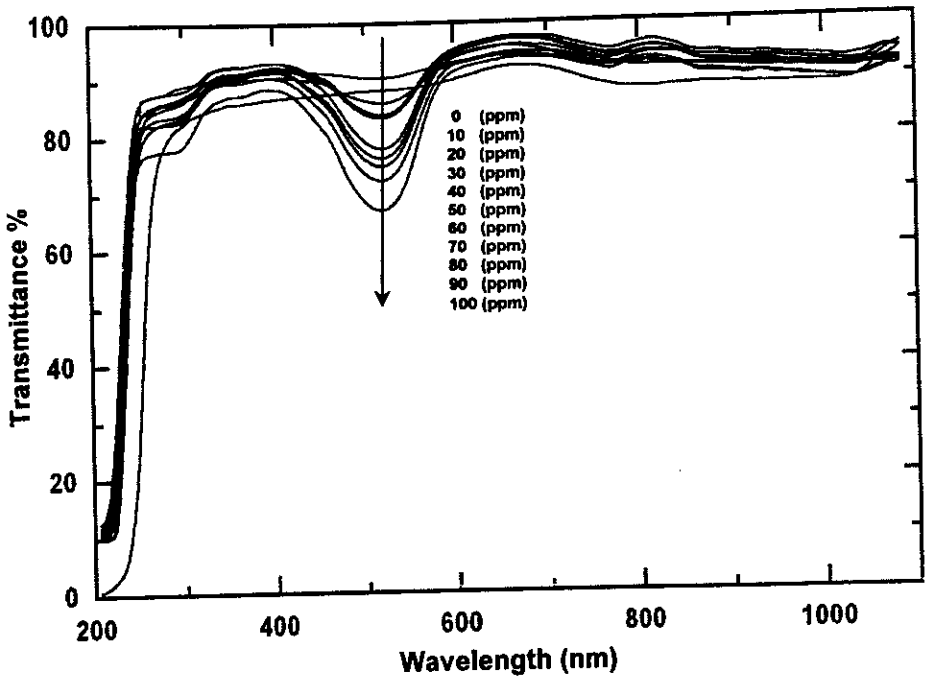

Fig.(4.1.13): Concentration dependence of Transmission spectra for the prepared (PMMA /MACROLEX Fluorescent Red G) films.

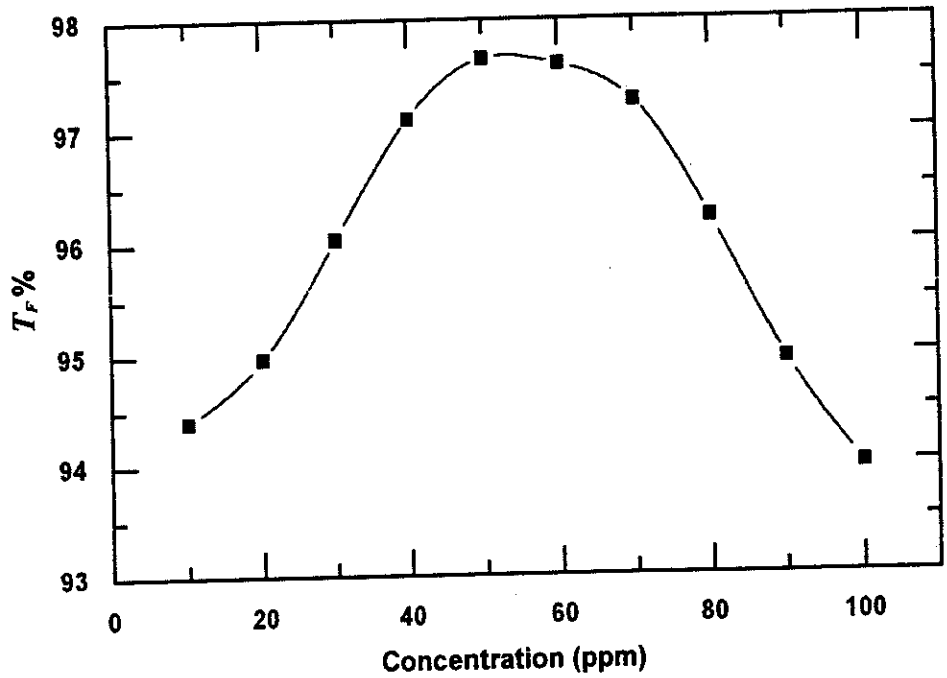

Fig.(4.1.14): The effect dye concentration on the film transmittance at the fluorescence peak, T_F, for (PMMA/MACROLEX Fluorescent Red G) films.

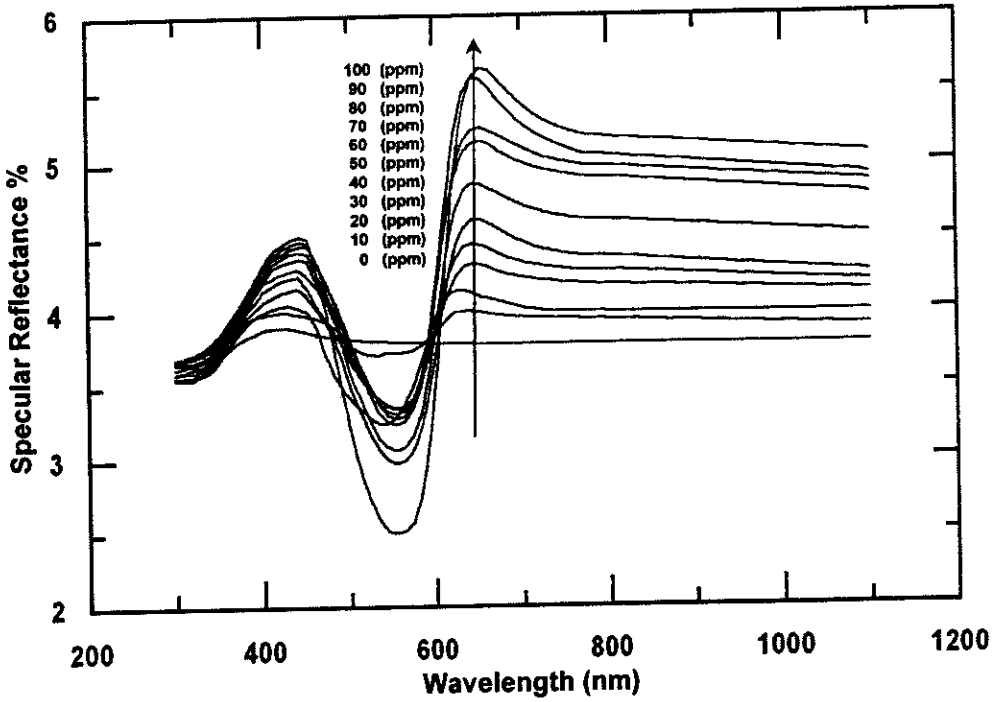

Fig.(4.1.15): The specular reflection spectra for all the investigated (PMMA/ MACROLEX Fluorescent Red G) films.

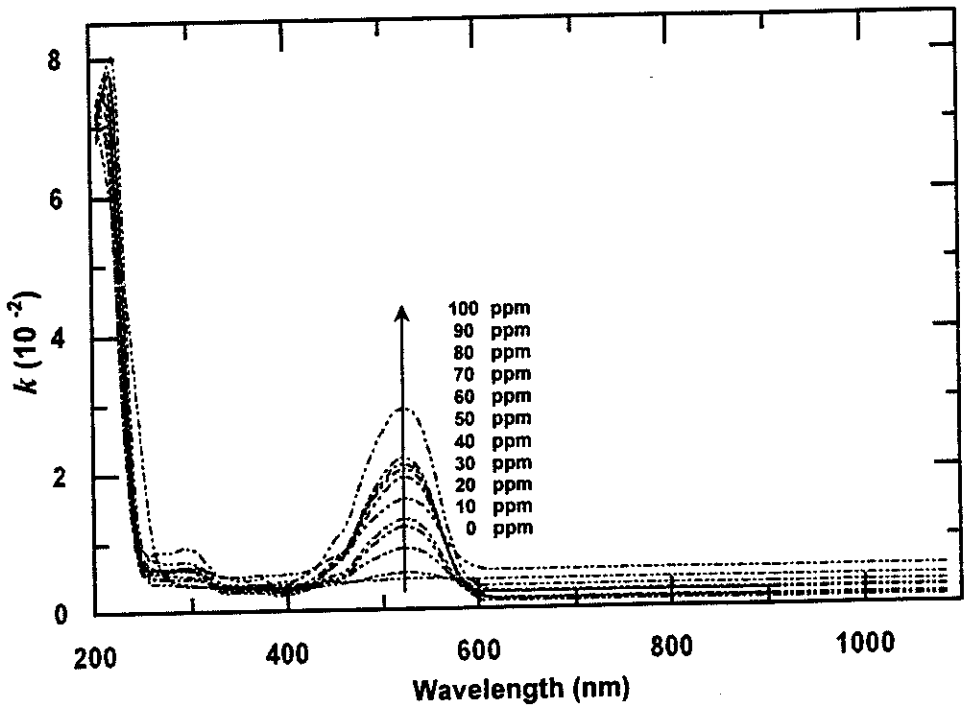

Fig.(4.1.16): The Effect dye concentration on the attenuation coefficient, k , of (PMMA /MACROLEX Fluorescent Red G) films.

The refraction of a medium can be described by a single quantity called complex refractive index ñ which is defined using the following equation [93,100],

$$\tilde{n} = n + ik \tag{4.1.1}$$

where n is the normal refractive index and k is the attenuation coefficient which is directly related to the absorption coefficient of the material α at a given wavelength λ according to [93, 100],

$$k = \alpha\lambda / 4\pi \tag{4.1.2}$$

Fig.(4.1.16) represents the spectral dependence of the attenuation coefficient k for all the fluorescent PMMA films. It is clear that k increases by increasing the dye concentration and tends to zero in the wavelength range of the fluorescence band, this indicates that the films are transparent in region of the films' fluorescence. Therefore the refractive index n can be calculated by using Equation (2.36) [55,100],

$$R_f = (n\text{-}1)^2 / (n+1)^2$$

where R_f is the Fresnel's reflection coefficient.

Fig.(4.1.17) shows the spectral dependence of the refractive index n for all the fluorescent PMMA films in the wavelength range 300-1100 nm. It is obviously noted that the values of n are increased in the wavelength region of the fluorescence band and then show normal dispersion according to Cauchy's dispersion formula [117 -119],

$$\frac{dn}{d\lambda} = -\frac{2B}{\lambda^3} \tag{4.1.3}$$

where B is a characteristic constant depending on the material type.

The increase of the refractive index n by increasing the dye concentration is attributed to an increase of the number of atomic refractions due to the increase of the mean molecular polarizability $\overline{\alpha}$ in agreement with Lorentz-Lorentz equation[120,121],

$$\frac{n^2-1}{n^2+2}\frac{M_n}{\rho}=\frac{4}{3}\pi N_A\ \overline{\alpha} \qquad (4.1.4)$$

where M_n is the molecular weight of the polymeric repeat, ρ is the molecular density and N_A is Avogadro's number.

The trapping efficiency η_{trap} was calculated from the refractive index n of the films using Eq.(2.38)[55],

$$\eta_{trap} = (1\text{-}1/n^2)^{0.5}$$

Fig.(4.1.18) represents a plot of η_{trap} against the dye concentration, it is clear that the value of η_{trap} is increased by increasing the refractive index n which is related to the dye concentration. This can be attributed to the decreasing of the critical angle and consequently reducing the escape fluorescent photons from the critical cones [88].

The trapped photons are assumed to propagate without losses by total internal reflection to the collecting edge, but it depends on the nature of the reflecting surfaces and edges. The partial yield η_{TIR} defined as the total internal reflection efficiency is given by Eq.(2.42) [55],

$$\eta_{TIR} = R_1^{n_1}$$

where n_i is the mean number of total internal reflections and R_i is the measured total internal reflection coefficient, the values of n_i were derived from the Eqs(2.39-40 & 2.43-44)[54,55]. Fig.(4.1.19) shows the dependence of η_{TIR} on the dye concentration, it is clear that the value of η_{TIR} increases by increasing the dye concentration with a maximum value (96.64%) at the dye concentration of 100 ppm. This can be attributed to the decrease of total internal reflection losses due to the increase of both dye dispersion and the surface smoothing [40,122].

According to the photon flow diagram depicted in Fig.(2.16), the conversion yield η_{conv} defined as the ratio of the number of photons available in the film N to the number of incident photons N_o, was calculated by using Eq.(2.46) [55],

$$\eta_{conv} = (1 - R_f)\,\eta_{trap}\,\eta_{abs}\,\eta_F = N/N_o$$

where (1- R_f) is the fraction of the incident light collected by the film. The dependence of η_{conv} on the dye concentration shows a maximum conversion efficiency (23.36%) for the film of 50 ppm, Fig.(4.1.20). This result is in good agreement with the fluorescence efficiency of the films, since increasing the dye concentration caused the formation of excited state dimers (excimers) which are weakly fluorescent [19,104].

4.1.7 Dye Self-Absorption

The stokes efficiency η_{stok} which is the ratio of the average energy of the fluorescent photons to the average energy of the absorbed photons is given by Eq.(2.33) [47],

$$\eta_{stok} = \langle \nu_F \rangle / \langle \nu_a \rangle$$

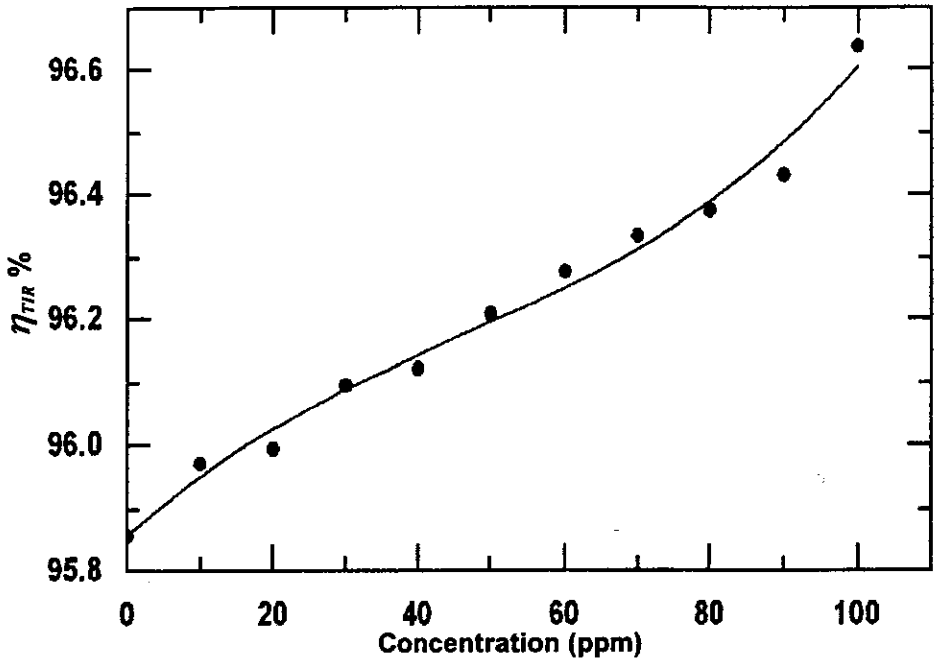

Fig.(4.1.19): The concentration dependence of the total internal reflection efficiency, η_{TIR}, for (PMMA/ MACROLEX Fluorescent Red G) films.

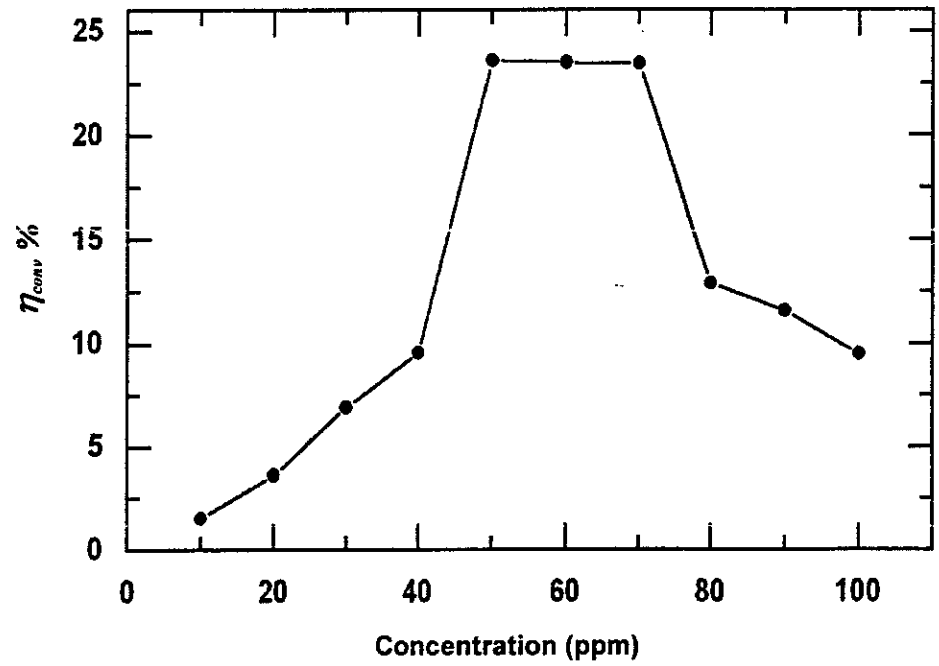

Fig.(4.1.20): Concentration dependence of the conversion efficiency, η_{conv}, for (PMMA/ MACROLEX Fluorescent Red G) films.

where ν_F and ν_a are the wavenumbers at the fluorescence and absorbance maxima respectively. The values of η_{stok} were extracted from the values of $\lambda_{F(max)}$ and $\lambda_{a(max)}$ listed in Table (4.1.1). It was observed that values of η_{stok} are decreased by increasing the dye concentration, to a minimum value (83.22%) for the concentration of 100 ppm. This means that the energy loss due to stokes shift (1- η_{stok}) is increased by increasing the dye concentration due to the aggregation of the dye molecules at the mentioned concentration.

On the other hand the self-absorption of the dye aggregates and its effect on the fluorescent light transport to the concentrator edges has been studied using the fluorescence polarization anisotropy technique. The degree of polarization can be expressed as Eq.(2.24) [103,104],

$$P = (I_{//} - I_{\perp}) / (I_{//} + I_{\perp})$$

where $I_{//}$ and $I_{\perp}$ are the relative intensities of fluorescence polarized parallel and orthogonal to the electric vector of the incident radiation respectively. Figs.(4.1.21 & 22) show the polarized excitation and fluorescence spectra for the fluorescent PMMA films of 10 and 100 ppm dye concentrations respectively. It is noticed that for the lowest dye concentration (10 ppm), the obtained polarization spectrum is rather ideal in that the values of P are almost constant across the long wavelength of the excitation and fluorescence bands. Dissimilarly, for the highest dye concentration (100 ppm), the fluorescence is less polarized and subsequently self-absorbed.

The degree of polarization can be measured by the reduced fluorescence anisotropy A given by Eq.(2.27) [103],

$$A = (2P)/ (3-P)$$

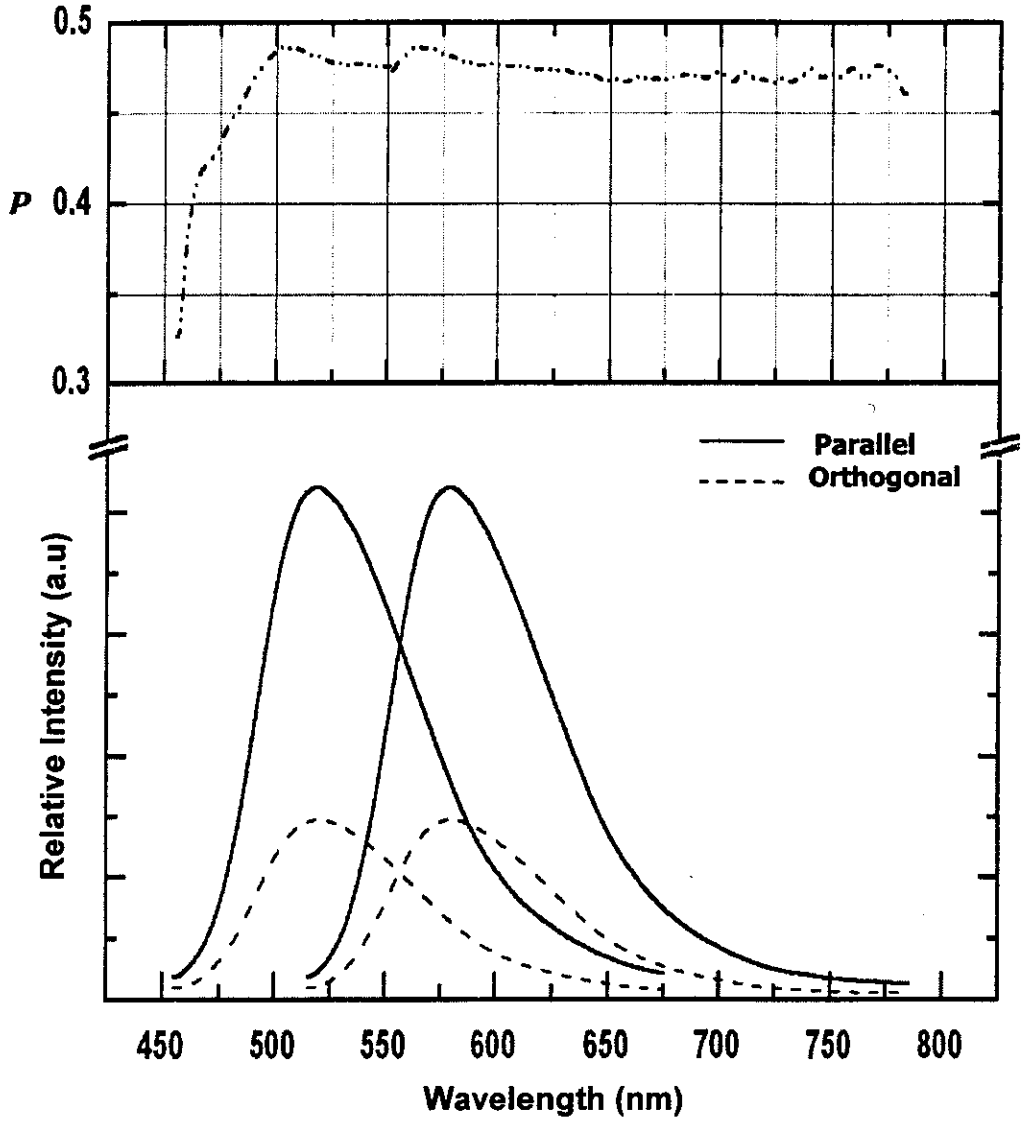

Fig.(4.1.21): Spectra of polarized fluorescence excitation (left) and fluorescence (right) for (PMMA/10 ppm MACROLEX Fluorescent Red G) film obtained by parallel and orthogonal orientations with respect to the polarization direction of the incident light. The polarization spectrum is plotted in the upper box.

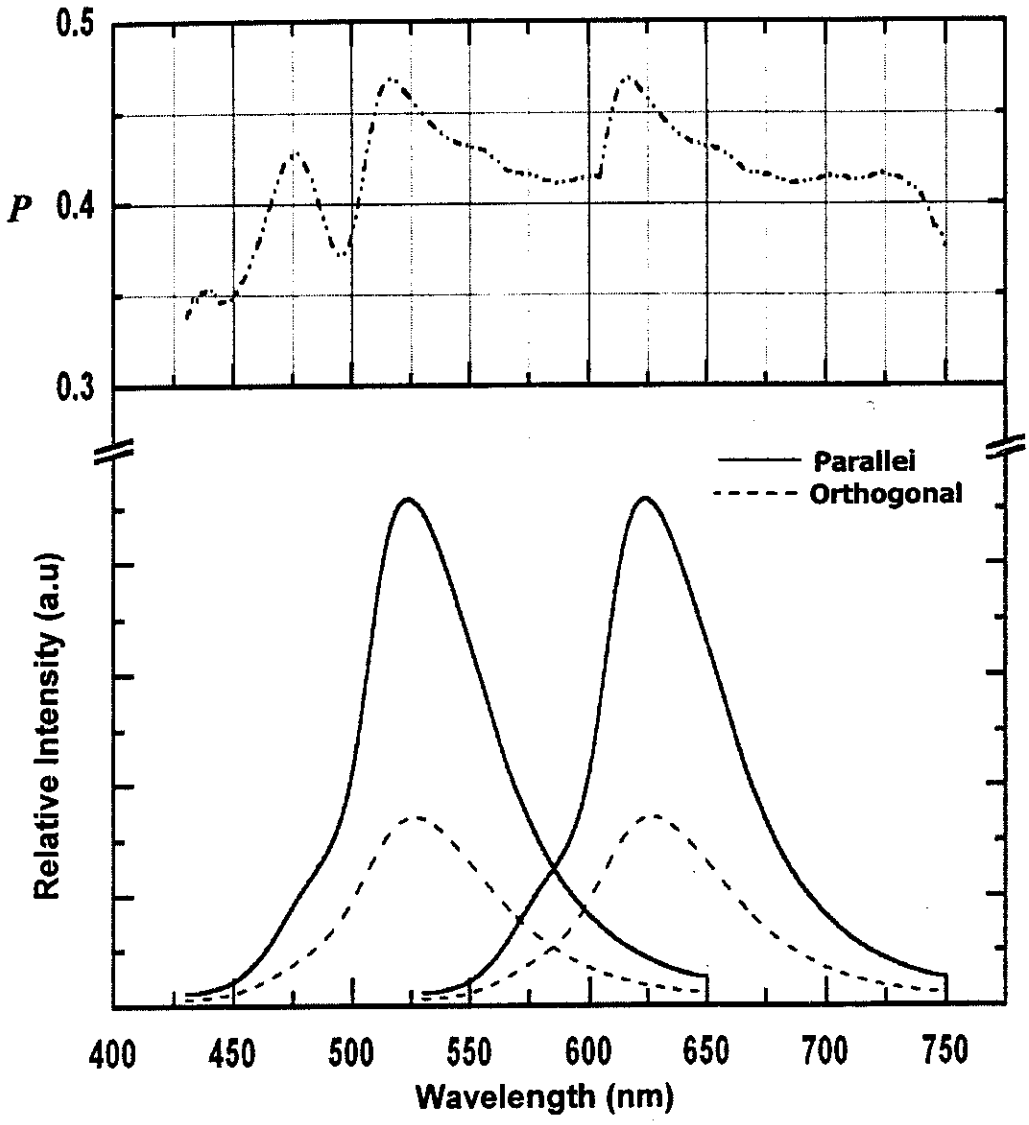

Fig.(4.1.22): Spectra of polarized fluorescence excitation (left) and fluorescence (right) for (PMMA/100 ppm MACROLEX Fluorescent Red G) film obtained by parallel and orthogonal orientations with respect to the polarization direction of the incident light. The polarization spectrum is plotted in the upper box.

The self-absorption probability ($1-\eta_{self}$) can be deduced using the following relation (2.34) [49,81],

$$(1-\eta_{self}) = [1-A_F/A_o]/\eta_F\,\eta_{trap}\,(1-A_F\,A_o)$$

where A_o is the highest measured reduced anisotropy value at very low concentration and pathlength; A_F is the measured reduced anisotropy at the concentration and pathlength of interest. The calculated values of A_F and A_o were 36.23 and 38.24% respectively; this leading to high self-absorption probability, since the estimated value of η_{self} was only 66.60%.

4.1.8 Photostability

4.1.8.1 Photoresponse of the Optical Absorption Spectra

The accelerated photoresponse of 100 ppm dye embedded PMMA film towards the UV-VIS radiation was tested indoors for 24 hrs using an artificial light source from xenon arc lamp. The change in the absorption spectra was monitored at different times during the irradiation period and plotted as shown in Fig.(4.1.23.a). The dye photodegradation a_t/a_o , which is the percentage change of optical density is plotted versus the exposure time as illustrated in Fig.(4.1.23.b). It is obviously noted that the photodegradation curve seems to accelerate with a relatively fast rate, this behavior suggests two degradation rates obeying an exponential relation [19],

$$a_t/a_o = C_1 + C_2\,exp(-R_1t) + C_3\,exp(-R_2t) \qquad (4.1.5)$$

where C_1, C_2 and C_3 are constants and R_1 and R_2 are the photodegradation rate constants of the dye. The values of the rate constants are equal to 2.04×10^{-3} sec^{-1} and 1.076×10^{-7} sec^{-1} respectively. The four orders difference between R_1 and R_2 can be attributed to the existence of two mechanisms of

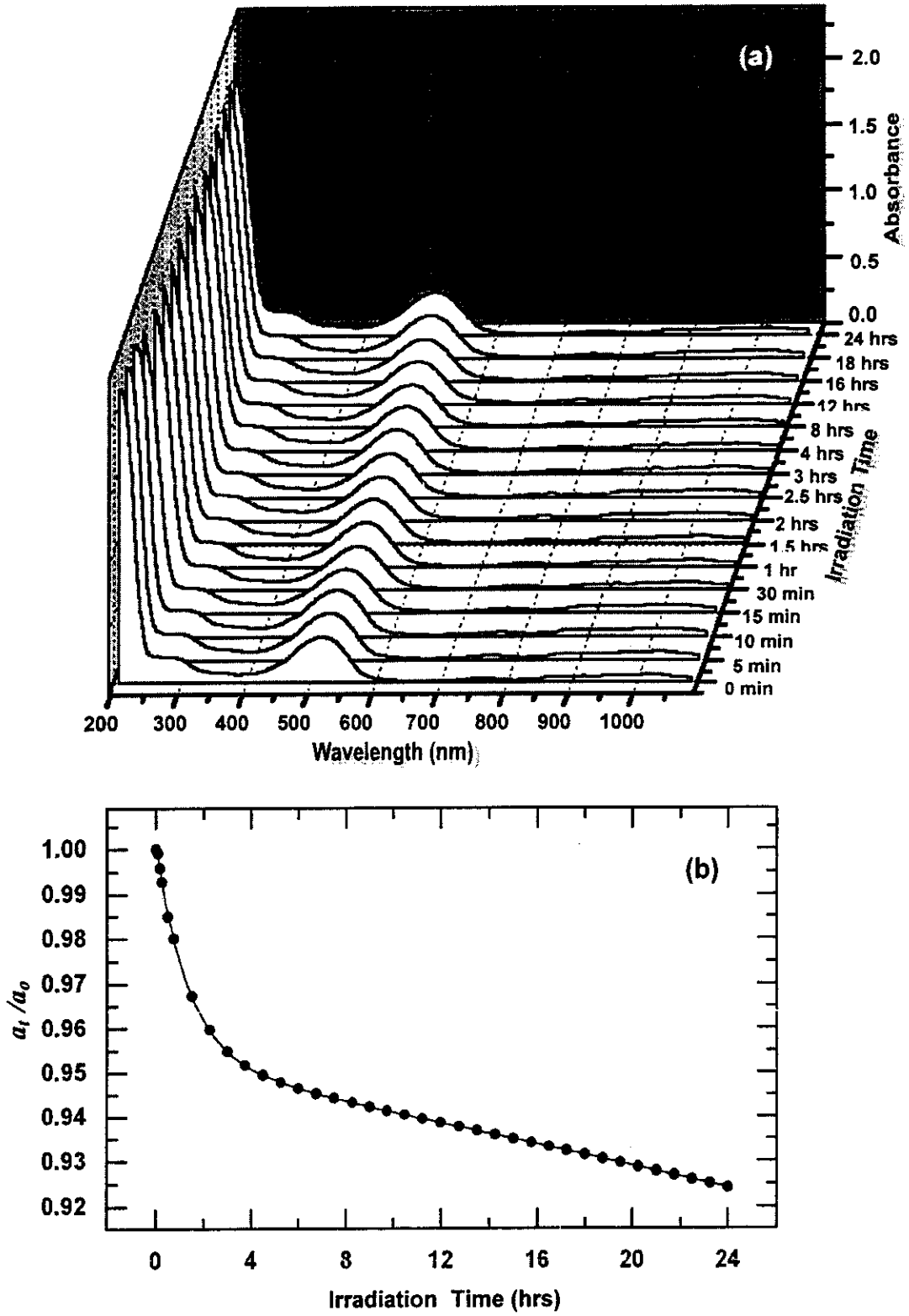

Fig.(4.1.23): (a) Time dependence of the absorption spectra of (PMMA/100 ppm MACROLEX Fluorescent Red G) film under photoirradiation with artificial sunlight and (b) The corresponding photodegradation curve after indoor exposure to artificial sunlight from Xenon arc lamp for 24 hrs.

dye photodegradation . The first concerns the dye molecules which may exist outside the core, and takes short time to photodecompose (large rate constant). The second mechanism concerns the caged dye molecules inside the core formed by three-dimensional chain network of PMMA; significantly the undestroyed dye molecules which may exist in deeper layers of PMMA. The later mechanism initiated after 2.2 hours of the photoirradiation (approximately 33 days of exposure to natural sunlight under normal atmospheric conditions). After 24 hrs of the photoirradiation (which is the period corresponding to about 1 year exposure to natural sunlight in the Egyptian climates), the dye absorbance reaches about 92.42 % of its initial value. This showed the way to study the effect of photoirradiation on the fluorescence spectra, since a considerable amount of the investigated dye remains in the film.

Fig.(4.1.24) shows the dependence of $(\alpha E)^2$ on the photon energy E for PMMA film embedded with 100 ppm of the investigated dye. These figures show a linear behavior that can be considered as an evidence of the direct allowed transition. The approximate value of E_{opt} is determined from the extrapolation of the straight line part to zero photon energy, and listed in Table (4.1.3). It is observed that, the values of E_{opt} are decreased by increasing the time of exposure to artificial sunlight and reached 5.050 eV after 3 hours (45 days exposure to natural sunlight). After 3 hours the values of E_{opt} are increased and reached 5.350 eV at 24 hours. The decrease in E_{opt} after 3 hours of photoirradiation is attributed to the increase of the degree of disorder due to the dye photodecomposition. According to the density of states model, the value of E_{opt} is decreased by increasing the degree of disorder of the amorphous phase. The noticeable increase in the values of E_{opt} after 3 hrs may be attributed to appearance of other types of optical transitions occurring from the higher vibrational levels of the ground state to higher sublevels of the first excited singlet state [80].

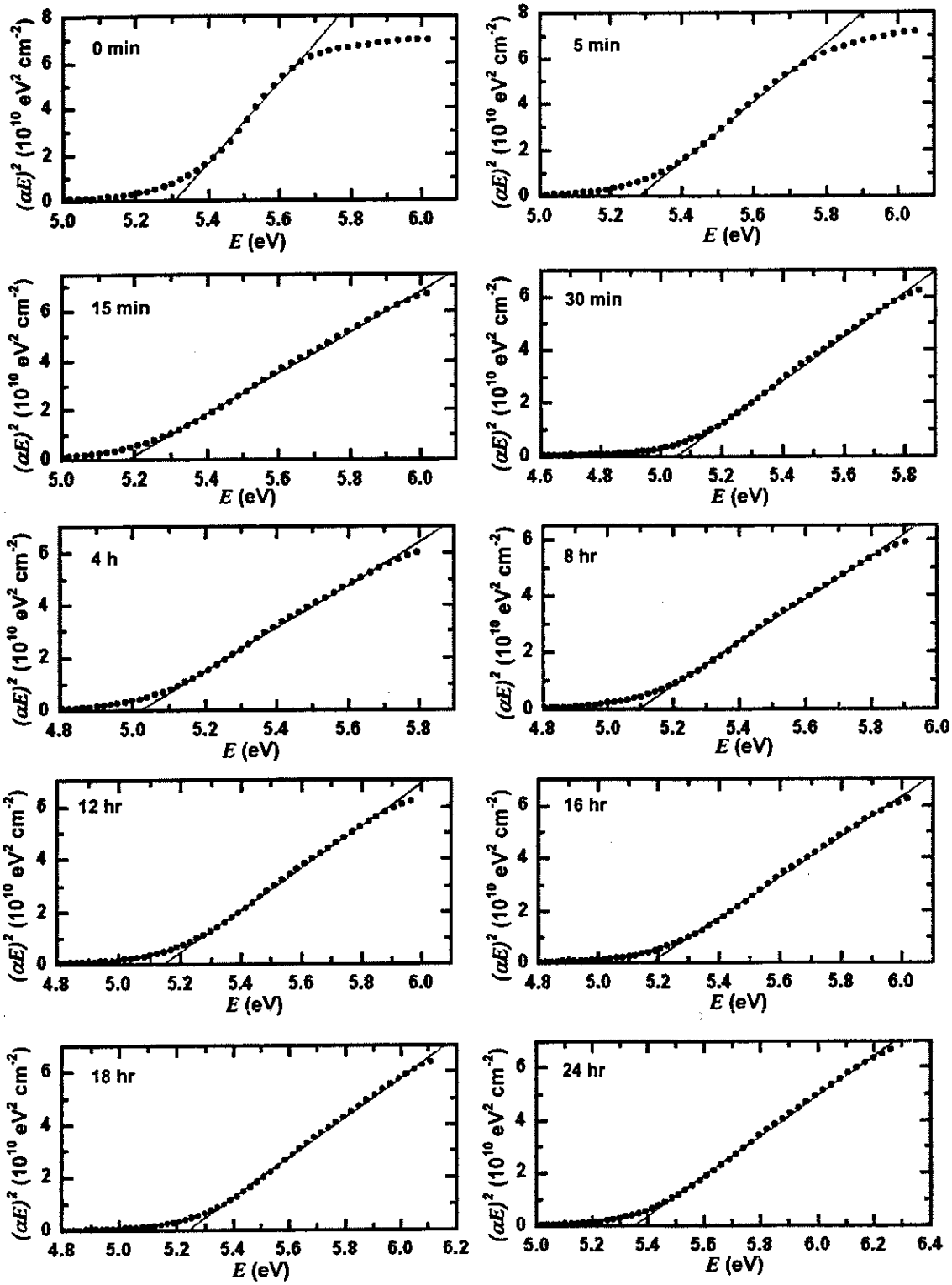

Fig.(4.1.24): The dependence of $(\alpha E)^2$ on photon energy (E) for (PMMA/100 ppm MACROLEX Fluorescent Red G) film at different periods of exposure to artificial sunlight from Xenon arc lamp.

Table(4.1.3): The optical parameters (E_{opt} and E_U) for the prepared (PMMA/100 ppm MACROLEX Fluorescent Red G) film exposed to artificial sunlight from Xenon arc lamp for 24 hrs.

Irradiation Time	E_{opt} (eV)	E_U (eV)
0	5.307	0.248
5 min	5.280	0.268
10 min	5.270	0.266
15 min	5.174	0.297
30 min	5.053	0.299
1 hr	5.050	0.299
1.5 hrs	5.050	0.299
2 hrs	5.050	0.299
2.5 hrs	5.050	0.299
3 hrs	5.050	0.299
4 hrs	5.016	0.305
8 hrs	5.097	0.320
12 hrs	5.141	0.336
16 hrs	5.174	0.344
18 hrs	5.239	0.351
24 hrs	5.350	0.356

The calculated values of E_U were calculated as the reciprocal gradient of the obtained straight line, from the relation between $ln\alpha$ versus the photon energy (Fig.4.1.25), and listed in Table (4.1.3). It is clear that the values of E_U are increased by increasing the irradiation time, due to the increase of internal potential fluctuations associated with the structural disorders. It can be stated that, the degradation of this dye introduced a set of localized energy levels that accordingly produced sets of very specific absorption wavelengths [18,19].

4.1.8.2 Photoresponse of the Fluorescence Spectra

The effect of accelerated photoresponse test on the fluorescence spectrum of 100 ppm dye embedded PMMA is illustrated in Fig.(4.1.26.a). It is noticed that the fluorescence intensity of the film is increased by 56.85% accompanied with a considerable blue shift from 623.4 nm to 597 nm in proportion to the irradiation time. This behavior suggests that the dimer molecules were decomposed by photo-irradiation and giving rise to the growth of monomer fluorescence [104]. Fig.(4.1.26.b) shows the dependence of the normalized fluorescence intensity on the time of photoirradiation according to the exponential growth relation,

$$I_t / I_i = A_1 - A_2 \exp(-k_1 t) \qquad (4.1.6)$$

where I_t/I_i represents the ratio of the fluorescence intensity after exposure time t to that before irradiation respectively and k_1 is the rate of the fluorescence intensity growth (monomer) which is found to be of the order of 1.133×10^{-4} sec^{-1}. These results indicate that there is another depressing effect due to the blue shift in the fluorescence wavelength for PMMA film of dimer concentration (100 ppm); pointing to the instability of the dimmer fluorescence properties by exposure to sunlight.

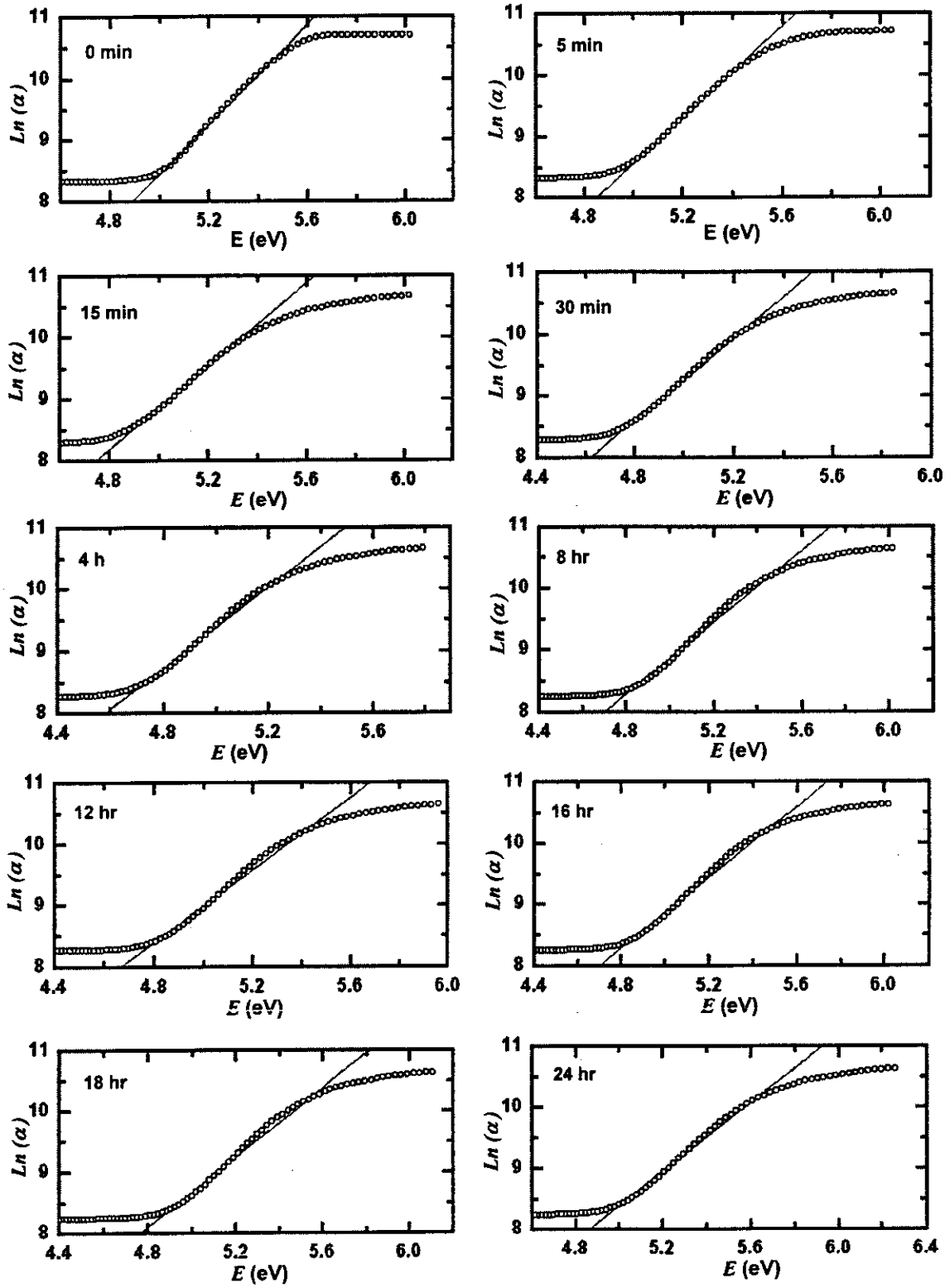

Fig.(4.1.25): The dependence of $ln(\alpha)$ on photon energy (E) for (PMMA/100 ppm MACROLEX Fluorescent Red G) film at different times of exposure to artificial sunlight from Xenon arc lamp.

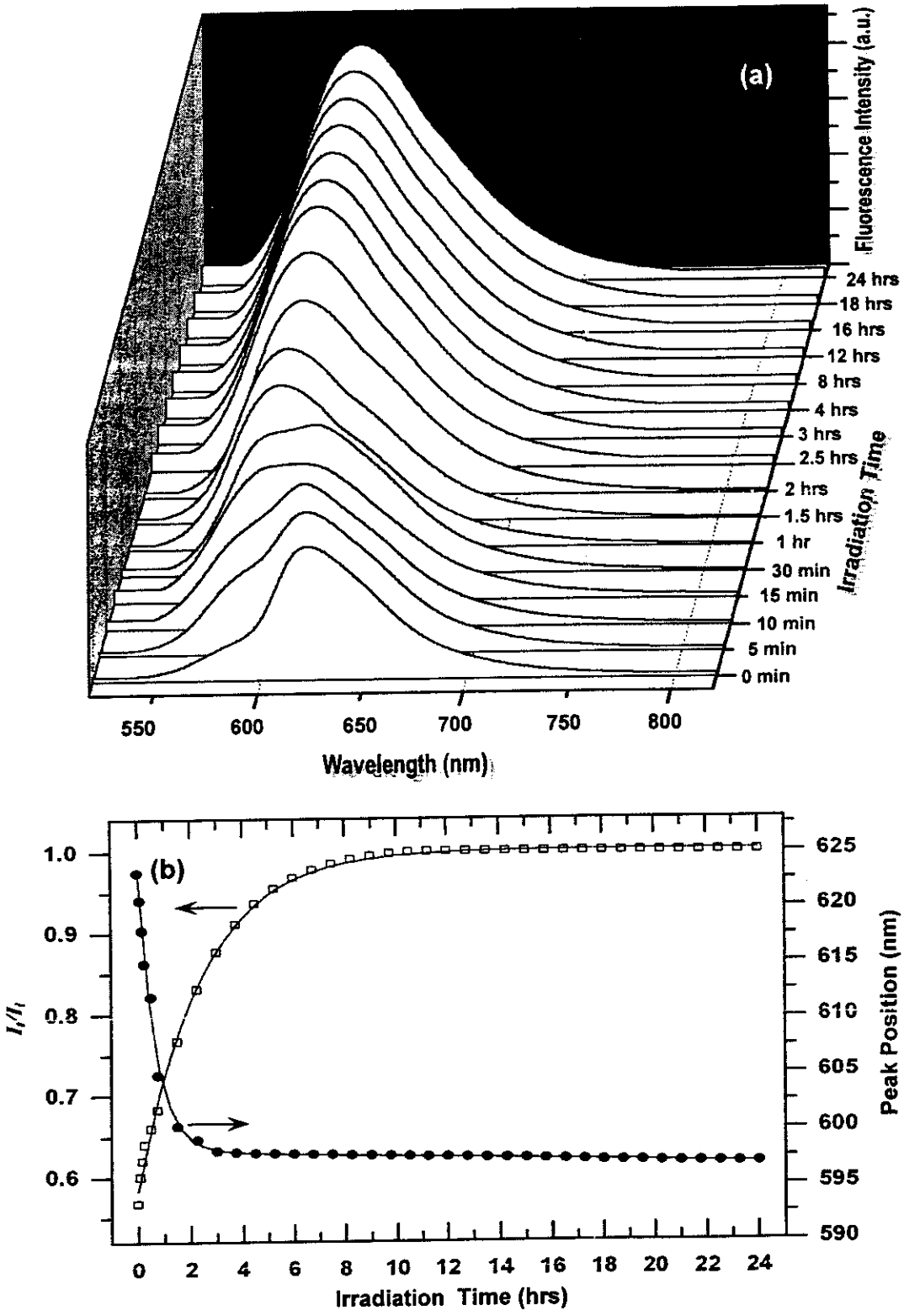

Fig.(4.1.26): (a) The time dependence of the fluorescence spectra of (PMMA/100 ppm MACROLEX Fluorescent Red G) film under photoirradiation with artificial sunlight and (b) the corresponding change in the fluorescence intensity, I_t/I_i and peak position during irradiation period.

4.1.9 Thermal Stability

4.1.9.1 Temperature Effect on the Optical Absorption Spectra

The absorption spectrum of 100 ppm dye doped PMMA film was recorded at different temperatures in the range (273-353 K). The dependence of $(\alpha E)^2$ and/or $\ln\alpha$ on the photon energy E was studied to calculate the values of the corresponding optical energy gap E_{opt} and Urbach's energy E_U, tabulated in Table (4.1.4). The data show that there is no major thermal effect on the dye molecules at temperatures below the glass transition temperature of PMMA matrix, in agreement with our published data[18].

4.1.9.2 Temperature Effect on the Fluorescence Spectra

The temperature effect on the fluorescence spectra of 100 ppm dye doped PMMA film was recorded at different temperatures in the range (273-353 K), the normalized fluorescence intensity against the temperature is plotted in Fig.(4.1.27.a). It is noted that as the temperature increases the fluorescence maximum decreases to 93.35% of its initial value. This can be attributed to the fact that, the increase of the ambient temperature leads to phonon assisted relaxation processes; the electronic excitation energy can be dissipated by the vibrations of the surrounding matrix and the energy levels of the fluorescent species[123]. This energy transfer occurs at a rate, $K_{ET}(T)$, which can be obtained from Fig.(4.1.27.b) using Arrhenius equation [124,125],

$$K_{ET}(T) = K_{ET}(\infty)\, exp(-E_a/RT) \qquad (4.1.7)$$

where E_a is the activation energy of the transfer process, R is the universal gas constant and $K_{ET}(\infty)$ equals to K_{ET} at $T=\infty$. The value of K_{ET} at a given

Table(4.1.4): Temperature effect on the optical parameters (E_{opt} and E_U) for (PMMA/100 ppm MACROLEX Fluorescent Red G) film.

Temperature (K)	E_{opt} (eV)	E_U (eV)
273	5.303	0.247
283	5.302	0.246
293	5.304	0.247
303	5.306	0.248
313	5.307	0.247
323	5.307	0.248
333	5.302	0.245
343	5.304	0.243
353	5.306	0.246

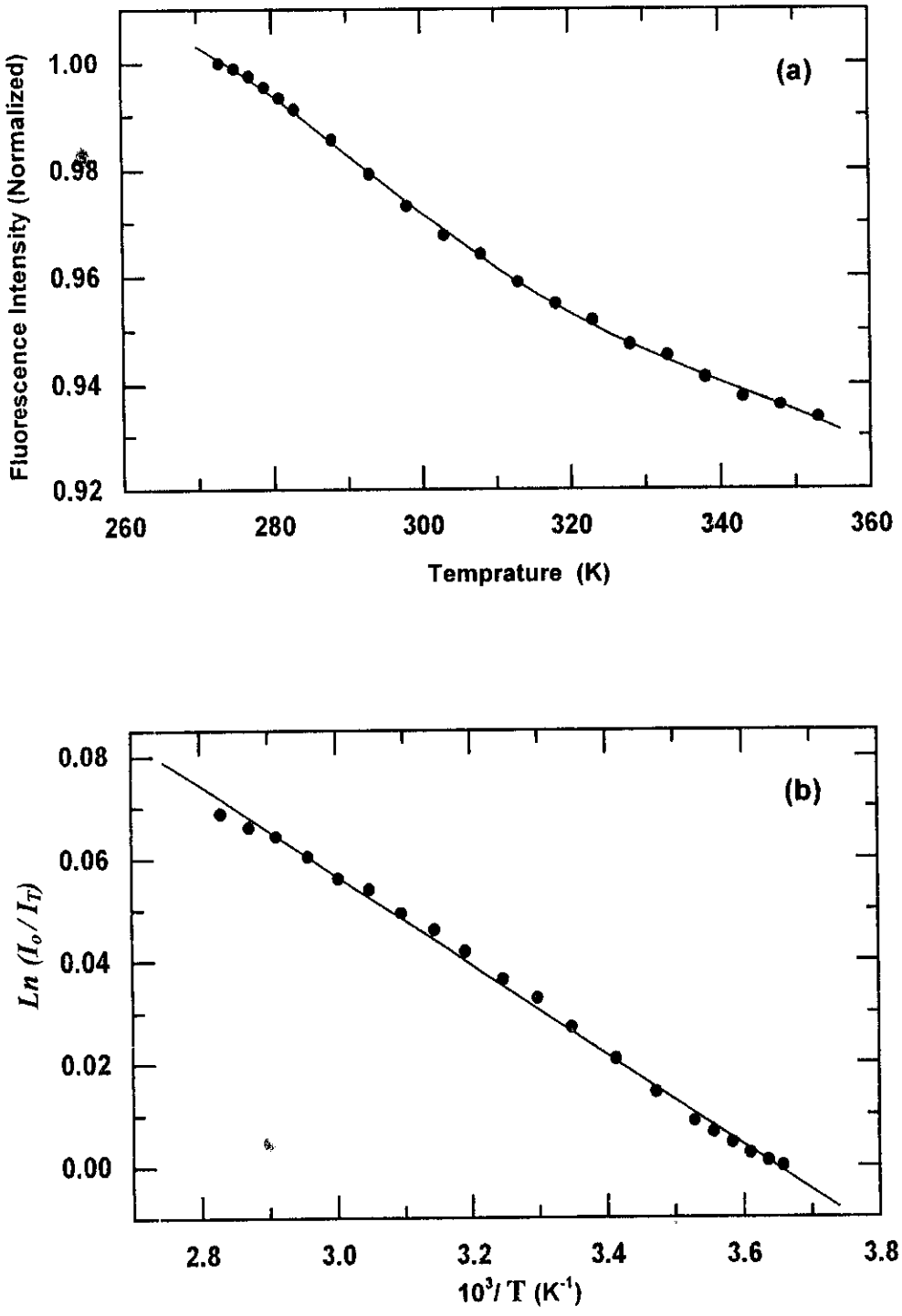

Fig.(4.1.27): (a) Fluorescence intensity as a function of temperature and (b) Semilogarithmic plot of fluorescence relative intensities, ln I_0/I_T vs. $10^3/T$ for PMMA/100 ppm MACROLEX Fluorescent Red G film.

temperature is proportional to the relative fluorescence intensity of the dye molecule (I_o/I_T) where I_o and I_T are the fluorescence intensities at zero and T temperatures respectively. Arrhenius plot of $\ln(I_o/I_T)$ versus. $10^3/T$ gives a reasonably good linear fit and the calculated value of E_a is 0.794 kJ/mol. After cooling the sample to room temperature the fluorescence intensity retained to its initial value; indicating that the dye fluorescence doesn't suffer from thermal degradation in the range of ambient temperatures (0-80 °C).

4.1.10 Optical Efficiency

The impact of the above spectroscopic features on the performance of the 100 ppm dye embedded PMMA film was found by calculating the value of the optical efficiency η_{opt}; which is defined as the energy coming out from the plate edges to the energy falling on the plate surface. The value of η_{opt} can be obtained from the spectroscopic efficiency parameters by applying Eq.(2.31) [33, 55],

$$\eta_{opt} = (1-R_f)\ \eta_{abs}\ \eta_F\ \eta_{trap}\ \eta_{stok}\ \eta_{self}\ \eta_{mat}\ \eta_{TIR}\ \eta_{lat}$$

where η_{lat} is the efficiency of the Lateral reflections which depend on the geometry of the polygon considered. The associated partial yield η_{lat} can be defined from Eq.(2.45) [55],

$$\eta_{lat} = r^{x}$$

where r is the reflection coefficient of the edges and X = 1.5 for rectangular geometry[54, 55], η_{lat}= 97%. The calculated value of η_{opt} was 4.43%, which is very low due to the originated dramatic losses in the values of η_F, η_{stok} and η_{self} as a result of the dimerization of fluorescent dye molecules.

4.1.11 Section Summary

This section outlined that there is no molecular interaction between the vibrational energy states of PMMA and the investigated dye molecules; indicating that the dye molecules are just physically entrapped in the core of the three-dimensional space network of PMMA. The photophysical properties of (PMMA/ MACROLEX Fluorescent Red G) films showed the maximum conversion efficiency (η_{conv}=23.36%) for the film of dye concentration 50 ppm; this value was a result of only a small absorbed fraction of the incident solar photons (η_{abs}=35.43%). By increasing the dye concentration to 100 ppm the value of η_{abs} showed a remarkable increase to 55.23% with a large depressing effect on the conversion efficiency (η_{conv}=9.52%). This effect was explained on the basis of fluorescence quenching due to the non-radiative energy transfer to the dye dimers and self-absorption of the fluorescent light by the dye molecules itself. On the other hand, the highest trapping efficiency (η_{trap}= 78.79%) and the total internal reflection efficiency (η_{TIR}= 96.64%) were obtained for the film of the highest dye concentration (100 ppm). All of the above considerations showed that increasing the dye concentration up to 100 ppm caused a large negative effect on the optical efficiency value (η_{trap}) ; which was found to be of the order 4.43%. More to the point, the increasing of dye concentration did not add any improvement in the photostability of the film, (Fig.(4.1.23-26)). From the prior discussion we can infer that, although PMMA bears excellent optical properties as a matrix of organic fluorescent dyes, it has a limitation to increase the dye concentration due to the formation of excited state dimers (excimers) which are weakly fluorescent. To overcome these entire problems, PMMA matrix had to be modified by an inorganic material to provide an extra efficient host for higher concentrations of organic fluorescent dyes[16,126].

Section 2

Photophysical Properties of PMMA/SiO_2 hybrids

Transparent organic-inorganic hybrid thick films based on PMMA entrapped different concentrations (0.1, 0.2, ... 0.5 wt%) of hydrophilic nanosilica (SiO_2 nanoparticles) were prepared. Such composites are used as host media in optical applications such as lasers, optics, sensors and nonlinear optical applications [15,37]. Spectroscopic tools were applied in order to determine the optimum SiO_2 concentration corresponding to the best optical properties for a matrix used for organic fluorescent dyes.

4.2.1 FT-IR Spectral Characterization

FT-IR transmission spectra were studied in order to exemplify some information about the interactions between the vibrational energy states of the molecules of both PMMA and hydrophilic SiO_2 nanoparticles. Fig.(4.2.1) shows the FT-IR transmission spectra for of PMMA and PMMA/0.1wt% SiO_2 films in the wavenumber range (4000-400 cm^{-1}); as a representative diagram. The disappearance of the C=C stretching mode (1650-1610 cm^{-1}) characterizing MMA, pointing to the complete polymerization of monomer for the hybrid film. This indicates that the polymerization of MMA is not decelerated by introducing the inorganic phase. The comparison between the two spectra shows that the most interesting feature is the shape and position of ester carbonyl groups (C=O stretching mode) expanded in the band (1800-1500 cm^{-1}), Fig.(4.2.2). It is observed that although the vibrational peaks of C=O stretching mode have the same position (1728 cm^{-1}); the band width (FWHM) is reduced from 50 cm^{-1} for PMMA to 43 cm^{-1} for PMMA/SiO_2. The band narrowing accompanied with the weakness of the intensity of the

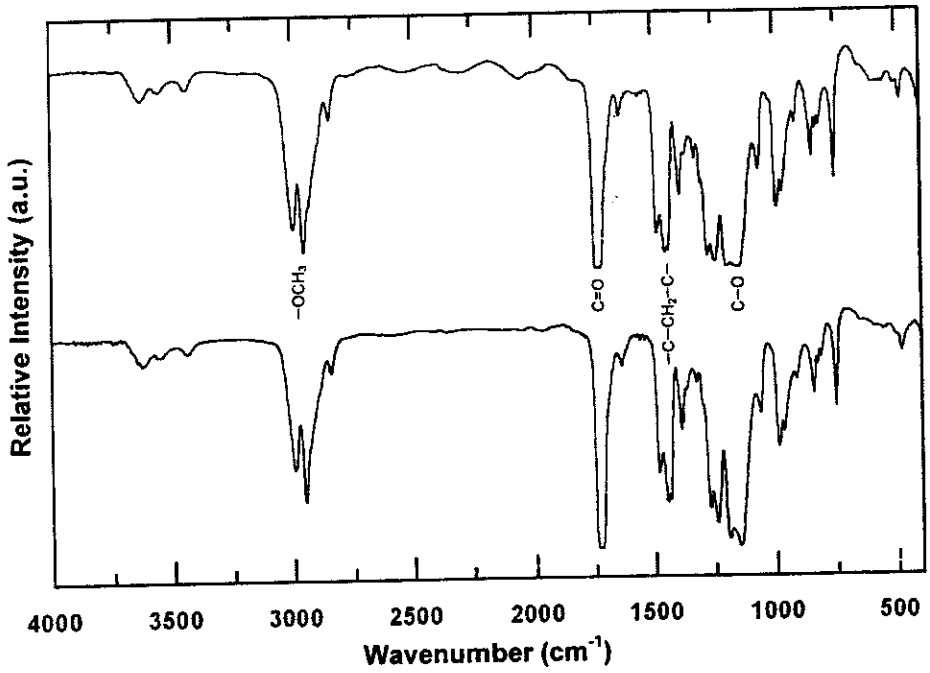

Fig.(4.2.1): FT-IR transmission spectra of (a) PMMA and (b) PMMA/0.1 wt% SiO_2 films; the main characteristic groups are depicted on the spectra.

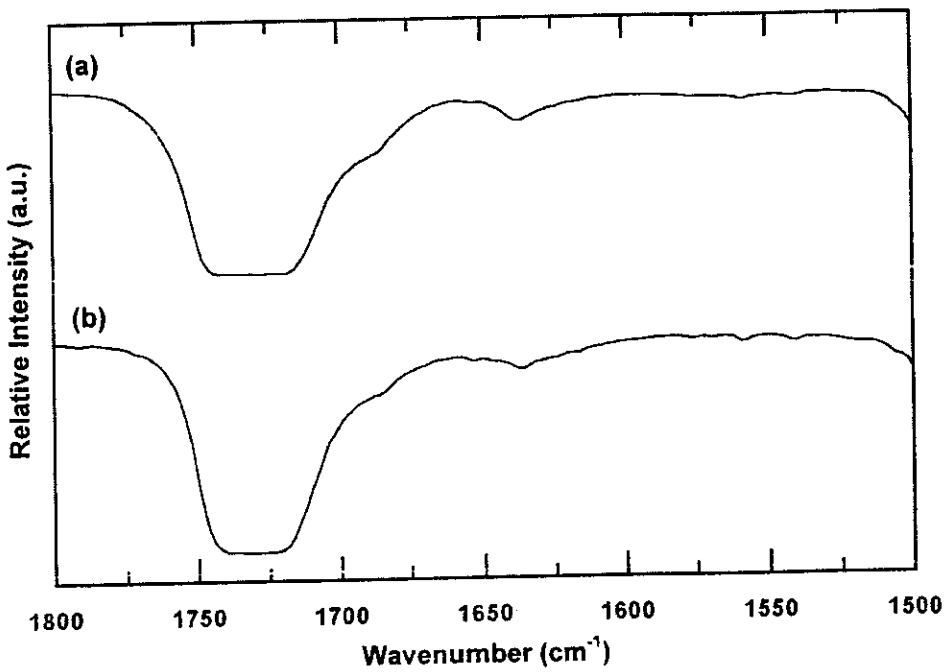

Fig.(4.2.2): Expanded FT-IR transmission spectra in the range (1800-1500 cm^{-1}) (a) PMMA and (b) (b) PMMA/0.1 wt% SiO_2 films.

shoulder appeared at 1685 cm^{-1} for pure PMMA; is attributable to the ester carbonyl groups which are hydrogen-bonded to surface silanol groups (Si—OH) [127]. This can be explained by the acidic feature Si—OH group and the strong amphoteric character of C=O group which acts as a basic site or proton acceptor. The presence of the 1728 cm^{-1} band in the hybrid film, which is largely attributed to the non-bonded C=O groups, confirms that the majority of them are actually free from hydrogen bonding. The formation of PMMA layer on the surface of hydrophilic nanosilica is schematically shown in Fig.(4.2.3) [127].This proposed molecular interaction is simply an interfacial phenomenon between the organic PMMA and inorganic silica phases; PMMA molecules which are above the bonded layer of the hybrid matrix will behave in a fashion similar to those in pure PMMA matrix. Therefore, both the chemical and physical properties of PMMA should be largely retained in PMMA/SiO_2 hybrids [128].

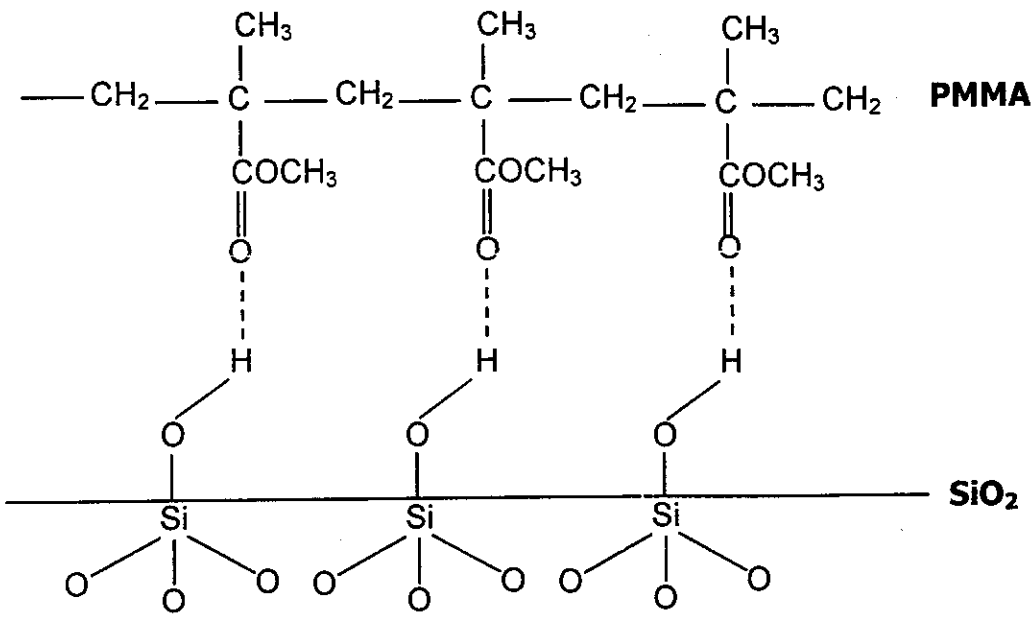

Fig.(4.2.3): Hydrogen bonding between ester carbonyl groups and silanol groups.

4.2.2 Optical Absorption Spectroscopy

The absorption spectra for all the prepared PMMA/SiO_2 hybrid films were recorded in the wavelength range (190-1100 nm) as plotted in Fig.(4.2.4). It is noticed that the absorption band characterizing π-π^* transition in the carbonyl group of PMMA is blue shifted by increasing the concentration of SiO_2 nanoparticles [18]. This can be attributed to the increase of the vibrational modes due to the formation of hydrogen bonding between C=O groups of PMMA and surface Si—OH groups in nanosilica [129].

The attenuation coefficient was calculated according to Eq.(4.1.2) [93],

$$k = \alpha\lambda / 4\pi$$

Fig.(4.2.5) represents the spectral dependence of the attenuation coefficient k for all PMMA/SiO_2 hybrid films calculated as mentioned before. It is clear that k decreases by increasing SiO_2 concentration and tends approximately to zero in the wavelength region beyond 250 nm , this indicates that all the prepared PMMA/SiO_2 hybrid films are transparent to the visible spectra [100].

4.2.3 Interband Transitions

The absorption coefficient α of pure PMMA and different doping levels of SiO_2 nanoparticles was calculated at different values of wavelength. The optical band gap E_{opt} was determined from the analysis of the spectral dependence of the absorption coefficient near the absorption edge. In the range $1 \leq \alpha \leq 10^4$ cm^{-1}, the absorption coefficient for a simple parabolic band can be expressed by Eq.(2.9) [93],

$$\alpha E = M (E - E_{opt})^{m}$$

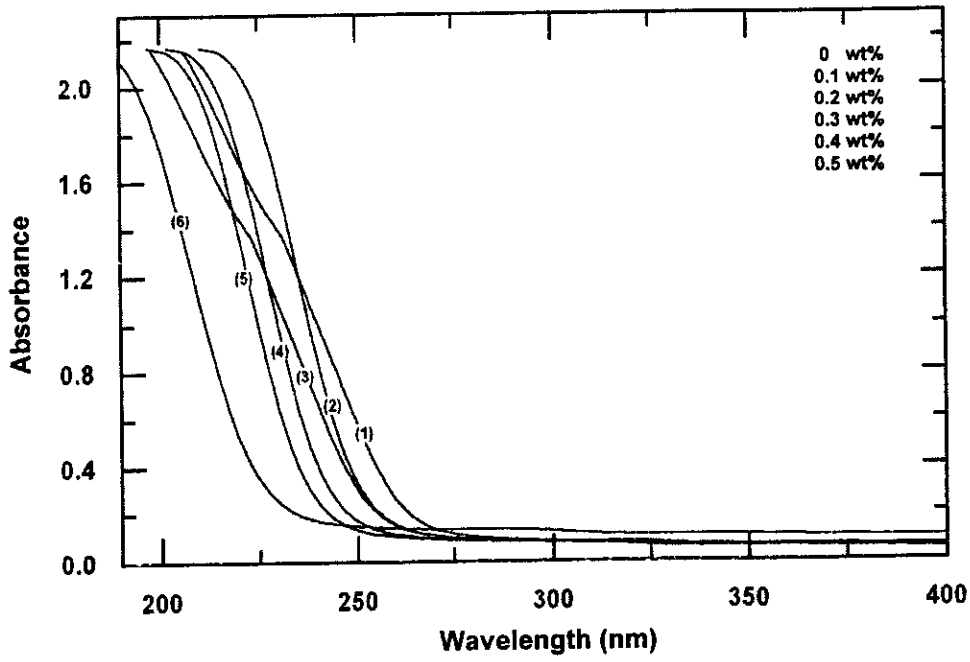

Fig.(4.2.4): The effect of SiO_2 nanoparticle concentration on the absorption spectra of PMMA/SiO_2 hybrid films.

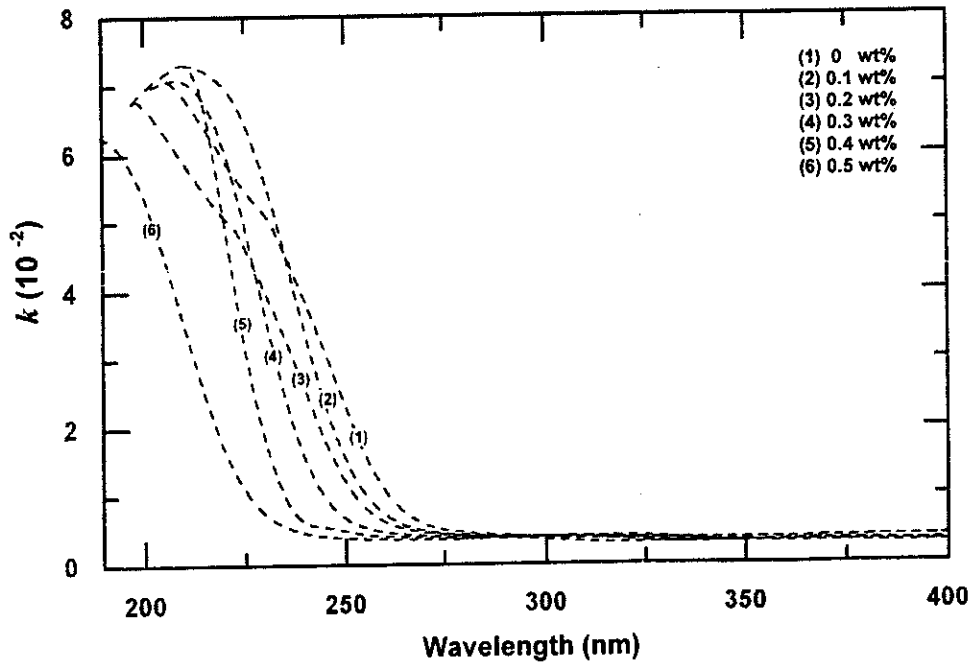

Fig.(4.2.5): The effect of SiO_2 nanoparticle concentration on the attenuation coefficient , k , of PMMA/ SiO_2 hybrid films.

Plots of $(\alpha E)^2$ versus E near the absorption edge for PMMA and PMMA-SiO_2 films showed a linear fit over a wide range of photon energy as shown in Fig.(4.2.6). This linearity indicates the existence of direct allowed transitions in the studied systems, the extrapolation of this linear dependence to the abscissa yields the corresponding values of E_{opt} tabulated in Table (4.2.1). The variation of E_{opt} by increasing nanosilica concentration reflects the role of SiO_2 in modifying the electronic structure of the PMMA matrix. This considerable variation can be attributed to the appearance of different polaronic and defect levels in the band structure of PMMA. The density of states, N(E), was found to be proportional to the concentration of these defects and consequently to SiO_2 content [96,116].

The Urbach's tail which is directly related to the exponential tail for the density of states of the band edge, can be calculated from Eq.(2.8) [101],

$$\alpha(\nu) = \alpha_o \exp(E/E_U)$$

The values of E_U were calculated as the reciprocal slope of the obtained straight line from the relation between $\ln\alpha$ versus the photon energy (Fig.4.2.7), and listed in Table (4.2.1). It is observed that the value of E_U for pure PMMA film is less than those for hybrid PMMA-SiO_2 films, confirming the increase of defect levels in the allowed band gap.

The dramatic increase of both E_{opt} and E_U by increasing nanosilica content can be explained on the following facts. When a sufficient amount of SiO_2 is dispersed in a system at rest, it can form a silica network due to hydrogen bonding as shown in Fig.(3.2). This exceptional ability of nanosilica to provide rheology control in various systems, depends largely on nanosilica concentration which affects the tendency of its aggregates to link together producing thixotropic behavior [130].

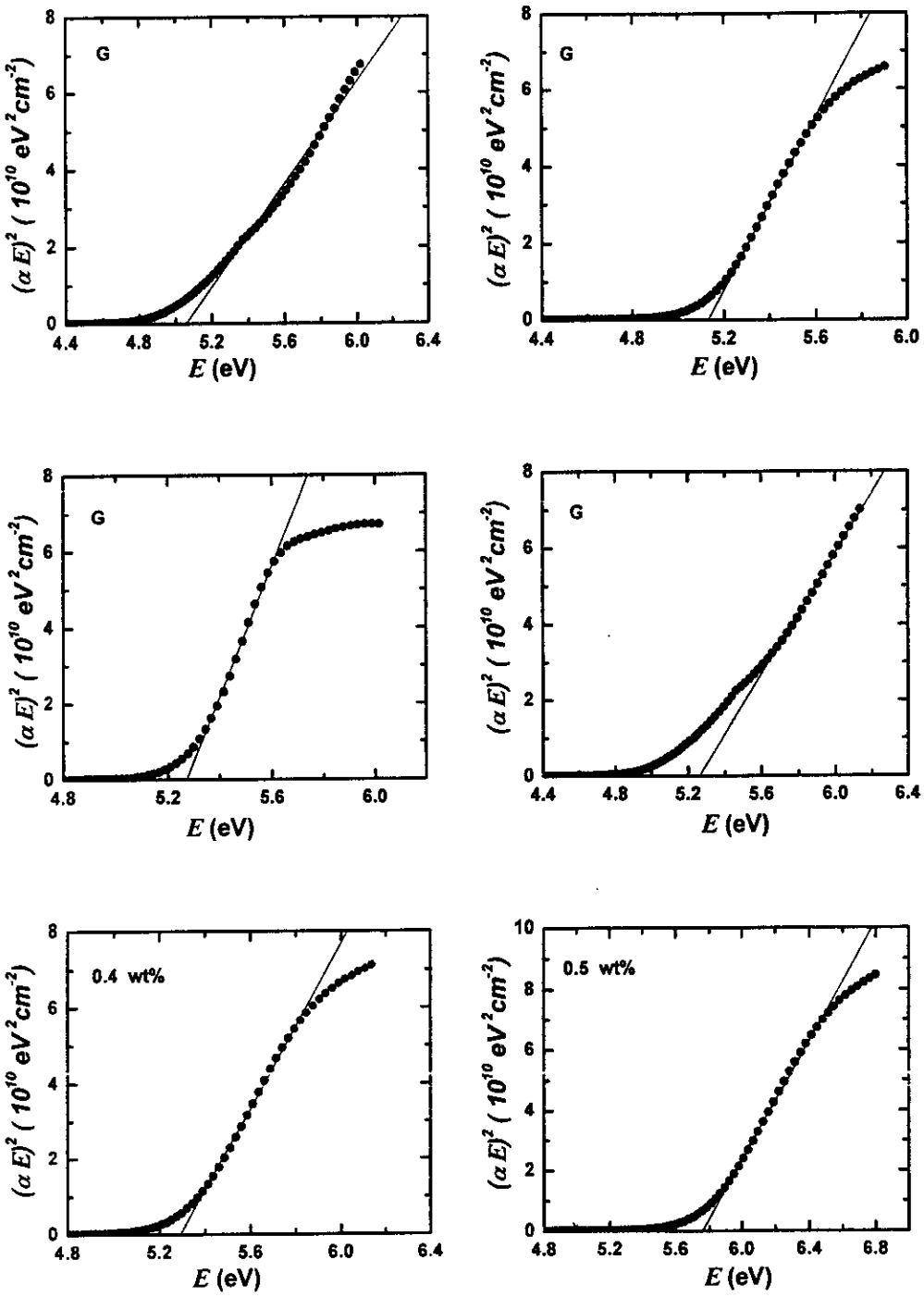

Fig.(4.2.6): The dependence of $(\alpha E)^2$ on photon energy (E) for the prepared (PMMA/SiO_2) films.

Table (4.2.1): The effect of concentration on the optical band gap E_{opt}, and the tail width E_U for the (PMMA/SiO_2) films.

Concentration (wt%)	E_{opt} (eV)	E_U (eV)
0	5.005	0.199
0.1	5.130	0.221
0.2	5.271	0.214
0.3	5.259	0.254
0.4	5.293	0.276
0.5	5.760	0.313

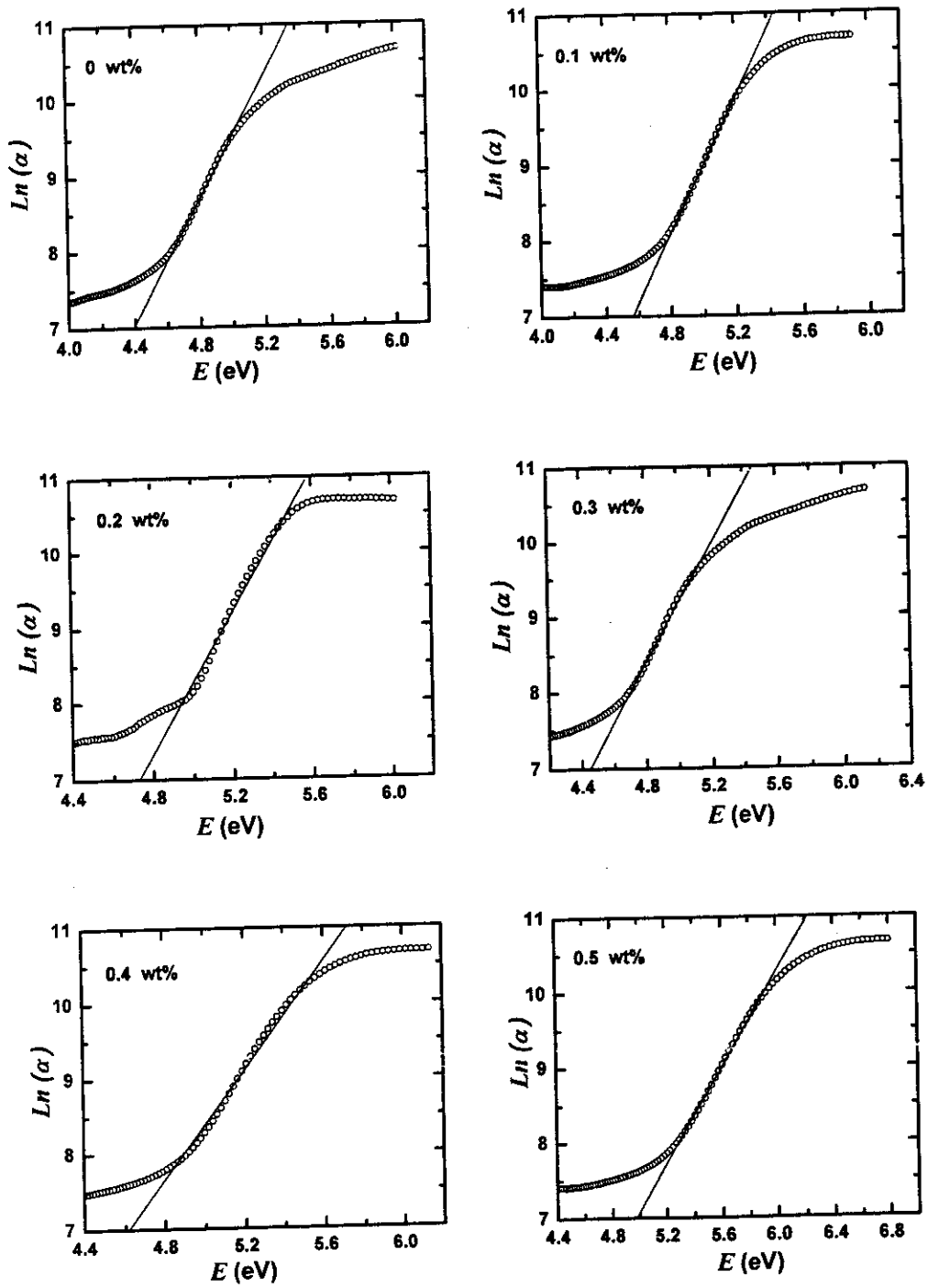

Fig.(4.2.7): The dependence of $ln(\alpha)$ on the photon energy (E) for the investigated ($PMMA/SiO_2$) films.

In our case a small concentration of nanosilica is inserted in the PMMA syrup, so the polar end of C=O groups of PMMA is adsorbed on the surface of Si—OH groups of nanosilica through hydrogen bonding (Fig.(4.2.3)). This bond prevents the formation of nanosilica network in the same manner as the chain terminating substance operates in a polymerization reaction. Accordingly, the viscosity of PMMA/ SiO_2 system is lowered and causes large deformations of the viscoelastic state permitted by PMMA segmental motions[131]. In other words electron phonon coupling become more pronounced and caused the charge carrier scattering which raises the energy required for the electronic transition (increase E_{opt}) [20].

4.2.4 Refractive Index and Guiding Properties

The spectral dependence of the specular reflection spectra for all PMMA/SiO_2 hybrid films are shown in Fig.(4.2.8), in the wavelength range (300-1100 nm). All the curves show that there are no minima due to the absorption of the visible wavelength, pointing to the fact that all of PMMA/SiO_2 hybrid films are colorless [104].

Since the films lied in the transparent range according to the calculated values of attenuation coefficient k, the refractive index n can be calculated by using Equation (2.36) [55,100],

$$R_f = (n-1)^2 / (n+1)^2$$

Fig.(4.2.9) shows the spectral dependence of the refractive index n for all PMMA/SiO_2 hybrid films in the wavelength range 300-1100 nm. It is obviously noted that the values of n are increased by increasing the SiO_2 concentration and showed that the maximum values lie around ≈420 nm. For wavelengths larger than 420 nm the refractive index showed normal dispersion behavior according to Cauchy's formula Eq.(4.1.3) [117-119].

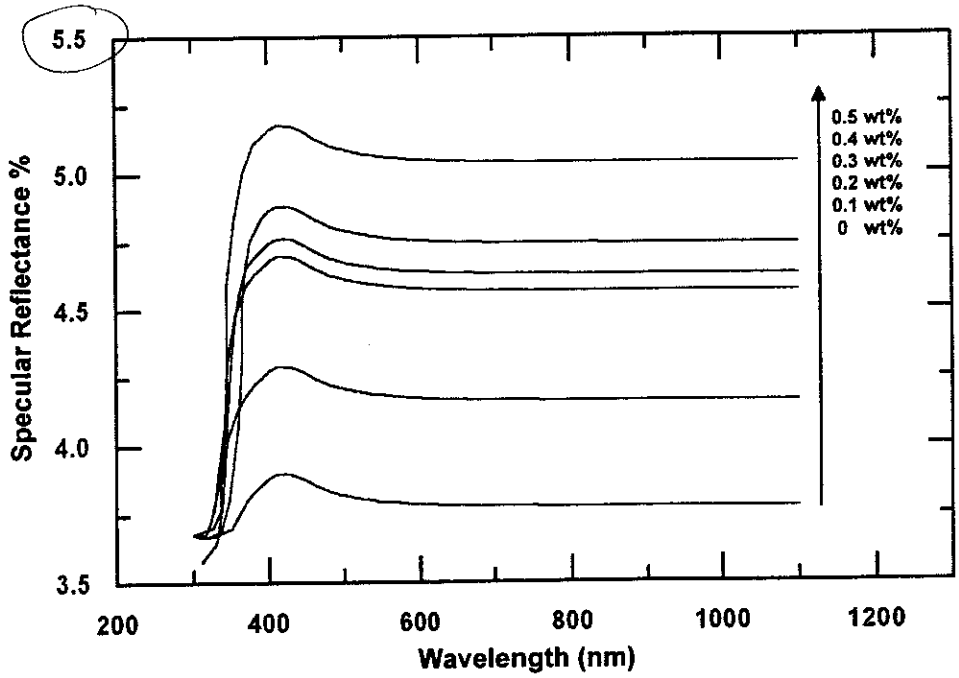

Fig.(4.2.8): Specular Reflection spectra for PMMA/SiO_2 hybrid films.

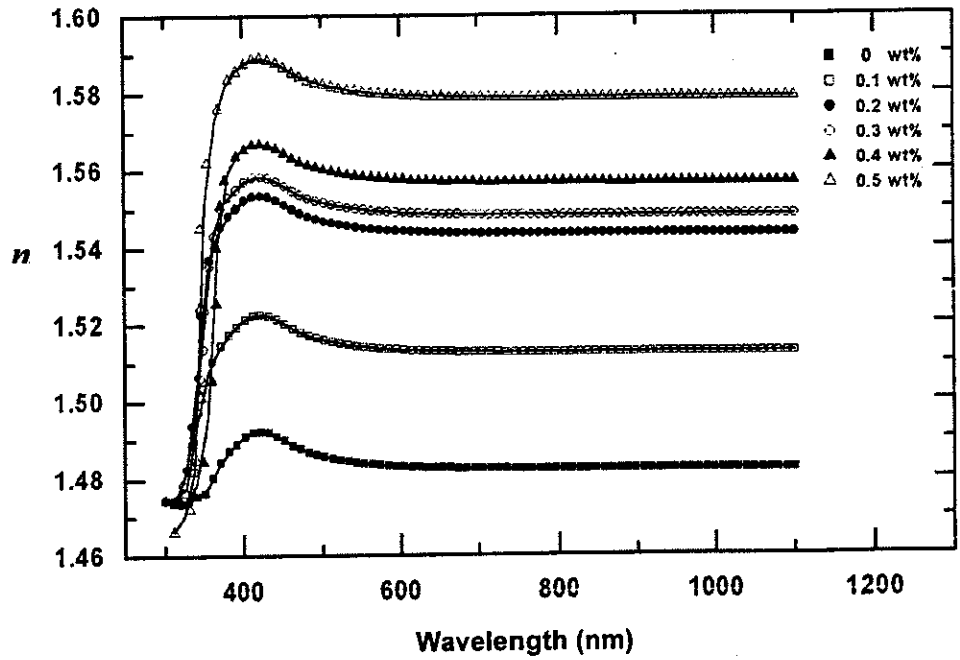

Fig.(4.2.9): The spectral dependence of the refractive index, n, for all PMMA/SiO_2 hybrid films.

It is also noted that the refractive indices of the hybrid PMMA/SiO_2 films are higher than those of the parent materials (n=1.49 for PMMA and 1.46 for SiO_2). This increase can be explained on the basis of Lorentz-Lorentz equation [120,121], since the incorporation of hydrophilic SiO_2 nanoparticles enlarged the number of atomic refractions due to the increase of the mean molecular polarizability.

Fig.(4.2.10) shows the dependence of the trapping efficiency η_{trap} on the concentration of SiO_2 nanoparticles, which reveals that the hybrid PMMA-SiO_2 tolerates the trapping of a larger fraction of photons and consequently improves the guiding properties [54,55].

4.2.5 Transmission Spectroscopy

The transmission spectra for all PMMA/SiO_2 hybrid films were recorded in the wavelength range (190-1100 nm), see Fig.(4.2.11). Despite the fact that all the films are transparent to human eye, their transmittance decreased by increasing the concentration of SiO_2 nanoparticles from 94% for PMMA to ~ 82% for PMMA/ 0.5 wt% SiO_2. This decrease can be attributed to the light scattering resulting from the aggregation of SiO_2 nanoparticles by increasing concentration [132].

4.2.6 Section Summary

This section outlined that the molecular interaction in the prepared PMMA/SiO_2 hybrids occurs only at the boundary of the two phases via hydrogen bonding between ester carbonyl and silanol groups[127]. Consequently, the bulk properties of each phase are largely retained leading to enhanced optical properties of a totally different material [16]. The optical properties of hybrid (PMMA/ SiO_2) films showed the increase of the UV transparency of the films by increasing SiO_2 concentration.

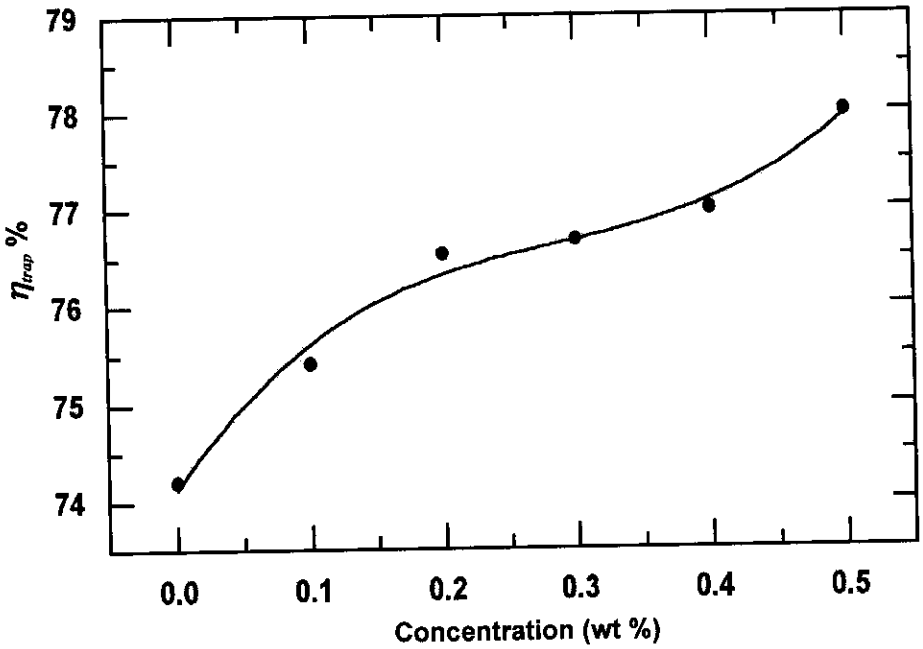

Fig.(4.2.10): Effect of SiO_2 nanoparticle concentration on the trapping efficiency, η_{trap}, for all PMMA/SiO_2 hybrid films.

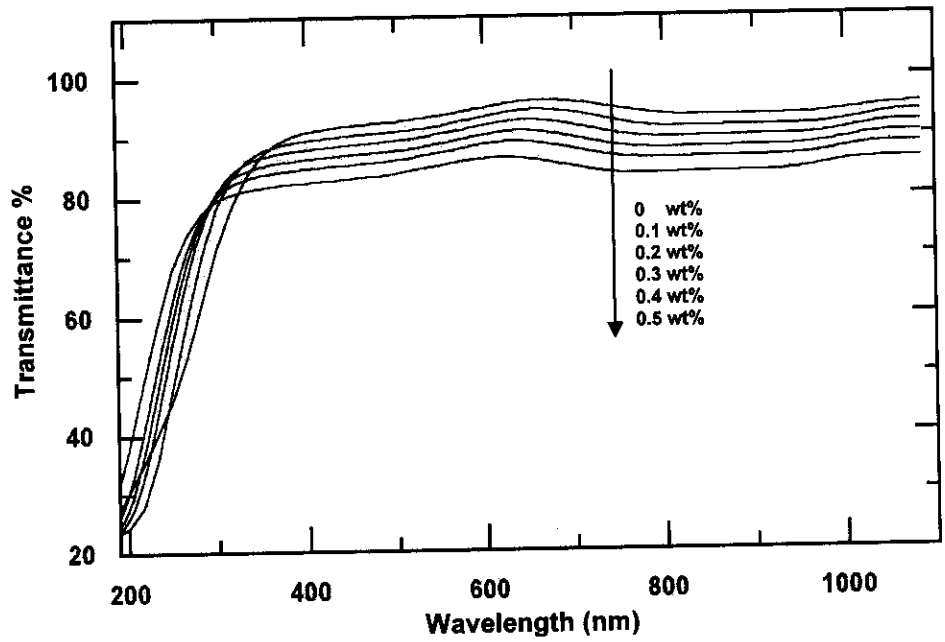

Fig.(4.2.11): Effect of SiO_2 nanoparticle concentration on the transmission spectra for all PMMA/ SiO_2 hybrid films.

Furthermore, the trapping efficiency (η_{trap}) was enhanced from 74.22% for PMMA to 77.70% for the film of 0.5 wt% SiO_2 concentration. All of these features were accompanied with a decrease in the film transmittance which decreased from 94% for PMMA to about ≈82% for PMMA/ SiO_2 hybrid film. Therefore, the hybrid matrix of 0.1 wt% SiO_2 concentration should be chosen to be the matrix for the dye under study due to its relatively high transmittance (92%) extended to a wider range of the near-UV radiation in comparison with PMMA. Meanwhile, it has also a relatively higher refractive index (1.523) compared to PMMA (1.492) and SiO_2 (1.46); leading to an improvement of the value of η_{trap} enlarged to 75.40%. Further more, this hybrid film has a large value of the optical band gap (5.005 eV) compared to that of PMMA film (5.130 eV). This property is advantageous, since it is desirable to choose FSC matrices which have large band gap compared to the absorption edge of the fluorescent dye[18,80]. To realize the choice of a suitable hybrid matrix for the investigated dye; the effect of the hybrid PMMA-SiO_2 hybrid matrix on the dimerization of dye molecules and the photophysical processes will be studied. It will also be advantageous to incorporate such matrix with very high dye concentrations, especially in our study, the dye owes a coumarin molecule which has the ability to be adsorbed on the hydrophilic SiO_2 nanoparticles by hydrogen bonding to surface silanol groups.

Section 3

Tailoring of efficiently fluorescent PMMA/SiO_2 Hybrids for solar energy conversion

The effect of the incorporation of 0.1 wt% hydrophilic nanosilica in PMMA/ 100 ppm MACROLEX Fluorescent Red G film was studied as a way of solving the problem of the dye dimerization. After that, a series of fluorescent PMMA/SiO_2 hybrid films embedded with different dye concentrations (50....200 ppm); were investigated to reach improved absorption, fluorescence, trapping and guiding efficiencies.

4.3.1 FT-IR Spectral Characterization

FT-IR transmission spectra were studied in order to exemplify some information about the interactions between the vibrational energy states of the molecules of both the dye molecules and hydrophilic SiO_2 nanoparticles in PMMA/SiO_2 hybrid matrix. Fig.(4.3.1) shows FT-IR transmission spectra of PMMA and PMMA/ 0.1 SiO_2 wt% films embedded with 100 ppm MACROLEX Fluorescent Red G dye in the wavenumber range (4000-400 cm^{-1}); the main vibrational characteristic groups are depicted on the spectra. An inspection of the spectra showed the disappearance of C=C stretching mode (1650-1610 cm^{-1}) characterizing MMA, pointing to the complete polymerization of monomer for the two films. Besides, it is noted that the two spectra are not completely identical; for the dye doped hybrid matrix there is a remarkable change of the intensity of the main vibrational bands of PMMA accompanied with an elevation in the base line of the spectrum. The expanded spectrum in the range (1800-1500 cm^{-1}) depicted in Fig.(4.3.2), corroborates that for the dye doped hybrid matrix the stretching mode of C=O appeared is blue

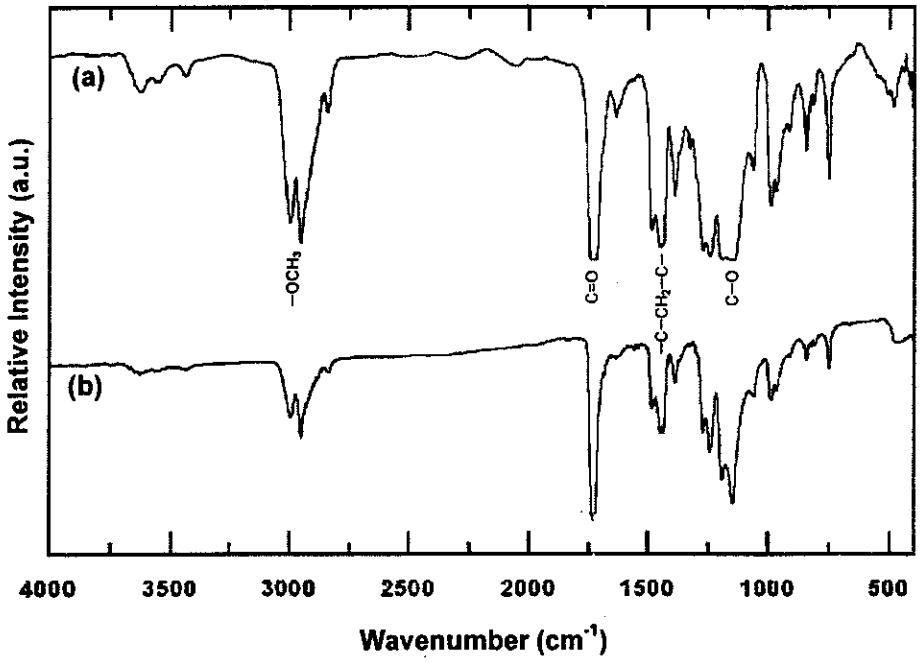

Fig.(4.3.1): FT-IR transmission spectra of (a) PMMA and (b) PMMA/0.1 wt% SiO_2 hybrid embedded with 100 ppm MACROLEX Fluorescent Red G films; the main characteristic groups are depicted on the spectra.

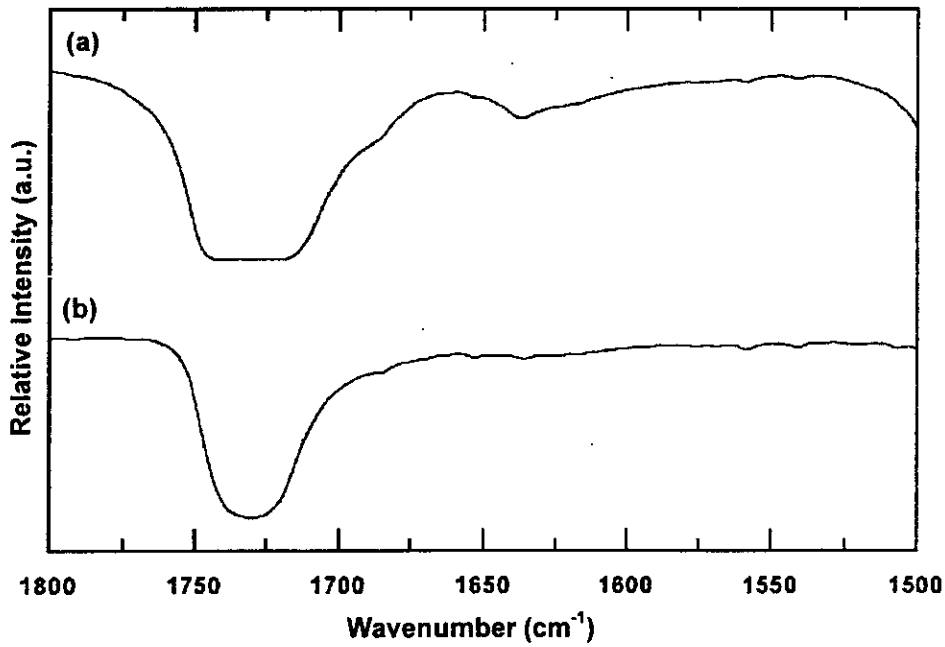

Fig.(4.3.2): Expanded FT-IR transmission spectra in the range (1800-1500 cm^{-1}) (a) PMMA and (b) PMMA/ PMMA/0.1 wt% SiO_2 embedded with 100 ppm MACROLEX Fluorescent Red G film.

shifted to (1730 cm^{-1}) and the band width (FWHM) is reduced from 50 cm^{-1} to 38 cm^{-1}. The complete change of the band shape of carbonyl group accompanied with the weakness of the intensity is attributable to the presence of another molecular interaction due to hydrogen bonding between aromatic carbonyl groups present in coumarin molecule of the dye and the surface silanol groups (Si—OH) of hydrophilic nanosilica. Eventhough the FT-IR bands of silica are very weak compared with the strong bands of PMMA; the effect of silica is more pronounced after doping PMMA with dye. This can be referred to the spectral deformations caused by the presence of siloxane (Si—O—Si 400-1500 cm^{-1}) and silanol (Si—OH 835-955 cm^{-1}) stretching modes on which the bands of PMMA are superimposed [127]. It is implied that the high electronegativity of oxygen atom which present in carbonyl group of coumarin molecule and also the acidic feature of silanol group, progressed the hydrogen bonding between the dye and SiO_2 nanoparticles [133,134]. The bonding of both the chains of PMMA and coumarin molecules of the dye to the surface silanol groups as schematically shown in Fig.(4.3.3).

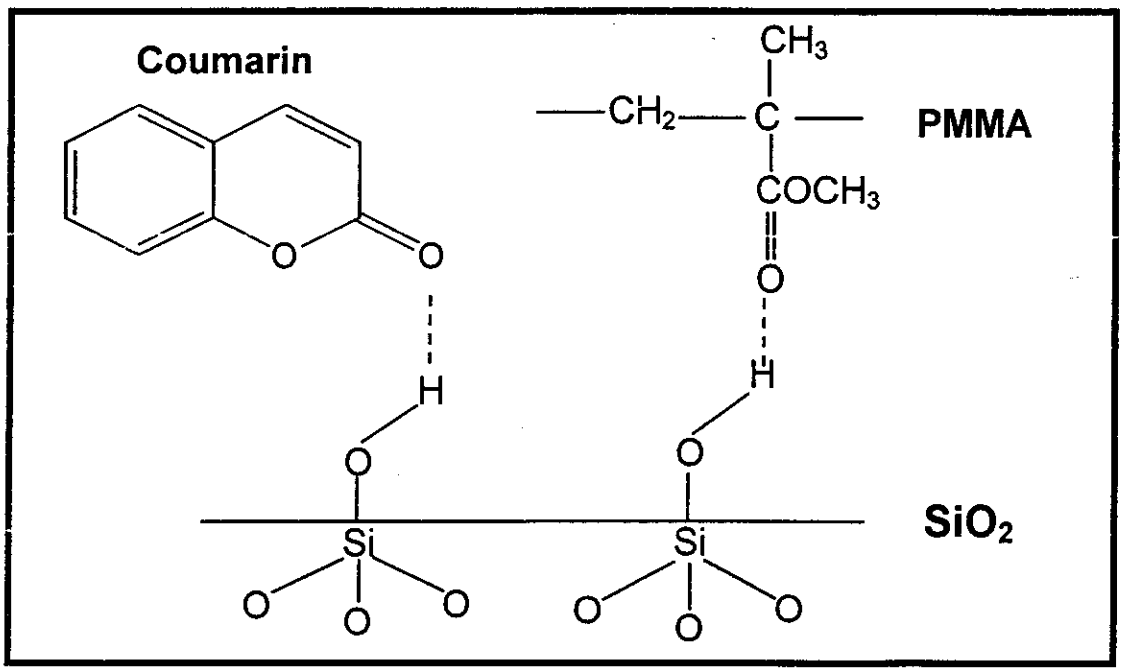

Fig.(4.3.3): Hydrogen bonding between silanol groups and carbonyl groups of PMMA and coumarin molecules.

4.3.2 Incorporation Models of Organic Laser Dyes in PMMA and Hybrid PMMA/SiO_2 Hosts

Based on the abovementioned results, two models for incorporating organic dyes in PMMA and PMMA/SiO_2 matrices are proposed, as depicted in Fig.(4.3.4). Model (a) stands for PMMA matrix with large cores in which the dye molecules are just physically incorporated. At high dye concentrations the dye molecules have a large tendency to be aggregated in these cores, as outlined in section (4.1). On the other hand model (b) demonstrates that the dye molecules are shown to have a relatively uniform dispersion in undersized cores formed by PMMA/SiO_2 cages of the hybrid PMMA/SiO_2 network. In such cores the dye molecules are assumed to be adsorbed on hydrophilic SiO_2 nanoparticles by hydrogen bonding to surface silanol groups. It has to be pointed out that the proposed model in Fig.(4.3.4.b) is just an idealized case, since a patch-like structure[127] of PMMA is likely to be present. Accordingly, there is a probability of the dye dimerization but at relatively higher concentration than 100 ppm [135,136].

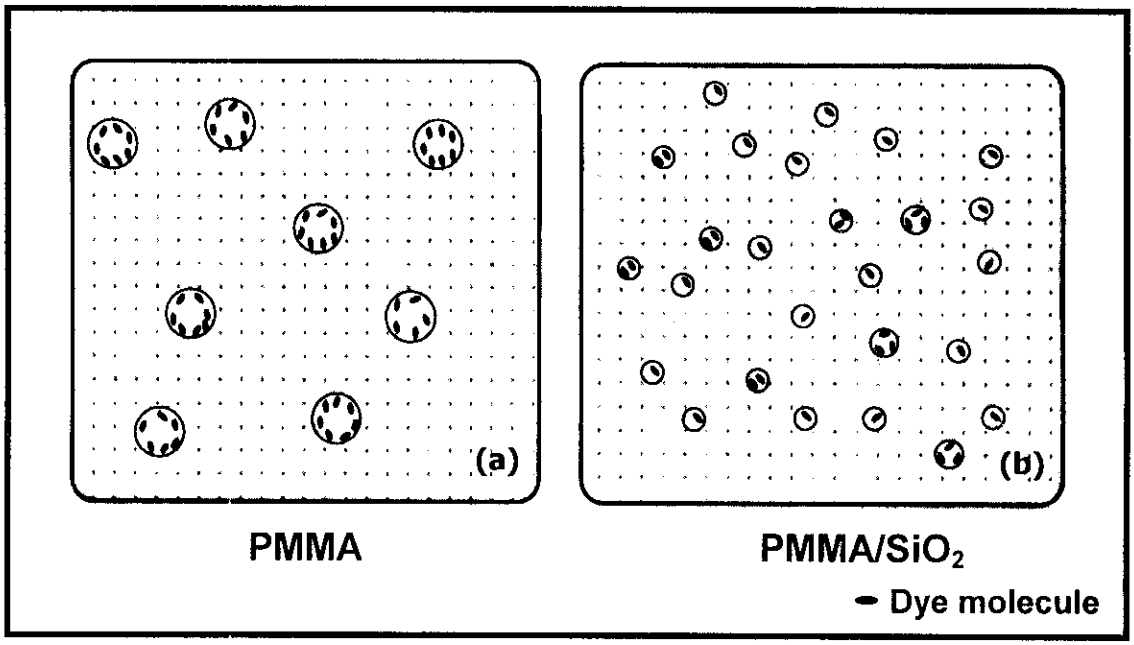

Fig.(4.3.4): The proposed incorporation models of MACROLEX Fluorescent Red G dye in ; (a) PMMA and (b) PMMA/SiO_2 matrices.

4.3.3 Optical Absorption Spectroscopy

The optical absorption spectra for all the prepared fluorescent PMMA/SiO_2 hybrid films were recorded in the wavelength range (190-1100 nm) and plotted in Fig.(4.3.5), it is noted that the spectra resembles that depicted in Fig.(4.1.3). Two major bands are observed, the first one lies in the UV region around ≈214 nm characterizing π-π^* transition in C=O molecules of PMMA which are free from hydrogen bonding with surface Si—OH groups. The second one appears around ≈520 nm corresponding to the electronic transition to the first excited singlet state ($s_o \rightarrow s_1$) of the dye molecules [18,113]. The increase in the absorbance value by increasing the dye concentration is attributed to the increase of the number of the absorbing species (chromophores) according to Beer's law [90,91] (Eq.2.3).

The absorption efficiency, η_{abs} was calculated for all the fluorescent hybrid PMMA/SiO_2 films from Eq. (2.32) as [55],

$$\eta_{abs} = 1 - 10^{-\alpha d}$$

Fig.(4.3.6) shows that the absorption efficiency η_{abs} increases by increasing the dye concentration and reaches its highest value (63.36 %) for the film of 200 ppm dye concentration. On the other hand, the value of η_{abs} is decreased for the concentrations of 50 and 100 ppm from 35.43 and 55.23 % in PMMA to 29.69 and 45.92% in hybrid PMMA/SiO_2 matrix respectively. This decrease is attributed to the fact that the entrapped dye molecules are isolated in the individual cages of PMMA/SiO_2 network. So there is a great ability to reach unconventional high dye concentrations since the ground state interactions between the dye molecules and the matrix impurities are greatly reduced [13,15].

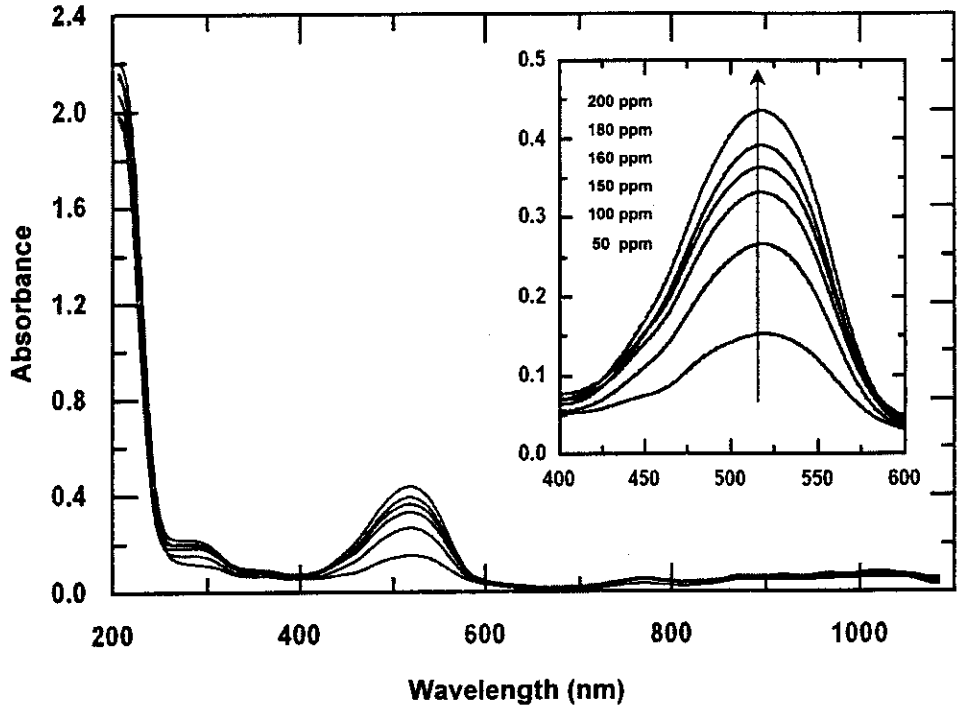

Fig.(4.3.5): The effect of MACROLEX Fluorescent Red G concentration on the absorption spectra of (PMMA-0.1 wt% SiO_2) hybrid films, the bands concerning the dye only are magnified (inset).

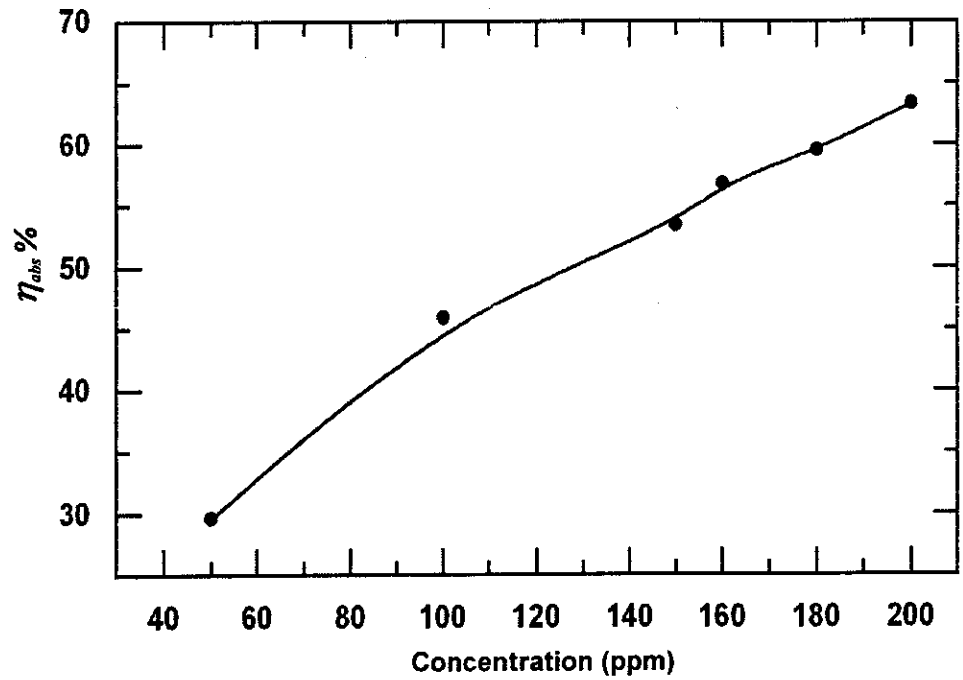

Fig.(4.3.6): The concentration dependence of the absorption efficiency, η_{abs}, for (PMMA-0.1 wt% SiO_2) hybrid / MACROLEX Fluorescent Red G films.

The matrix efficiency η_{mat} for all the fluorescent PMMA/ SiO_2 hybrid films can calculated by applyiing Eq.(2.41) [55],

$$\eta_{mat} = 10^{-\alpha(\lambda_F)\bar{d}}$$

From Fig.(4.3.7), it is clear that the values of η_{mat} are slightly increased by increasing the dye concentration, until reaching a highest value 89.78 % for the hybrid film of concentration 200 ppm. This value indicates low matrix absorption of the fluorescent light [38,40], eventhough this concentration doubles the dimerization concentration of PMMA matrix (section 4.1).

4.3.4 Fluorescence Spectroscopy

The effect of the dye concentration on the fluorescence spectra of the investigated fluorescent hybrid films is illustrated in Fig.(4.3.8); the intensity and position of the fluorescent peaks are plotted against the dye concentration in Fig.(4.3.9). It is observed that there is a remarkable blue shift of the fluorescence maximum accompanied with the intensity increase for 100 ppm dye incorporated PMMA/SiO_2 matrix, than that of the same concentration in PMMA matrix (Fig.(4.1.6)). This can be attributed to the unique PMMA-SiO_2 cage; that the only possible reorientation of the cage walls is the rotation around Si—O—H bonds, i.e., relocation of hydrogen bonding to the dye. Under this restricted cage freedom, the rotational movements allow the stabilization of the dye molecule excited-state by the interactions with the cage [13]. As discussed above, the walls of PMMA/SiO_2 cage are polar than that of PMMA; this allows further corroboration of the remarkable fluorescence blue shift [80,103]. Fig.(4.3.10) illustrates that the excitation and fluorescence spectra for 100 ppm dye incorporated film look like mirror image of each other; confirming that the vibrational states of the electronic transitions occurred in existent chromophores and fluoropores are similar to some extent. So, the excitation and fluorescence spectra of the

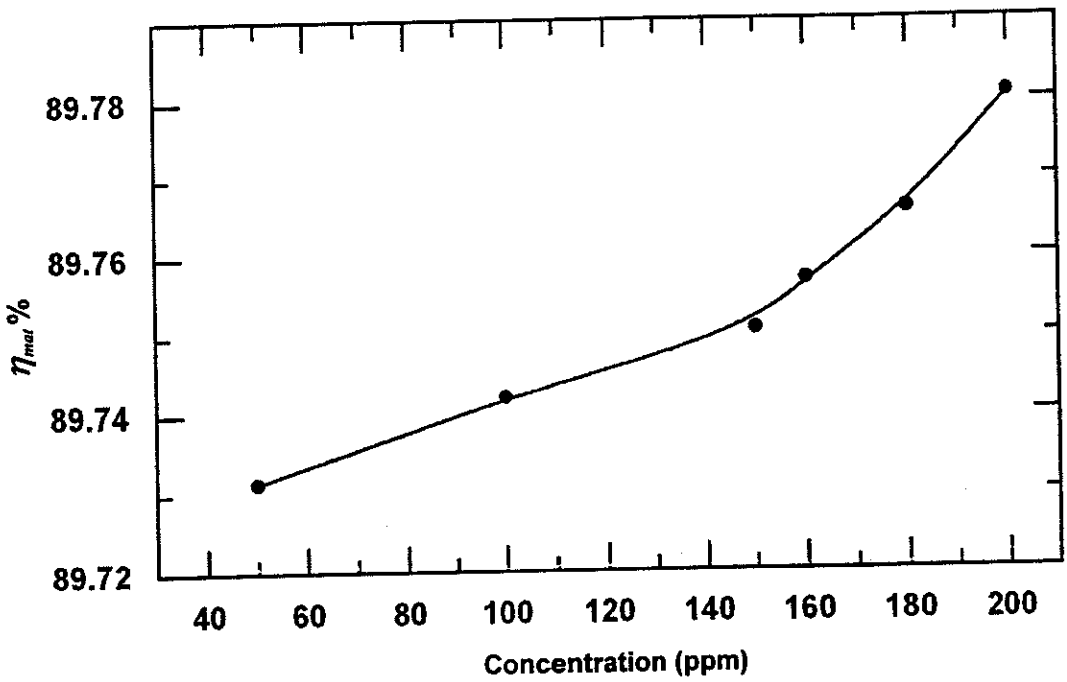

Fig.(4.3.7): Concentration dependence the matrix efficiency, η_{mat} , for (PMMA-0.1 wt% SiO_2) hybrid / MACROLEX Fluorescent Red G films.

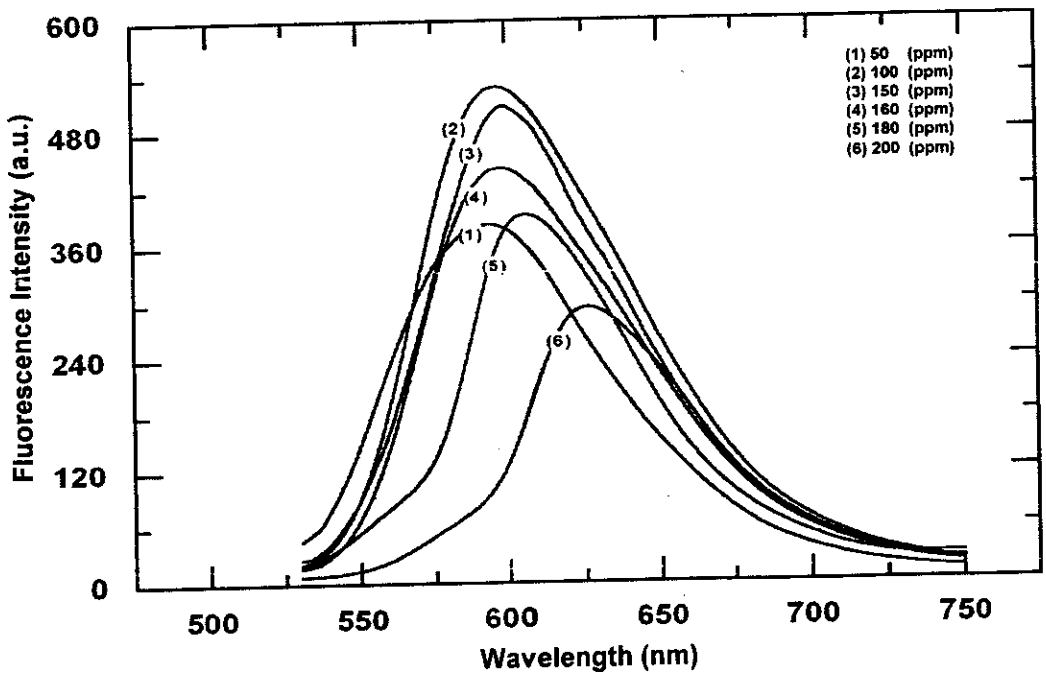

Fig.(4.3.8): Fluorescence spectra of (PMMA-0.1 wt% SiO_2) hybrid / MACROLEX Fluorescent Red G films.

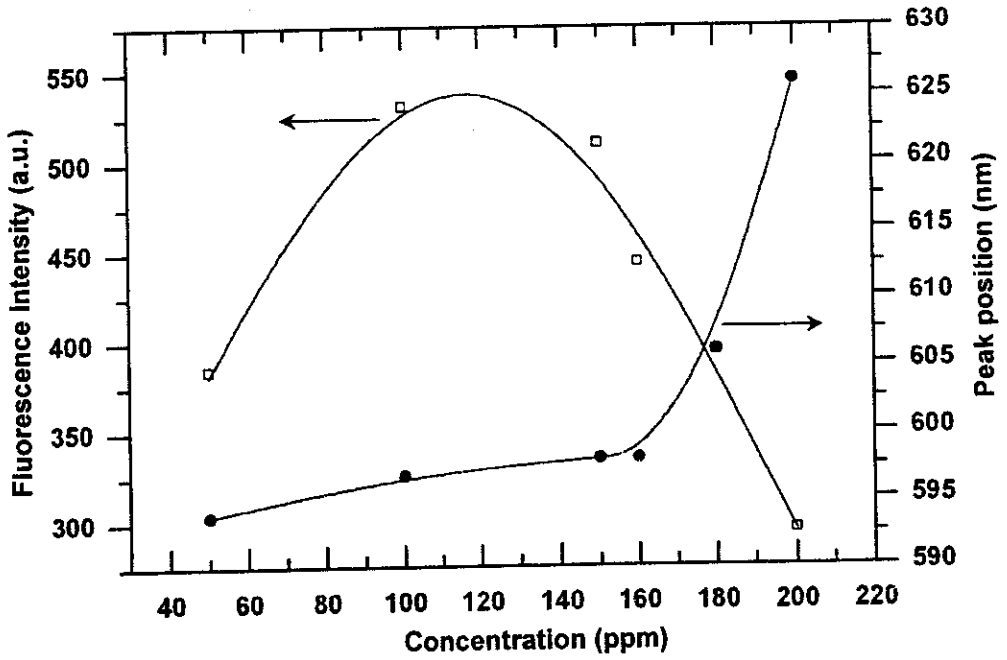

Fig. (4.3.9): The change of the fluorescence intensity and peak position for all the prepared (PMMA-0.1 wt% SiO_2) hybrid/MACROLEX Fluorescent Red G films.

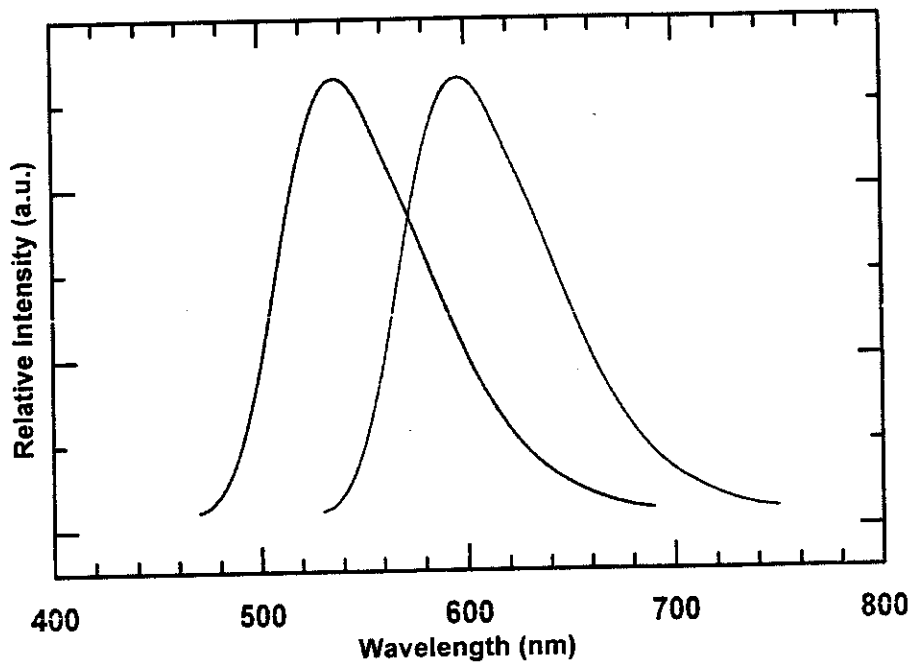

Fig.(4.3.10): Mirror image relationship of excitation (left) and fluorescence (right) spectra for (PMMA-SiO_2) /100 ppm MACROLEX Fluorescent Red G) film.

fluorescent hybrid film proceed similarly in each direction from the wavelength corresponding to the electronic transition[90]. The new distribution of the dye molecules in PMMA/SiO_2 film incorporated with 100 ppm dye concentration can be explicated by the three-dimensional synchronous excitation and fluorescence spectra plotted in Fig.(4.3.11) and the corresponding contour plot is depicted in Fig.(4.3.12). One distinct maximum can be observed at the coordinates (exc., fluo.) = (518, 596.8 nm), which is very close to the excitation and fluorescence of isolated (monomer) dye molecules mentioned in section (4.1). It is also observed that the contour lines become narrower than the case of PMMA matrix; pointing to a more confined distribution of the dye molecules which are anchored on the surface of hydrophilic SiO_2 nanoparticles or in the core formed by PMMA-SiO_2 cage. This suggests that the incorporation of SiO_2 in the fluorescent PMMA film reduced the translational freedom of the dye molecules and subsequently the intermolecular deactivation processes of fluorescence [114]. In addition the solid cage reduces the internal rotational modes of the dye, probably to a greater extent than the relatively flexible organic polymer molecules; since the rotational relaxation of the excited state of organic laser dyes is one of the main modes of the non-radiative energy losses [13]. The achieved enhancement in the fluorescence after incorporating 100 ppm dye molecules in PMMA/SiO_2 hybrid matrix is found to be followed by a staged reduction accompanied with the appearance of a new fluorescence band red shifted to 626 nm for the hybrid film of 200 ppm. This may be attributed to the formation of dye dimers formation due to the presence of the patch-like PMMA structure in the hybrid PMMA/SiO_2 matrix, as mentioned in the FT-IR results. The evidence of dimer formation can be well-known by the following study of the spectroscopic parameters[115].

The absolute fluorescence quantum yield η_F, of fluorescent PMMA/SiO_2 hybrid films was calculated, relative to Rhodamine 101 doped in

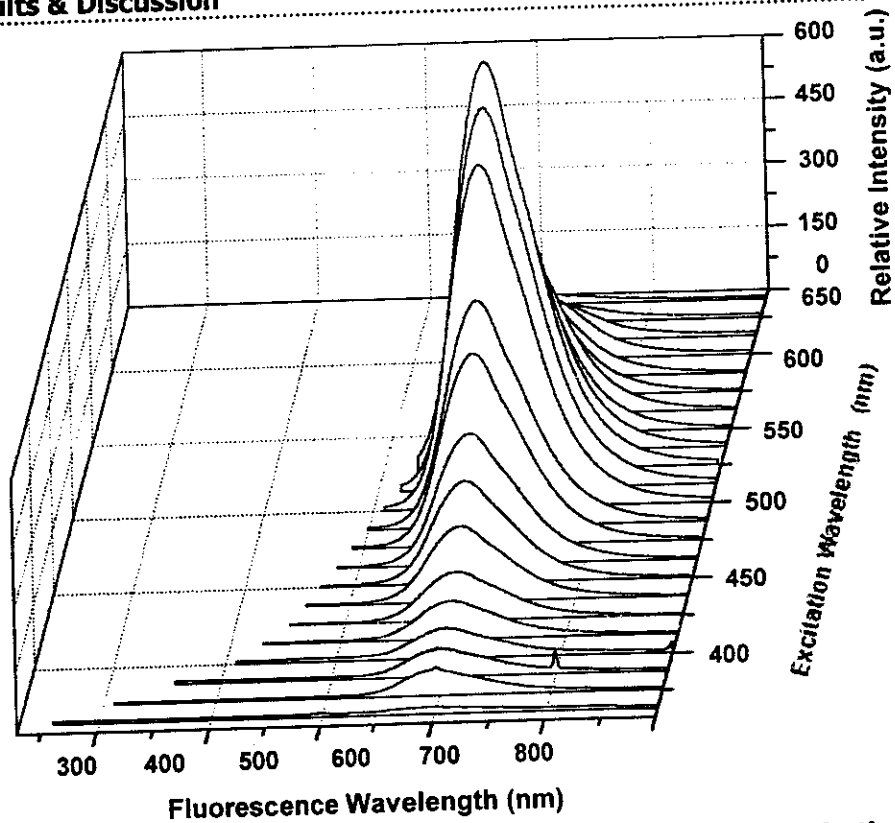

Fig.(4.3.11): Three dimensional representation of a synchronous excitation and fluorescence spectra of (PMMA-0.1 wt% SiO_2)/100 ppm MACROLEX Fluorescent Red G film.

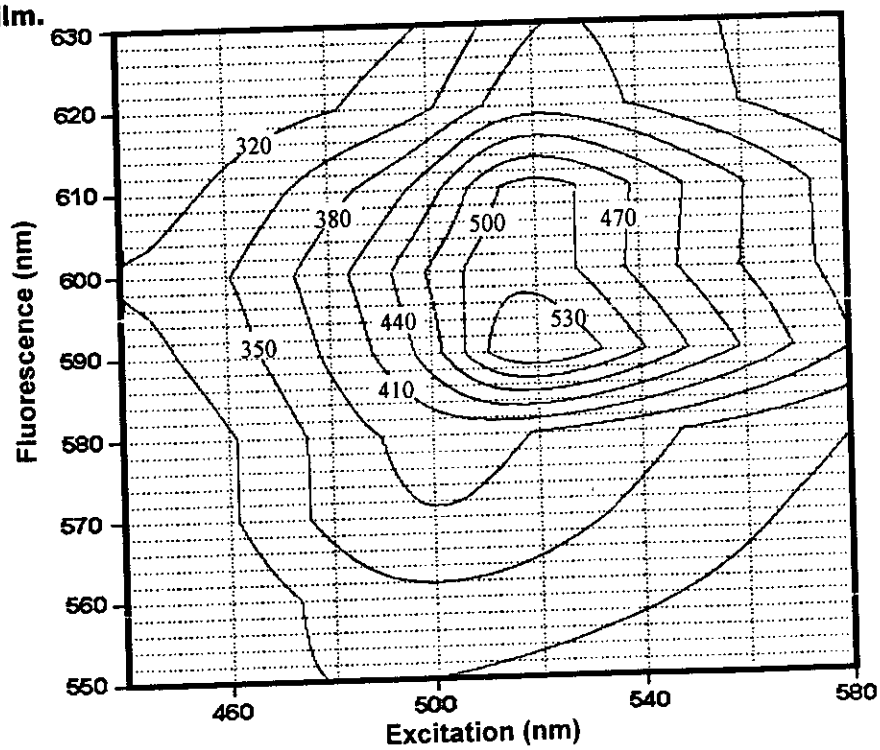

Fig.(4.3.12): Surface map representation of a synchronous excitation and fluorescence spectra of (PMMA-0.1 wt% SiO_2)/100 ppm MACROLEX Fluorescent Red G film.

PMMA/SiO_2 film as a reference sample using Eq. (2.21) [103-107],

$$\eta_F = \eta_{ref} (a / a_{ref}) (n / n_{ref}) (S_{ref}/S)$$

In addition, the Stokes shift $\Delta\lambda_s$, which is a measure of self-absorption of the fluorescent light, was calculated from Eq.(2.22) [19],

$$\Delta\lambda_S = \lambda_{F(max)} - \lambda_{a(max)}$$

The values of $\lambda_{a(max)}$, $\lambda_{F(max)}$, $\Delta\lambda_S$ and η_F are listed in Table (4.3.1). The observed decrease in η_F accompanied with the increasing values of $\Delta\lambda_S$ at concentrations higher than 100 ppm can be attributed mainly to the starting of the formation of excited state dimers (excimers) and higher aggregates which have small values of η_F [103,115]. Despite the fact that the concentrations of the fluorescent hybrid films are extremely higher than those in fluorescent PMMA films, they have a noticeably larger values of η_F. The dimerization and aggregation of the dye molecules in the hybrid PMMA/SiO_2 matrix have gained an intensive and on-going study because of the strong effects of the hybrid matrix on the spectral properties. It seems that the proposed PMMA-SiO_2 cage has a strong effect on reducing the probability of the formation of dimers which are not only weakly fluorescent but also absorb the fluorescence from the monomer. This means that the effect Förster-type energy transfer to the excited state dimers (excimers) is more limited by incorporating the dye in a relatively rigid PMMA/SiO_2 matrix than flexible chain PMMA matrix [135,136].

4.3.5 Interband Transitions

The UV absorption edge was analyzed in the range (190-350 nm) and the calculated values of the absorption coefficient α are found to lie in the range $1 \leq \alpha \leq 10^4$ cm^{-1}, the absorption coefficient for a simple parabolic band

Table(4.3.1): The effect of dye concentration on the absorption and fluorescence maxima $\lambda_{a(max)}$ and $\lambda_{F(max)}$, stokes shift $\Delta\lambda_S$ and the fluorescence quantum yield η_F for (PMMA-0.1 wt% SiO_2) hybrid MACROLEX Fluorescent Red G films.

Concentration (ppm)	$\lambda_{a(max)}$ (nm)	$\lambda_{F(max)}$ (nm)	$\Delta\lambda_S$ (nm)	η_F %
50	517.50	593.80	76.30	65.20
100	518.00	596.80	78.80	90.10
150	517.00	598.00	81.00	86.50
160	517.00	598.00	81.00	75.30
180	518.00	606.00	88.00	66.90
200	518.00	626.00	108.00	50.10

can be expressed by Eq.(2.9) [116],

$$\alpha E = M (E - E_{opt})^{m}$$

Fig.(4.3.13) shows the plots of $(\alpha E)^2$ versus the photon energy E for the investigated fluorescent PMMA/SiO_2 hybrid films, these plots show a linear behavior that can be considered as an evidence of the direct transition. The approximate value of E_{opt} is determined and listed in Table(4.3.2). The dependence of E_{opt} on the dye concentration shows a maximum value for the film of 150 ppm. This behavior is well correlated to that observed in the calculated values of the fluorescence quantum yield shown in Table (4.3.1) .

The Urbach's tail which is directly related to the exponential tail for the density of states of the band edge, can be calculated from [101],

$$\alpha(\nu) = \alpha_o \, exp \, (E/E_U)$$

The values of E_U were calculated from the relation between $\ln\alpha$ versus the photon energy (Fig.4.3.14), and listed in Table (4.3.2).

The effect of the hybrid PMMA/SiO_2 matrix on the optical transitions in the FSCs can be clarified by making a comparison between the values of E_{opt} and E_U for fluorescent hybrid PMMA/SiO_2 films (Table (4.3.2)) and those for fluorescent PMMA films (Table (4.1.2)). For the dye concentration of 100 ppm, it is noticeable that the value of E_{opt} is decreased from 5.307 eV in PMMA matrix to 5.273 eV in PMMA-SiO_2 matrix. On the otherhand, the value of Urbach's energy is increased from 0.248 eV to 0.281 eV. This can be explained by the formation of induced Frenkel exciton-like states due to the adsorption of aromatic C=O group of the coumarin molecule on the surface of SiO_2 nanoparticles (see FT-IR results). Frenkel excitons are light initiated electron hole pairs of very small radii and large binding energies which

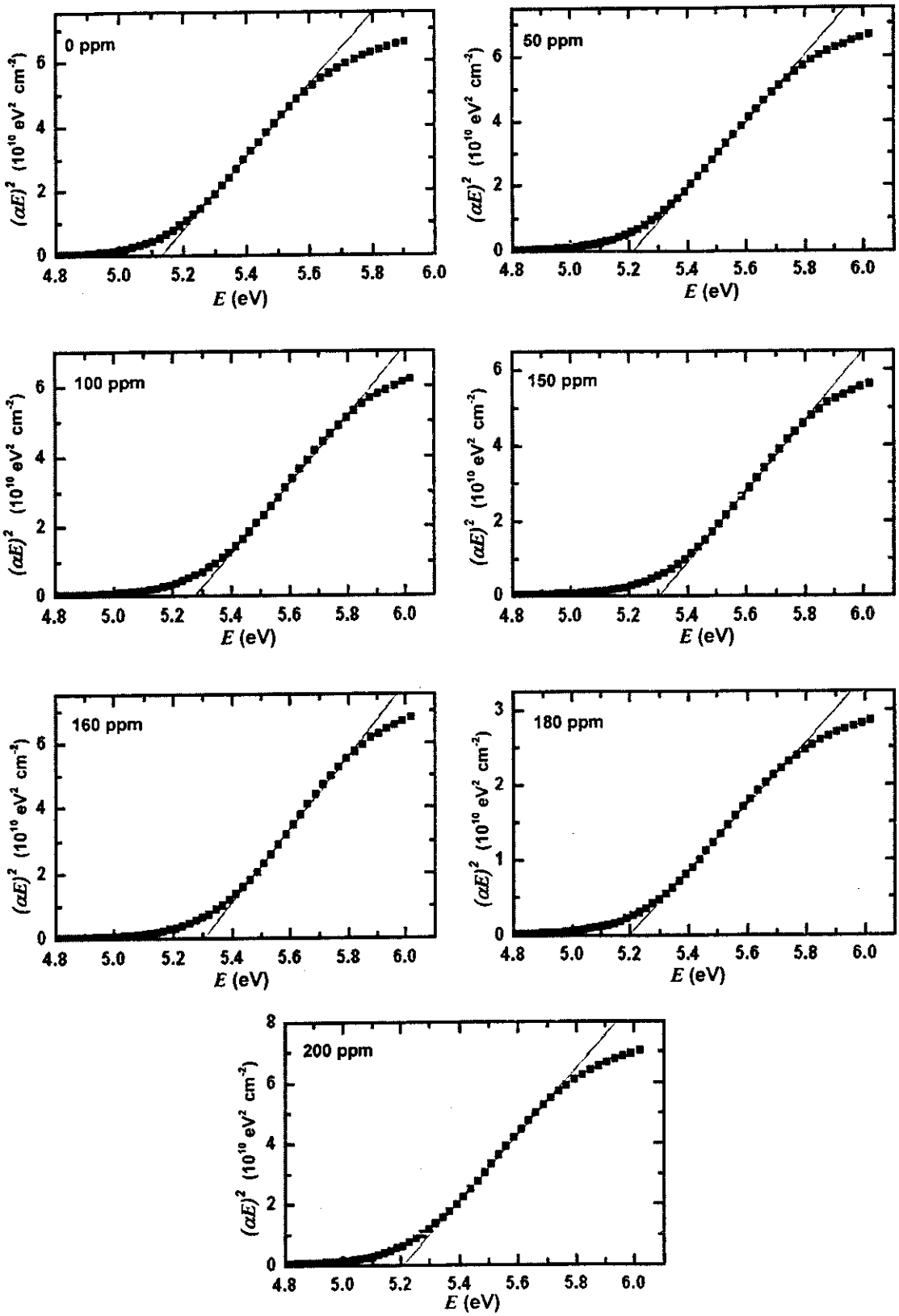

Fig.(4.3.13): The dependence of $(\alpha E)^2$ on the photon energy (E) for all the prepared (PMMA-0.1 wt% SiO_2) hybrid/MACROLEX Fluorescent Red G films.

Table (4.3.2): The effect of concentration on the optical band gap E_{opt}, and the tail width E_U for the investigated (PMMA-0.1 wt% SiO_2) hybrid/MACROLEX Fluorescent Red G films.

Concentration (ppm)	E_{opt} (eV)	E_U (eV)
0	5.130	0.215
50	5.214	0.258
100	5.273	0.281
150	5.304	0.304
160	5.301	0.308
180	5.195	0.313
200	5.209	0.318

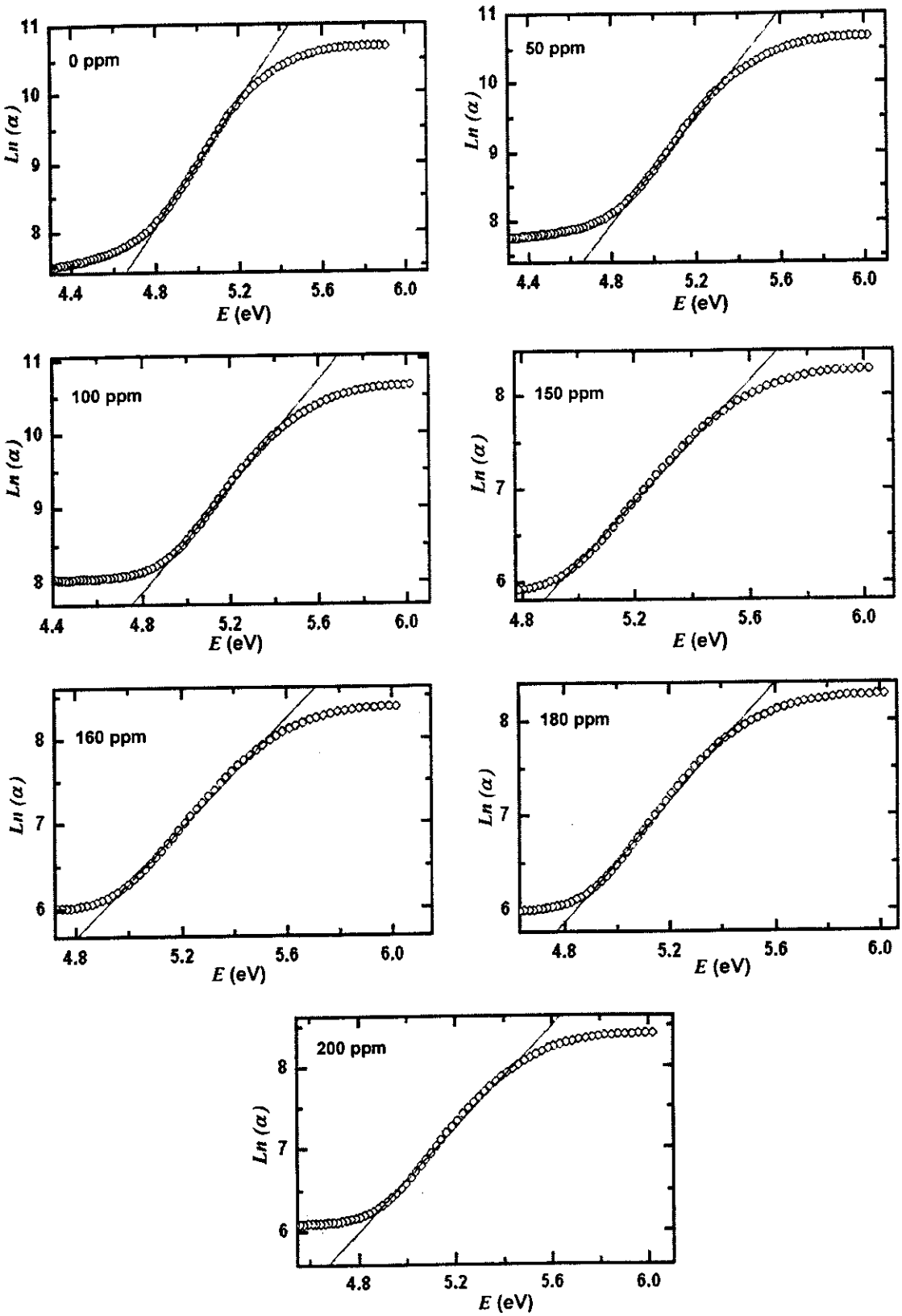

Fig.(4.3.14): The dependence of $ln(\alpha)$ on the photon energy (E) for the investigated (PMMA-0.1 wt% SiO_2) hybrid/MACROLEX Fluorescent Red G films.

increase their localization on the atomic sites at which they are created [93]. Accordingly, they are considered as excited states of individual matrix molecules on which they are localized. This leads to the isolation of the dye molecules from each other and shifting the dimerization threshold to higher values of dye concentration (from 100 ppm in PMMA film to 200 ppm in PMMA/SiO_2 hybrid film).

4.3.6 Transmission Spectroscopy

The transmission spectra for all the prepared fluorescent PMMA-SiO_2 hybrid films were recorded in the wavelength range (190-1100 nm) as depicted in Fig.(4.3.15). The effect of dye concentration on the film transmittance at the fluorescence maxima T_F is illustrated in Fig.(4.3.16). It is noticed that all the films exhibit high transmission values with a maximum value (98.77%) for the concentration 100 ppm due to its excellent fluorescence properties and the lacking of dye dimerization. The comparison between Figs.(4.1.14) and (4.3.16) reveals that the value of T_F for the dimer concentration in the hybrid matrix (96.25% for 200 ppm in PMMA/SiO_2) is higher than that in the polymer matrix (93.98% for 100 ppm in PMMA). This behavior is well correlated to the fluorescence properties.

4.3.7 Refractive Index and Guiding properties

The spectral dependence of the specular reflection spectra for all the investigated fluorescent hybrid films in the wavelength range (300-1100 nm) is shown in Fig.(4.3.17). All the curves show a minimum in the wavelength range of the absorption band followed by a maximum one in the wavelength range of the fluorescence band. The determined wavelength of the maximum reflectance is found to increase by increasing the dye concentration; in good agreement with the behavior observed in the fluorescence spectra.

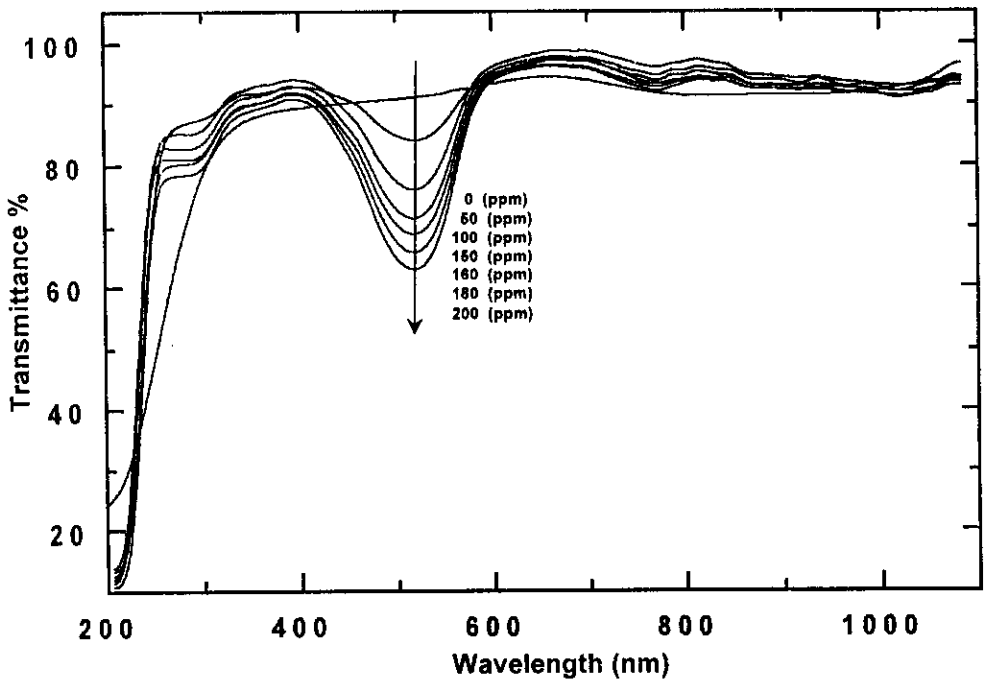

Fig.(4.3.15): Transmission spectra of (PMMA-0.1 wt% SiO_2) hybrid /MACROLEX Fluorescent Red G films.

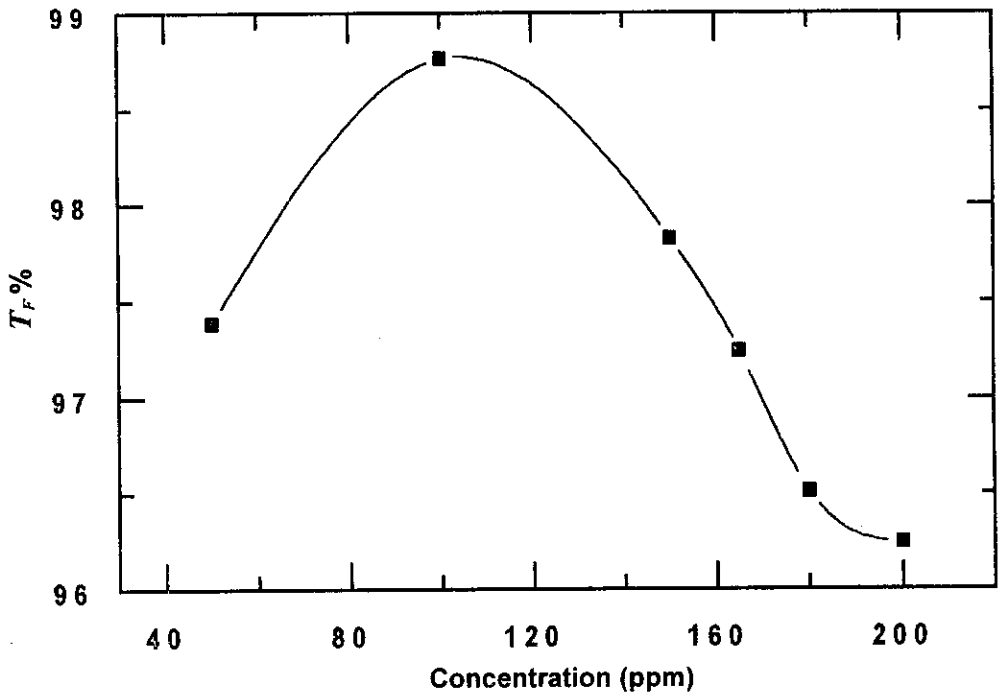

Fig.(4.1.16): The effect of dye concentration on the film transmittance at the fluorescence peak, T_F, for (PMMA-0.1 wt% SiO_2) hybrid/MACROLEX Fluorescent Red G films.

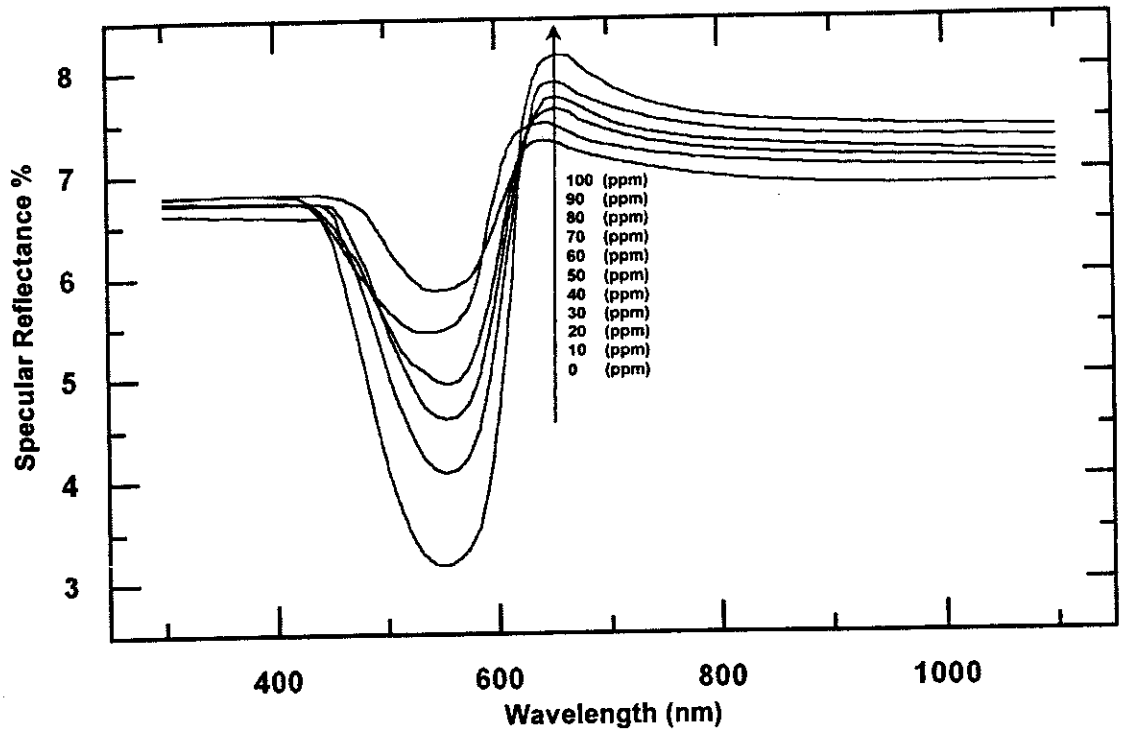

Fig.(4.3.17): Specular Reflection spectra for MACROLEX Fluorescent Red G/ (PMMA-0.1 wt% SiO_2) hybrid films.

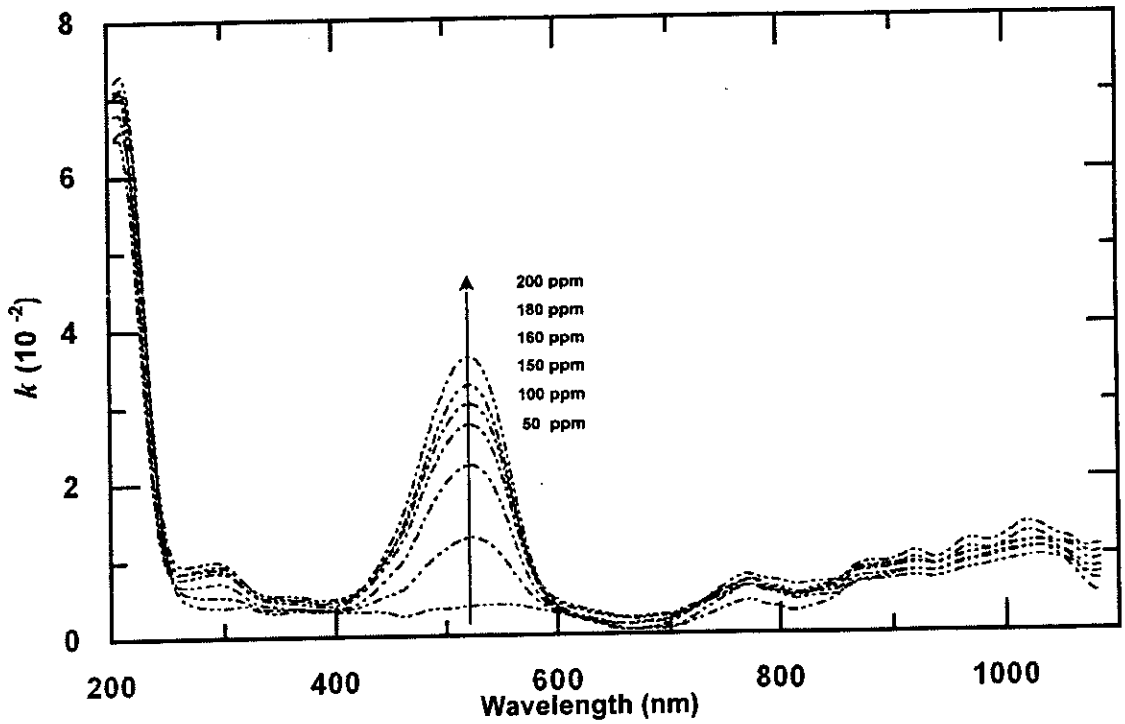

Fig.(4.3.18): Effect of MACROLEX Fluorescent Red G concentration on the attenuation coefficient of (PMMA-0.1 wt% SiO_2) hybrid films.

To evaluate the complex refractive index of the fluorescent hybrid PMMA/SiO_2 films, it is important to determine the attenuation coefficient k which is directly related to the absorption coefficient of the material α at given wavelength λ according to Eq.(4.1.2) [93, 100],

$$k = \alpha\lambda / 4\pi$$

Fig.(4.3.18) represents the spectral dependence of the attenuation coefficient k for all the fluorescent PMMA films. It is clear that k increases by increasing the dye concentration and tends to zero in the wavelength region of the fluorescence band; this indicates that the films are in the transparent range. For that reason the refractive index n can be calculated from the approximated Eq.(2.36) [55,100],

$$R_f = (n-1)^2/(n+1)^2$$

Fig.(4.3.19) shows the spectral dependence of the refractive index n for all the fluorescent PMMA films in the wavelength range 300-1100 nm. It is obviously noted that values of n are increased in the wavelength region of the fluorescence band and then show normal dispersion according to Cauchy's formula, Eq.(4.1.3)[117-119]. It is also plainly observed that the maximum values of refractive indices for 50 and 100 ppm dye concentrations are increased from 1.548 and 1.624 in PMMA (Fig.(4.1.17)) to 1.742 and 1.753 in PMMA-SiO_2 hybrid films. This increase can be explained on the basis of Lorentz-Lorentz equation (4.1.4)[120,121], since intermolecular interactions between the dye molecules and SiO_2 nanoparticles enlarged the mean molecular polarizability and subsequently the number of atomic refractions.

The trapping efficiency η_{trap} was calculated from the refractive index n of the films using Eq.(2.38)[55],

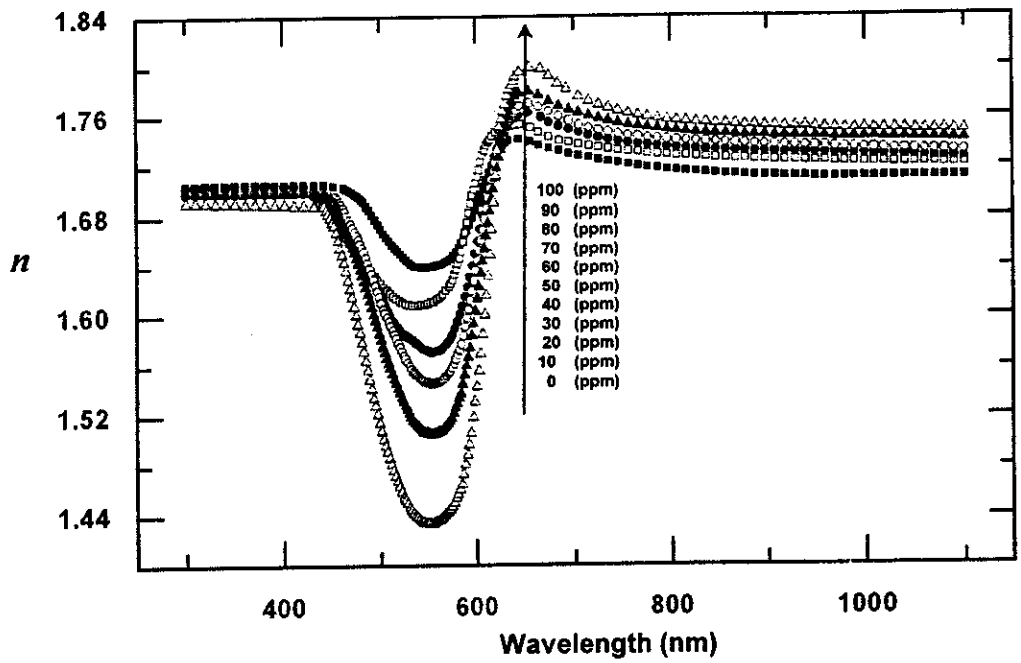

Fig.(4.3.19): The spectral dependence of the refractive index, n , for MACROLEX Fluorescent Red G /(PMMA-0.1 wt% SiO_2) hybrid films.

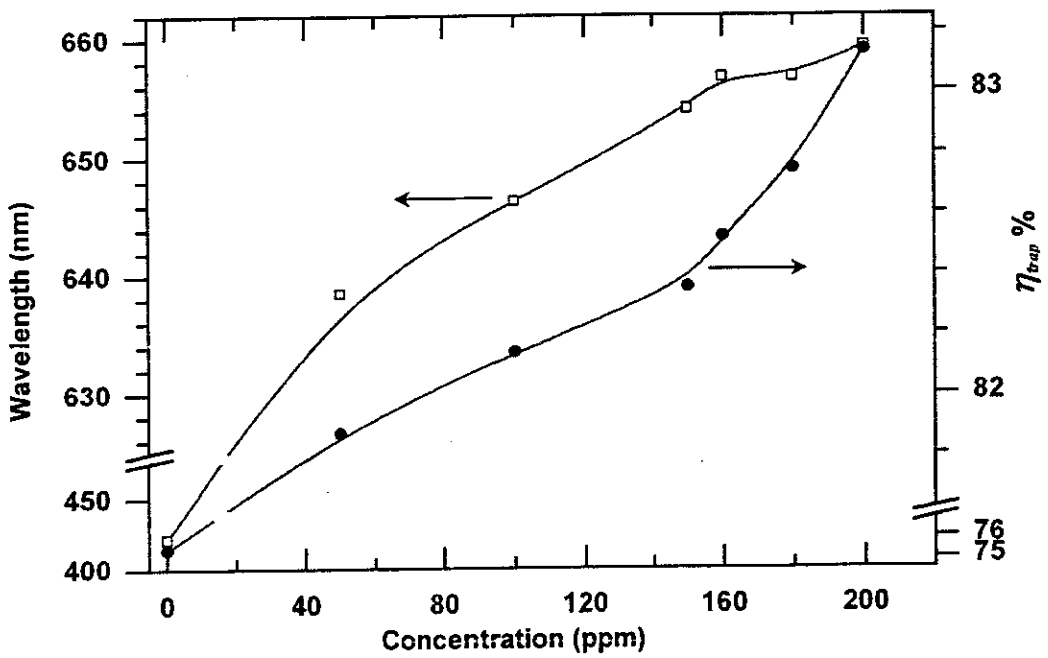

Fig.(4.3.20): The trapping efficiency, η_{trap} , and the peak position for (PMMA-0.1 wt% SiO_2) hybrid / MACROLEX Fluorescent Red G films.

$$\eta_{trap} = (1\text{-}1/n^2)^{0.5}$$

Fig.(4.3.20) represents a plot of η_{trap} against dye concentration. It is clear that the values of η_{trap} for the fluorescent hybrid films are larger than those of fluorescent PMMA films (Fig.(4.1.18). This means that incorporating of organic fluorescent dyes in the hybrid matrices decreases the critical angle and accordingly reduce the fraction of fluorescent photons escaped from the critical cones [88].

The trapped photons are assumed to propagate without loss by total internal reflection to the collecting edge. Each internal reflection will not be total because of the surface defects among other manufacture factors. The partial yield η_{TIR} defined as the total internal reflection efficiency is given by Eq.(2.42) [55],

$$\eta_{TIR} = R_i^n$$

Fig.(4.3.21) shows the dependence of η_{TIR} on the dye concentration, it is clear that the value of η_{TIR} increases by increasing the dye concentration having its maximum value (98.46%) for the dye concentration 200 ppm. It is also evidently observed that the values of η_{TIR} for 50 and 100 ppm dye concentrations are increased from 96.21% and 96.64% in PMMA matrix (Fig.(4.1.19)) to 98.12% and 98.46% in PMMA-SiO_2 hybrid matrix. This reflects the color homogeneity and good surface preparation of the fluorescent hybrid matrices which decreased the total internal reflection losses and subsequently enhances the guiding properties [40,122].

The conversion yield η_{conv} which is the ratio of the number of photons available in the film N to the number of incident photons N_o , was calculated by using Eq.(2.46) [55],

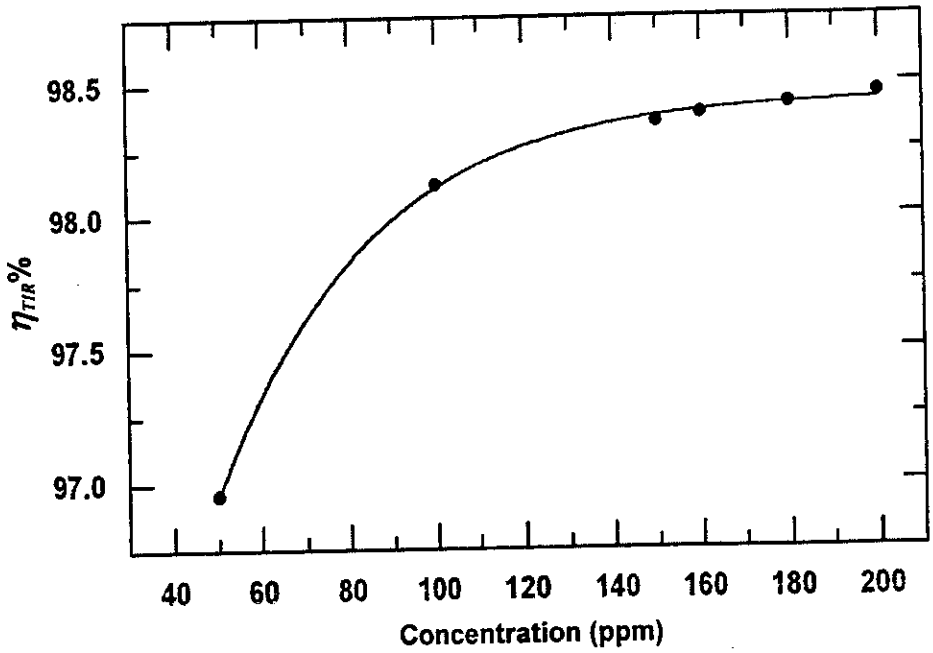

Fig.(4.3.21): Concentration dependence of the total internal reflection efficiency, η_{TIR}, for (PMMA-0.1 wt% SiO_2) hybrid/ MACROLEX Fluorescent Red G films.

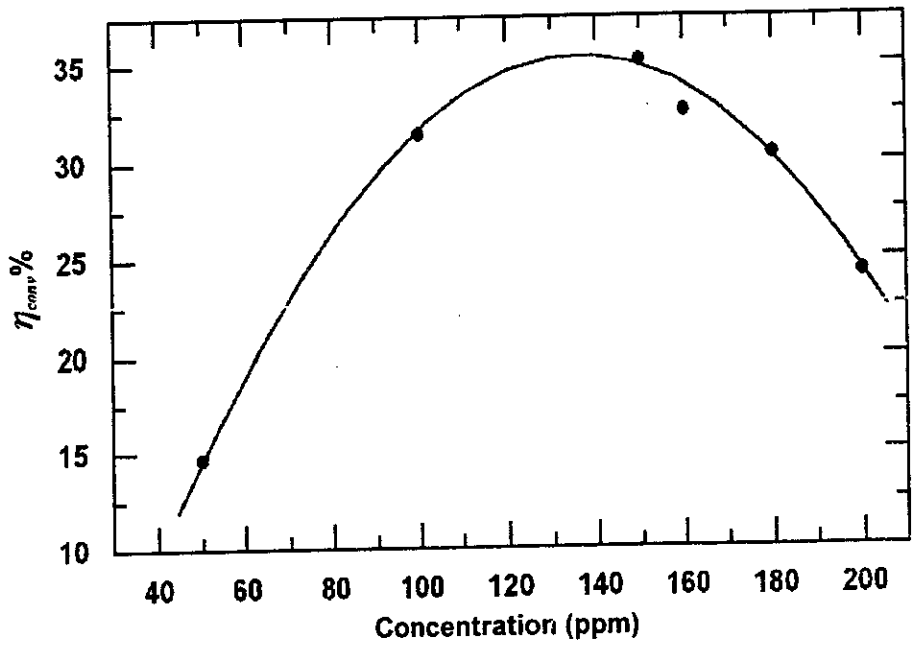

Fig.(4.3.22): Concentration dependence of the conversion efficiency, η_{conv}, for (PMMA-0.1 wt% SiO_2) hybrid/MACROLEX Fluorescent Red G films.

$$\eta_{conv} = (1 - R_f)\,\eta_{trap}\,\eta_{abs}\,\eta_F = N/N_o$$

Fig.(4.3.22) shows the dependence of η_{conv} on the dye concentration shows a maximum conversion efficiency (35.17%) for the film of 150 ppm. It is also noticed that the values of η_{conv} for 50 and 100 ppm dye concentrations are increased from 23.36% and 9.52% in PMMA (Fig.(4.1.20)) to 14.69% and 24.24% in PMMA-SiO_2 hybrid films. The observed decrease for the first concentration is attributed to the increase of the number of nonradiative energy transfer processes from the fluorophores which are adsorbed on the surface of SiO_2 nanoparticles by hydrogen bonding. On the otherhand the observed enhancement in η_{conv} for 100 ppm dye concentration is attributed to the growth of the dye fluorescence due to its isolation in the confined cage of PMMA/SiO_2 film (estimated in FT-IR study), thus very high dye concentrations can be incorporated without the formation of excited state dimers and other undesirable aggregations [19,104].

4.3.8 Dye Self-absorption

The stokes efficiency which is the ratio of the average energy of the fluorescent photons to the average energy of the absorbed photons is given by Eq.(2.33) [47],

$$\eta_{stok} = \langle \nu_F \rangle / \langle \nu_a \rangle$$

The values of η_{stok} were extracted from the values of $\lambda_{F(max)}$ and $\lambda_{a\,(max)}$ which are listed in Table (4.3.1). For the dye concentration of 100 ppm, it was observed that the values of η_{stok} are increased from 83.22% in PMMA matrix to 86.80% in PMMA/SiO_2 hybrid matrix. This leads to the reduction of the energy loss due to the stokes shift (1- η_{stok}) by the hybrid matrix [136].

On the other hand the self-absorption of the dye aggregates and its effect on the fluorescent light transport to the film edges has been studied by employing the fluorescence polarization anisotropy technique and by using Eq.(2.24) [103,104],

$$P = (I_{//} - I_{\perp}) / (I_{//} + I_{\perp})$$

Figs.(4.1.23-25) show the polarized excitation and fluorescence spectra for the fluorescent PMMA/SiO_2 films of 10 ,150, 200 ppm dye concentrations respectively. It is noticed that, for the hybrid film of concentration 150 ppm the calculated polarization spectrum is comparatively ideal in that the values of P are almost constant across the long wavelength of the excitation and fluorescence bands. Dissimilarly, for the highest dye concentration (200 ppm), the fluorescence is less polarized and subsequently self-absorbed. This confirms the shift in the dimerization threshold from 100 ppm in PMMA matrix to 200 ppm for PMMA/SiO_2 hybrid matrix.

The self-absorption probability (1-η_{self}) can be deduced using the following relation (2.34) [49,81],

$$(1- \eta_{self}) = [1- A_F/A_o]/ \eta_F \eta_{trap} (1- A_F A_o)$$

The efficiency limited by the energy loss due to self-absorption η_{self} can be deduced using the highest measured reduced anisotropy (A_o= 39.74%) for the hybrid film of 10 ppm and the reduced anisotropy A_F values for the concentrations of interest; mainly 150 ppm for monomer fluorescence and 200 ppm for dimer fluorescence. The calculated values of reduced anisotropy A_F were 39.15 and 37.69% for PMMA-SiO_2 films incorporated with 150 and 200 ppm dye concentrations; leading to values of η_{self} equal to 94.11% and 85.36%, respectively. This indicates that a greatly reduced self-

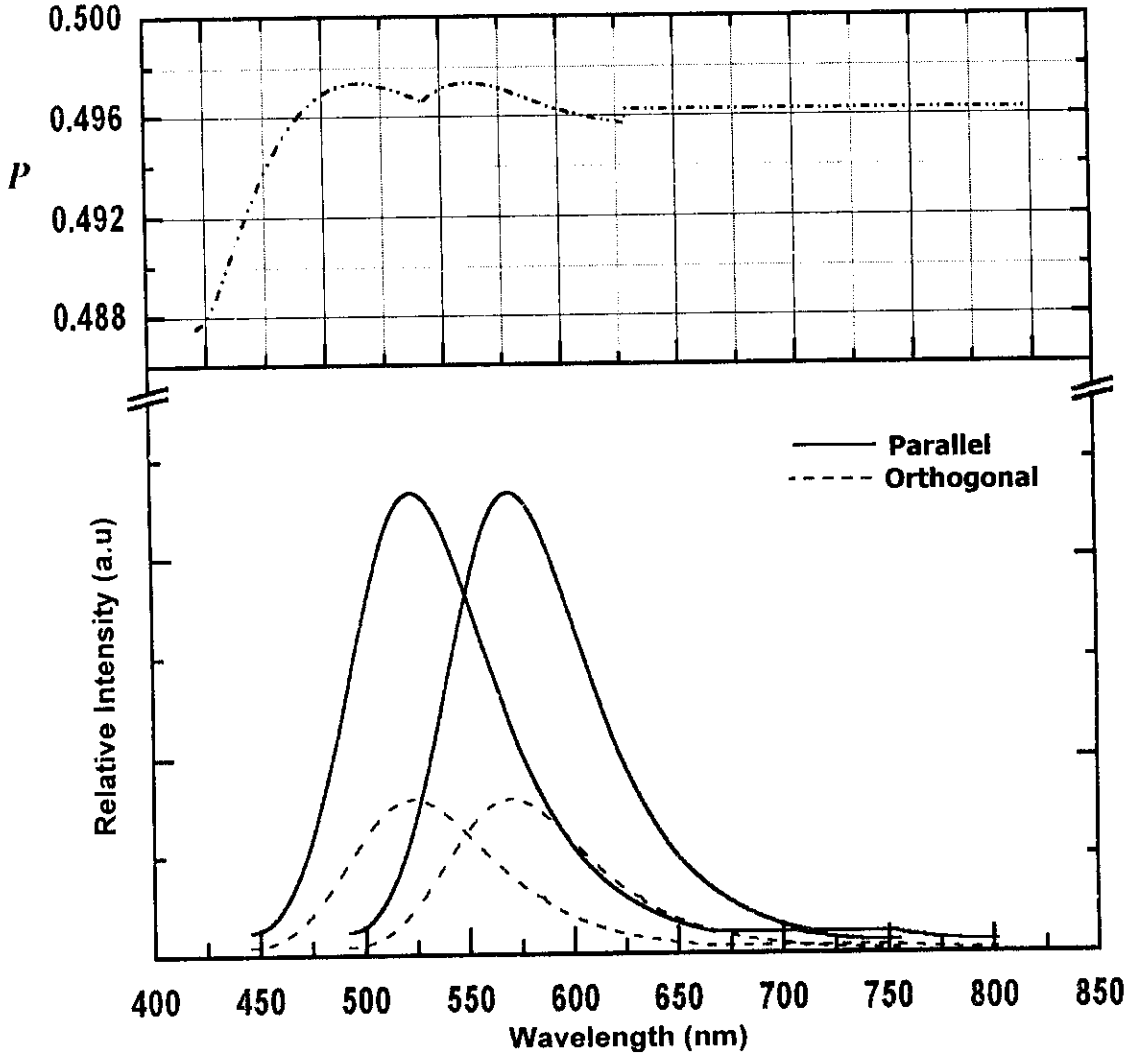

Fig.(4.3.23): The polarized fluorescence excitation (left) and emission (right) spectra for (PMMA-0.1 wt% SiO_2) hybrid /10 ppm MACROLEX Fluorescent Red G film obtained by parallel and orthognal orientation with respect to the polarization direction of the incident light. The polarization spectrum is plotted in the upper boxes.

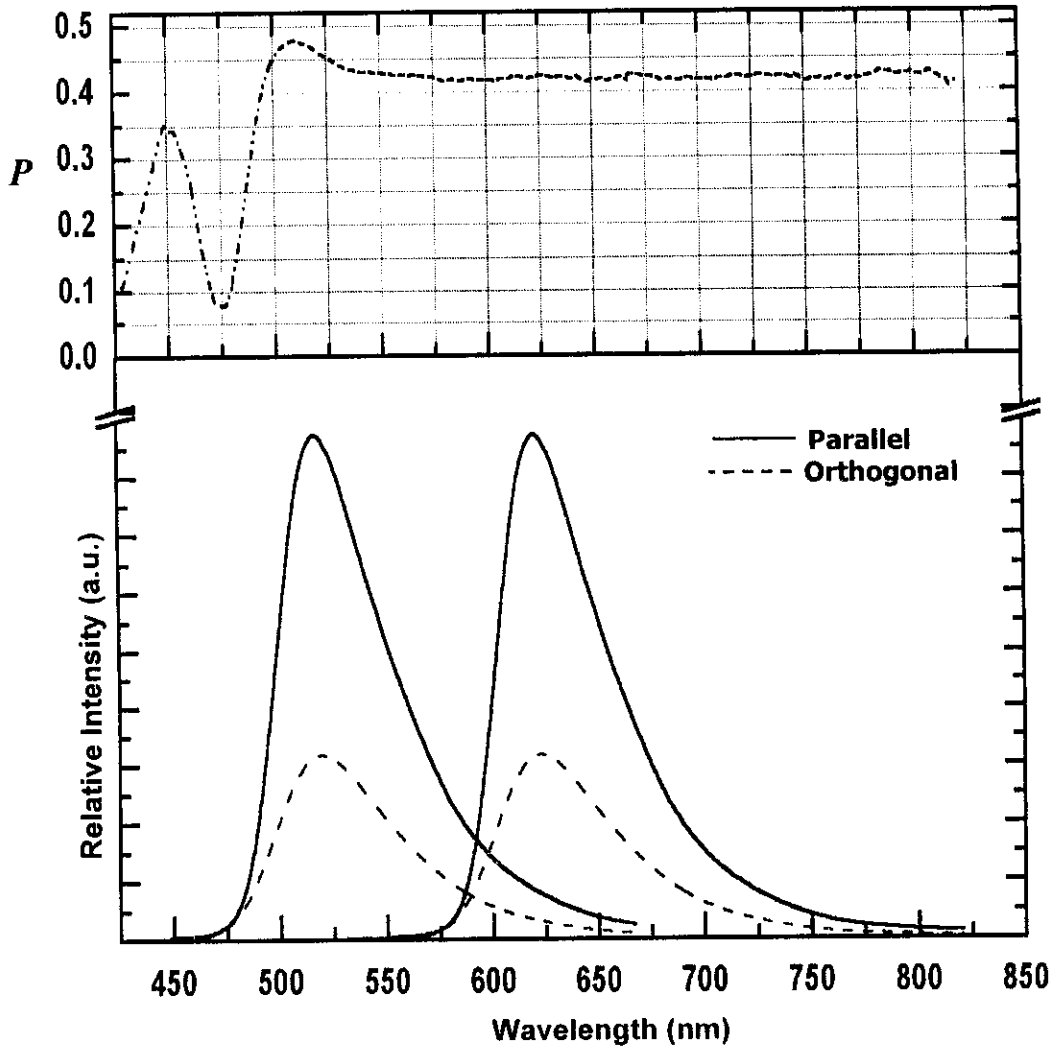

Fig.(4.3.24): The polarized fluorescence excitation (left) and emission (right) spectra for (PMMA-0.1 wt% SiO_2) hybrid /150 ppm MACROLEX Fluorescent Red G film obtained by parallel and orthognal orientation with respect to the polarization direction of the incident light. The polarization spectrum is plotted in the upper boxes.

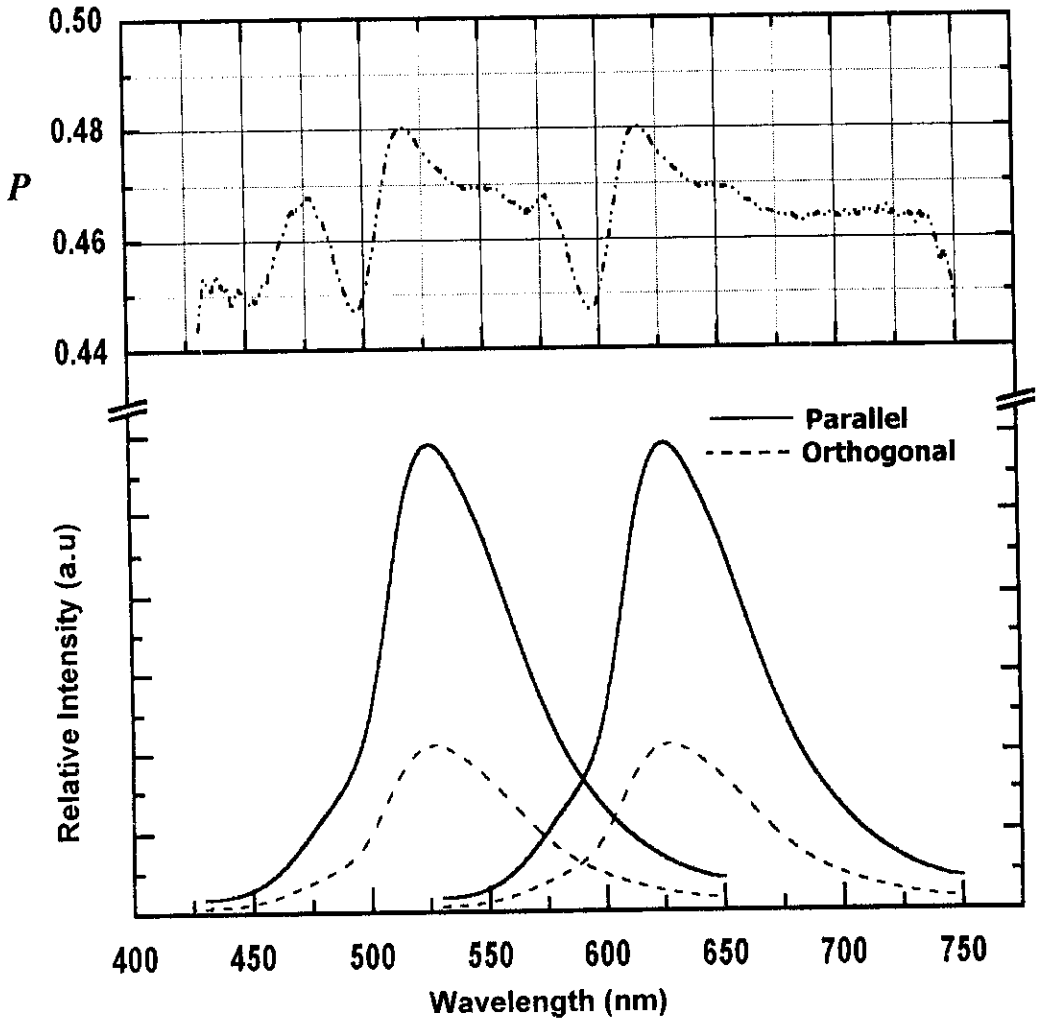

Fig.(4.3.25): The polarized fluorescence excitation (left) and emission (right) spectra for (PMMA-0.1 wt% SiO_2) hybrid /200 ppm MACROLEX Fluorescent Red G film obtained by parallel and orthognal orientation with respect to the polarization direction of the incident light. The polarization spectrum is plotted in the upper boxes.

absorption probability of fluorescent photons can be acheived by embedding the dye molecules in the hybrid PMMA/SiO_2 matrix rather than the relatively flexible PMMA matrix [135,136].

4.3.9 Photostability

The photostability of the absorption and fluorescence spectra were studied for the fluorescent hybrid films of 150 ppm and 200 ppm dye concentrations. These concentrations are corresponding to the maximum conversion efficiency for both the monomer and dimer dye molecules.

4.3.9.1 Photoresponse of the Optical Absorption Spectra

The mentioned fluorescent hybrid PMMA/SiO_2 films were exposed indoors to UV-VIS radiation for 24 hrs and the change in the absorption spectra was monitored at different times during the irradiation period and plotted as shown in Figs.(4.3.26.a) &(4.3.27.a). The optical gap E_{opt} and Urbach's energy E_U were estimated at different exposure times to artificial sunlight and listed in Tables (4.3.3) & (4.3.4). The tabulated values indicate that there is no significant variation in E_{opt} values near the absorption edge and also the same is observed for E_U values. From this observation one can consider that the hybrid PMMA/SiO_2 matrix is a good one for the dye under investigation and could act as an inert medium [18,80].

The dye photodegradation a_t/a_o, which is the percentage change of optical density is plotted versus the exposure time as illustrated in Figs.(4.4.26.b) & (4.4.27.b). It was found that for 150 ppm dye doped film; the behavior suggests two degradation rates obeying the exponential relation described by Eq. (4.1.5) [19],

$$a_t/a_o = C_1 + C_2\, exp(-R_1 t) + C_3\, exp(-R_2 t)$$

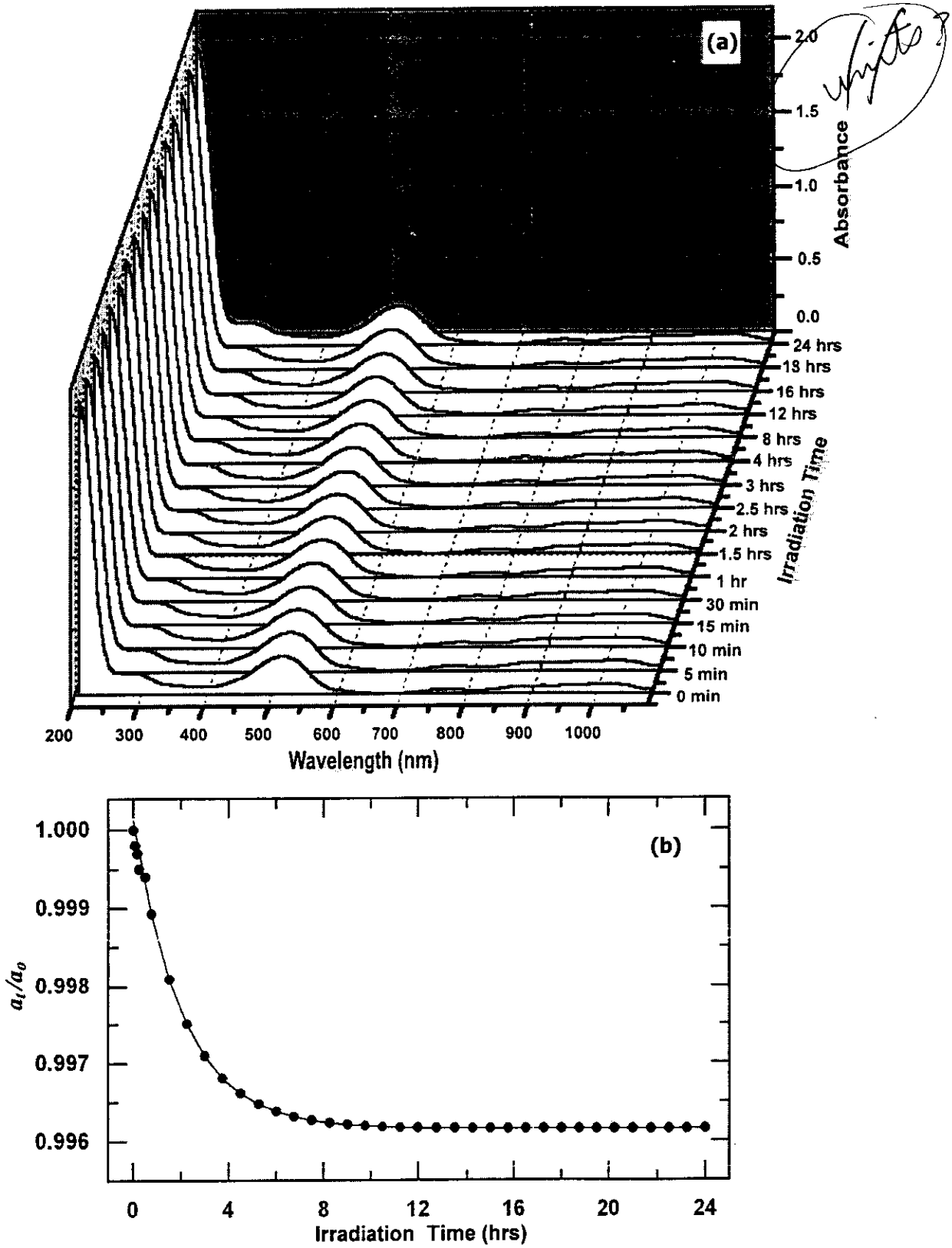

Fig.(4.3.26): (a) Time dependence of the absorption spectra of the as prepared (PMMA- 0.1 wt% SiO_2) hybrid /150 ppm MACROLEX Fluorescent Red G under photoirradiation with artificial sunlight and (b) The photodegradation curve of the as prepared PMMA/100 ppm MACROLEX Fluorescent Red G matrix, after indoor exposure to artificial sunlight from Xenon arc lamp for 24 hrs.

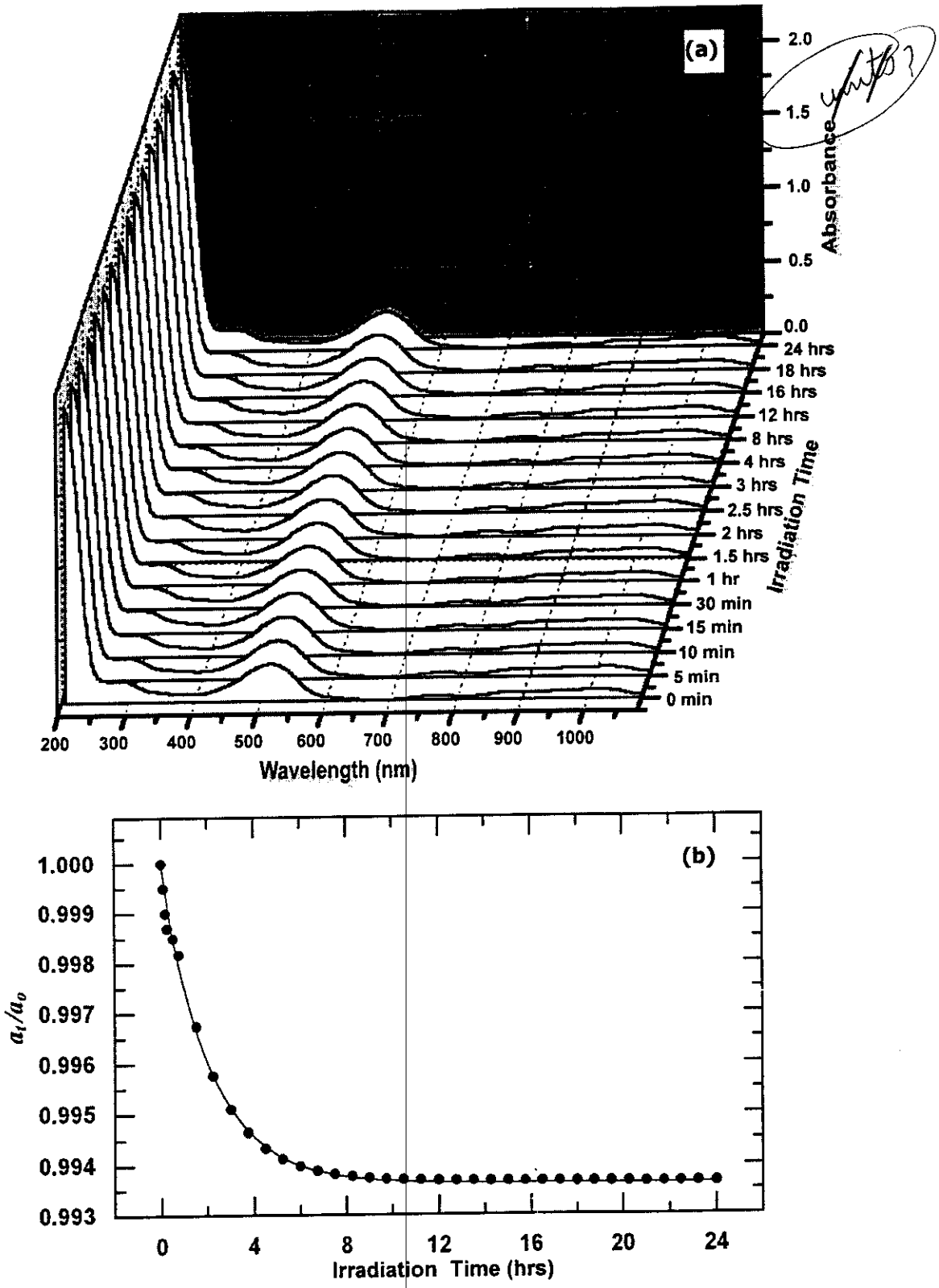

Fig.(4.3.27): (a) Time dependence of the absorption spectra of the as prepared (PMMA- 0.1 wt% SiO_2) hybrid /200 ppm MACROLEX Fluorescent Red G under photoirradiation with artificial sunlight and (b) The photodegradation curve of the as prepared PMMA/100 ppm MACROLEX Fluorescent Red G matrix, after indoor exposure to artificial sunlight from Xenon arc lamp for 24 hrs.

Table(4.3.3): The optical parameters (E_{opt} and E_U) for (PMMA- 0.1 wt% SiO_2) hybrid/150 ppm MACROLEX Fluorescent Red G exposed to artificial sunlight from Xenon arc lamp for 24 hrs.

Irradiation Time	E_{opt} (eV)	E_U (eV)
0	5.304	0.304
5 min	5.301	0.306
10 min	5.305	0.305
15 min	5.304	0.305
30 min	5.303	0.303
1 hr	5.302	0.304
1.5 hrs	5.303	0.306
2 hrs	5.304	0.303
2.5 hrs	5.300	0.306
3 hrs	5.302	0.304
4 hrs	5.303	0.304
8 hrs	5.301	0.304
12 hrs	5.301	0.303
16 hrs	5.302	0.305
18 hrs	5.303	0.302
24 hrs	5.304	0.303

Table(4.3.4): The optical parameters (E_{opt} and E_U) for (PMMA- 0.1 wt% SiO_2) hybrid/200 ppm MACROLEX Fluorescent Red G exposed to artificial sunlight from Xenon arc lamp for 24 hrs.

Irradiation Time	E_{opt} (eV)	E_U (eV)
0	5.209	0.318
5 min	5.208	0.317
10 min	5.207	0.316
15 min	5.208	0.317
30 min	5.206	0.317
1 hr	5.208	0.316
1.5 hrs	5.206	0.317
2 hrs	5.207	0.316
2.5 hrs	5.208	0.318
3 hrs	5.207	0.315
4 hrs	5.206	0.316
8 hrs	5.207	0.315
12 hrs	5.208	0.316
16 hrs	5.207	0.317
18 hrs	5.206	0.318
24 hrs	5.205	0.319